Heavy Neutrinos and Rare Decays

Dissertation

zur Erlangung des Grades

“Doktor der Naturwissenschaften”

am Fachbereich Physik

der Johannes Gutenberg-Universität
in Mainz

Zoltán Gagyi–Pálffy

geboren in Arad, Rumänien

Mainz 2004

Datum der mündlichen Prüfung: **19.02.2004**

Contents

Introduction

About to reach a history of fourty years, the Standard Model has proven itself as an outstanding description of the processes in the elementary particle physics. There is little doubt nowadays that a local quantum field theory based on the $SU(3)_c \otimes SU(2)_L \otimes U(1)_Y$ gauge group describes with an amazing precision all the experimental results obtained at the energies available in the current particle accelerators. The main theoretical predictions of the theory were confirmed one by one: the existence of the charm quark (foreseen in the GIM mechanism), the existence of the neutral currents, the physical evidence for the W and Z bosons and the quantitative relation between the corresponding masses, and many others. With high energy $e^+ - e^-$ colliders it was possible to study also the quantum structure of the theory. Running at the Z^0 resonance, the Large Electron-Positron Collider (LEP) at CERN was sensitive to the different loop-corrections, starting the era of the precision tests of the Standard Model.

With all these successes, the model still faces serious challenges. One of the most serious difficulties encountered is the theoretical description for the hadronic spectrum, strongly related to the problem of quark confinement in Quantum Chromodynamics (QCD), the gauge theory of strongly interacting quarks and gluons. Although an intuitive qualitative description was given by the discovery of asymptotic freedom in the strong interactions, quantitative results for the non-perturbative regime of QCD are still hard to obtain.

In the electroweak sector the origin of different particle masses is of crucial importance. In the Standard Model it is assumed that the initial gauge symmetry of the theory is spontaneously broken by the non-vanishing vacuum expectation value of a neutral scalar Higgs field. The peculiarity of the Higgs particle is that its mass is an independent parameter of the theory (at least at tree level) and up to now it has evaded detection. Precision

tests of the Standard Model taking into account radiative corrections impose only vague limits on its mass. After the discovery of the sixth (top) quark, the Higgs boson remained the last fundamental constituent of the model to be found. It will be the task of the next generation of high energy accelerators, in particular the Large Hadron Collider (LHC) at CERN, to detect this particle.

It is generally accepted that the Standard Model provides only an effective description of the fundamental interactions at the currently observable energies, and that it originates in a more fundamental theory. There is an intensive search for signals indicating the presence of this theory, mainly via discrepancies compared to the predictions of the Standard Model. The presence of "new physics" would manifest itself in new types of elementary particles, detected directly or through their effects in radiative corrections. A good example for such "new physics" are supersymmetric theories, and the search for the supersymmetric partners of the presently known particles is very seriously pursued at the different colliders.

An indirect way for detecting interactions of a new type is the search for evidence of processes forbidden or strongly suppressed in the Standard Model. The allowed rare processes usually are not possible at tree level and they are governed by loop-corrections. A significant departure of the experimental results from the range allowed by the theory could be seen as an effect of "new physics". For processes entirely forbidden in the Standard Model it would suffice merely their detection in order to conclude about the presence of "new physics".

We will dedicate this thesis to the study of such rare processes, in particular the leptonic decay $K_L \to e\mu$. The peculiarity of this process is that the lepton number corresponding to a given leptonic family is not conserved, as it happens in the Standard Model. This forbids the given decay to take place within the realm of the present theory. However, the conservation of leptonic number does not correspond to any gauge symmetry present in the theory and one has no reason to consider it a fundamental property. Given, however, the level of accuracy of the Standard Model, we will restrict ourselves to considering only minimal extensions of it. This will enable us to have new types of interactions present in our models, but on the other hand it will keep the necessarily arising complexity of the theory at an acceptable level.

We will adopt two particular models for completing our investigation. The first one

to be considered represents an extension of the Standard Model when heavy right-handed neutrinos are present, preserving the initial gauge structure. The second one is the result of more general considerations, a left-right symmetric theory based on the gauge group $SU(2)_L \otimes SU(2)_R \otimes U(1)_{B-L}$, also in the presence of heavy right-handed neutrinos, more natural in this particular model. It will be shown that both models can predict substantially increased values for the branching ratio of the chosen decay compared to previous results and in some cases these can reach the region of the presently observed experimental limit.

In this work we will stress also the necessary model-building in order to study rare decays in minimal extensions of the Standard Model. The particular left-right symmetric model is outlined, and although there will be no new results obtained in this domain, we stress the motivations of the particular choices for the different parameters occurring in the theory. The reason behind this detailed outline of the model is to offer a clear distinction between the mandatory aspects required by the particular symmetries and the several choices available for other parameters. Here we will single out a particular model which corresponds to fairly general and at the same time sufficiently realistic relations between the different available parameters, mainly concerning the vacuum expectation values of the different symmetry-breaking scalar multiplets. In the second chapter the question of non-vanishing neutrino masses is discussed, with explicit attention given to a model with two neutrino generations. This model will be shown to be consistent with additional heavy neutrinos having masses as light as $\sim$ 100 GeV. Mixings between the different massive neutrino families are also discussed and many useful relationships between the corresponding mixing matrix-elements are presented.

The main part of our work is dedicated to the study of the decay $K_L \to e\mu$ in the framework of the models outlined in the first two chapters. The third chapter is devoted to the study of this decay in an $SU(2)_L \otimes U(1)_Y$ model with heavy neutrinos, the fourth chapter applies the $SU(2)_L \otimes SU(2)_R \otimes U(1)_{B-L}$ model to the study of the same process. Our results will underline the dominant role played by the top quark appearing in the internal lines of the 1-loop Feynman diagrams contributing to the decay and also the considerable enhancement of the branching ratio obtained through chirality-changing interactions in the left-right symmetric model, leading to non-decoupling effects due to the presence of the heavy neutrinos. Our study is completed by addressing the question of gauge invariance

in the last chapter. To substantiate our results, a particular attention is paid to the gauge independence of this decay process at one loop level. Analogously with earlier studies on the $K^0 - \bar{K}^0$ mixing, it is explicitly shown how restoration of gauge invariance occurs in the decay amplitude containing the box diagrams, when the relevant Higgs-dependent self-energy and vertex graphs are taken into account. An on-shell skeleton renormalization scheme is adopted in order to achieve the first complete analysis of gauge invariance for $K_L \to e\mu$. As a striking difference compared to the $K^0 - \bar{K}^0$ mixing, it is found that in the Feynman-'t Hooft gauge, the gauge dependent complements may become dominant for a large range of parameters, an aspect that was not addressed in detail before.

Chapter 1

Left-right symmetric model of the weak interaction

The Standard Model of the elementary particle physics [1] based on the $SU(3)_c \otimes SU(2)_L \otimes U(1)_Y$ symmetry has proved itself extremely successful in providing a theoretical framework for the description of the low-energy weak phenomena. The present status of this model is still very robust, the high precision experiments carried out at LEP, being sensitive to the radiative corrections to the tree-level theory, are up to now in good coincidence with the theoretical expectations.

In spite of all the successes in the last decades, the Standard Model leaves a lot of questions unanswered. One of the unsolved problems is understanding the origin of parity violation in low-energy particle physics. In the Standard Model the parity violation is introduced "by hand" in the sense that the Lagrangian of the theory is constructed in a way that it violates parity because only the left-handed components of the fermions are subjected to the gauge interactions. One can have a different approach assuming that the dynamics is intrinsically left-right symmetric, the asymmetry observed in nature (like in β-decay and μ-decay, etc.) arising from the vacuum being non-invariant under parity symmetry. Within the framework of gauge theories this idea has found its realization in the $SU(2)_L \otimes SU(2)_R \otimes U(1)_{B-L}$ models [2] constructed in 1973–1974. An important characteristic of those models is that at low energies they reproduce all the features of the $SU(2)_L \otimes U(1)_Y$ model, and as we move higher in energies new effects associated

with parity invariance of the Lagrangian (such as a second neutral Z-boson, right-handed charged currents, right-handed neutrino) are supposed to appear.

Another concept concerning the weak interactions that finds its place naturally in a left-right symmetric model rather than the Standard Model is the neutrino mass. Recent results in solar and atmospheric neutrino oscillation experiments at Sudbury (SNO) [3,4] and Super-Kamiokande [5,6] provide strong evidence of non-vanishing masses for the neutrinos, ruling out non-standard solutions for the solar neutrino anomaly. There exist also astrophysical considerations [7] having to do with the missing mass of the universe, galactic clusters and galactic formation, which are easily understood if the neutrino has a non-vanishing mass in the eV range. The left-right symmetric models provide a natural framework to understand the existence of neutrinos with $m_\nu \neq 0$ in this range.

The lack of any physical meaning of the $U(1)$ generator in the conventional theory is yet another deficiency eliminated by the left-right symmetric models. In the latter, the $U(1)$ generator becomes the $B-L$ quantum number [8] and then all the weak interaction symmetry generators have physical meaning. As if suggesting a deeper symmetry structure in the $SU(2)_L \otimes U(1)_Y$ model the only anomaly-free quantum number left ungauged is $B-L$, and once $B-L$ is included as a gauge generator the weak group becomes $SU(2)_L \otimes SU(2)_R \otimes U(1)_{B-L}$ and the electric charge is given by

$$Q = I_{L3} + I_{R3} + \frac{B-L}{2} \ . \tag{1.1}$$

One can comment also on the status of CP-violation in gauge theories. It is interesting that in the standard $SU(2)_L \otimes U(1)_Y$ model, three generations are required to have non-trivial CP-violation and all CP-violations are parameterized by only one phase, δ_{KM}, the Kobayashi-Maskawa phase [9]. But the model provides no hint as to why the observed CP-violation has milliweak strength. The left-right symmetric models provide a more appealing alternative [10], where the smallness of CP-violation is related to the suppression of $V+A$ currents, i.e.,

$$\eta_{+-} \simeq \left(\frac{M_{W_L}}{M_{W_R}}\right)^2 \sin\delta \ , \tag{1.2}$$

where the coefficients η_{ij} are defined in the K^0 decays [11] as

$$\eta_{ij} = \frac{\langle \pi_i \pi_j | H_{wk} | K_L^0 \rangle}{\langle \pi_i \pi_j | H | K_S^0 \rangle} \ , \tag{1.3}$$

and $i, j = (+, -)$ or $(0, 0)$. If both parity and CP-violations owe their origin to spontaneous breakdown of gauge symmetries, Eq. (1.3) can be proved [12] for three generations and becomes valid regardless of the contribution of the Higgs sectors.

After outlining all these general reasons for the interest in left-right symmetric models, in the present chapter we will provide a closer insight in their structure, particularly focusing our attention to realistic vacuum expectation value scenarios. We will see that in such scenarios family lepton number violating processes can occur at a level close to their present experimental limit.

1.1 Fermion content of the theory

Choosing $SU(2)_L \otimes SU(2)_R \otimes U(1)_{B-L}$ as the gauge group for the left-right symmetric model of the weak interaction, we can define the lepton and quark multiplets as

$$Q'_i \equiv \begin{pmatrix} u'_i \\ d'_i \end{pmatrix} \; ; \quad L'_j \equiv \begin{pmatrix} \nu'_{l'_j} \\ l'_j, \end{pmatrix} \; , \tag{1.4}$$

where u'_i, d'_i are the u- and d-type quark flavors corresponding to the i-th generation ($u_i = u, c, t$; $d_i = d, s, b$), l'_j and $\nu'_{l'_j}$ being the negatively charged lepton and its corresponding neutrino of the j-th generation.

With this definition one can make the following assignments to the representations of the gauge group

$$\begin{aligned} Q'_L &: (\frac{1}{2}, 0, \frac{1}{3}) \; , \quad Q'_R : (0, \frac{1}{2}, \frac{1}{3}) \; , \\ L'_L &: (\frac{1}{2}, 0, -1) \; , \quad L'_R : (0, \frac{1}{2}, -1) \; , \end{aligned} \tag{1.5}$$

where the $U(1)$ generator corresponds to the $B - L$ quantum numbers of the multiplet. The formula for the electric charge then reads [8]

$$Q = I_{L3} + I_{R3} + \frac{B - L}{2} \; . \tag{1.6}$$

1.2 Gauge bosons of the theory

The gauge fields are introduced through the covariant derivative

$$D_\mu = \partial_\mu - ig_L W^a_{L\mu} T^a_L - ig_R W^a_{R\mu} T^a_R - ig' B_\mu S \ , \tag{1.7}$$

where T_L, T_R and S are the generators of the $SU(2)_L$, $SU(2)_R$ and $U(1)_{B-L}$ gauge groups, respectively.

This actually means that in addition to the three "left-handed" gauge bosons of the weak interaction present in the Standard Model there will be three additional "right-handed" gauge bosons corresponding to the new $SU(2)_R$ group. As the starting point for the model was the initially unbroken left-right symmetry, one must require equal strength for the left- and right-handed couplings,

$$g_L = g_R = g_w (= g) \ . \tag{1.8}$$

1.3 Higgs content of the theory

The Higgs multiplets of the minimal model are dictated by the intuitive dynamical requirement that they should be bilinear in the basic fermionic multiplets [13,14]. This leads to the scalar fields

$$\Phi : (\frac{1}{2}, \frac{1}{2}^*, 0) \ ; \quad \Delta_L : (1, 0, 2) \ ; \quad \Delta_R : (0, 1, 2) \ , \tag{1.9}$$

where the $SU(2)_L$, $SU(2)_R$ and $B - L$ quantum numbers are indicated in parentheses. It is convenient to represent these fields as 2×2 matrices

$$\Phi = \begin{pmatrix} \phi_1^0 & \phi_1^+ \\ \phi_2^- & \phi_2^0 \end{pmatrix} \ , \tag{1.10}$$

$$\Delta_L = \begin{pmatrix} \frac{\delta_L^+}{\sqrt{2}} & \delta_L^{++} \\ \delta_L^0 & \frac{-\delta_L^+}{\sqrt{2}} \end{pmatrix} \ , \tag{1.11}$$

$$\Delta_R = \begin{pmatrix} \frac{\delta_R^+}{\sqrt{2}} & \delta_R^{++} \\ \delta_R^0 & \frac{-\delta_R^+}{\sqrt{2}} \end{pmatrix} \ . \tag{1.12}$$

In order to work with correctly normalized fields, the neutral Higgs field ϕ^0 should be written in terms of correctly normalized real and imaginary components as

$$\phi^0 = \frac{1}{\sqrt{2}}(\phi^{0r} + \phi^{0i}) \ . \tag{1.13}$$

The scalar fields will transform according to the relation

$$\begin{array}{rclcrcl} \Phi & \longrightarrow & U_L \Phi U_R^\dagger & , & \tilde{\Phi} & \longrightarrow & U_L \tilde{\Phi} U_R^\dagger \ , \\ \Delta_L & \longrightarrow & U_L \Delta_L U_L^\dagger & , & \Delta_L^\dagger & \longrightarrow & U_L \Delta_L^\dagger U_L^\dagger \ , \\ \Delta_R & \longrightarrow & U_R \Delta_R U_R^\dagger & , & \Delta_R^\dagger & \longrightarrow & U_R \Delta_R^\dagger U_R^\dagger \ , \end{array} \tag{1.14}$$

where $U_{L,R}$ are the general $SU(2)_L$ and $SU(2)_R$ unitary transformations, and $\tilde{\Phi} \equiv \tau_2 \Phi^* \tau_2$, that is

$$\tilde{\Phi} = \begin{pmatrix} \phi_2^{0*} & -\phi_2^+ \\ -\phi_1^- & \phi_1^{0*} \end{pmatrix} \ . \tag{1.15}$$

.

1.4 The Higgs potential

According to the present approach, the scalar field potential must satisfy the left-right symmetry, which requires the potential to be invariant under the transformation

$$\Delta_R \longleftrightarrow \Delta_L \ , \quad \Phi \longleftrightarrow \Phi^\dagger \ . \tag{1.16}$$

The most general scalar field potential can not have any trilinear terms. That is because the Δ_L and Δ_R triplets have nonzero $B-L$ quantum numbers, so these must always appear in the quadratic combinations $\Delta_L^\dagger \Delta_L$, $\Delta_R^\dagger \Delta_R$, $\Delta_L^\dagger \Delta_R$ or $\Delta_R^\dagger \Delta_L$. But one can not combine these quadratic expressions with a single bidoublet Φ field in a way to form a $SU(2)_L$ or $SU(2)_R$ singlet. Analogously, one can not combine three bidoublets to form a singlet. The most general scalar field potential will take then the form

$$\begin{aligned} V \ = \ & -\sum_{i,j=1}^{2} \mu_{ij}^2 \mathrm{Tr}\Phi_i^\dagger \Phi_j + \sum_{i,j,k,l=1}^{2} \lambda_{ijkl} \mathrm{Tr}(\Phi_i^\dagger \Phi_j) \mathrm{Tr}(\Phi_k^\dagger \Phi_l) \\ & + \sum_{i,j,k,l=1}^{2} \lambda'_{ijkl} \mathrm{Tr}\Phi_i^\dagger \Phi_j \Phi_k^\dagger \Phi_l - \mu_2^2 \mathrm{Tr}(\Delta_L^\dagger \Delta_L + \Delta_R^\dagger \Delta_R) \end{aligned}$$

$$
\begin{aligned}
&+\rho_1[(\mathrm{Tr}\Delta_L^\dagger\Delta_L)^2+(\mathrm{Tr}\Delta_R^\dagger\Delta_R)^2] \\
&+\rho_2(\mathrm{Tr}\Delta_L^\dagger\Delta_L\Delta_L^\dagger\Delta_L+\mathrm{Tr}\Delta_R^\dagger\Delta_R\Delta_R^\dagger\Delta_R)+\rho_3(\mathrm{Tr}\Delta_L^\dagger\Delta_L)(\mathrm{Tr}\Delta_R^\dagger\Delta_R) \\
&+\rho_4(\mathrm{Tr}\Delta_L\Delta_L\mathrm{Tr}\Delta_R^\dagger\Delta_R^\dagger+\mathrm{Tr}\Delta_L^\dagger\Delta_L^\dagger\mathrm{Tr}\Delta_R\Delta_R) \\
&+\sum_{i,j=1}^{2}\alpha_{ij}\mathrm{Tr}\Phi_i^\dagger\Phi_j(\mathrm{Tr}\Delta_L^\dagger\Delta_L+\mathrm{Tr}\Delta_R^\dagger\Delta_R) \\
&+\sum_{i,j=1}^{2}\beta_{ij}(\mathrm{Tr}\Delta_L^\dagger\Phi_i\Phi_j^\dagger\Delta_L+\mathrm{Tr}\Delta_R^\dagger\Phi_i^\dagger\Phi_j)\Delta_R \\
&+\sum_{i,j=1}^{2}\gamma_{ij}\mathrm{Tr}\Delta_L^\dagger\Phi_i\Delta_R\Phi_j^\dagger\ , \qquad (1.17)
\end{aligned}
$$

where $\Phi_1\equiv\Phi$ and $\Phi_2\equiv\tilde{\Phi}$. In order to satisfy the required symmetry transformations, the following constraints are imposed on the Higgs-particle couplings (some of them being equivalent to conditions for hermicity of the potential):

$$
\begin{aligned}
\mu_{ij} &= \mu_{ji}\ ,\quad \lambda_{1212}=\lambda_{2121}\ ,\quad \lambda_{iijk}=\lambda_{iikj} \\
\lambda_{ijkk} &= \lambda_{jikk}\ ,\quad \lambda'_{ijkl}=\lambda'_{lijk}=\lambda'_{klij}=\lambda'_{jkli}\ , \\
\alpha_{ij} &= \alpha_{ji}\ ,\quad \beta_{ij}=\beta_{ji}\ ,\quad \gamma_{ij}=\gamma_{ji}\ . \qquad (1.18)
\end{aligned}
$$

As one can immediately see, there are combinations proportional to $\mathrm{Tr}\Delta_L^\dagger\Phi_i\Delta_R\Phi_j^\dagger$ which are in general allowed by the left-right symmetry. However, in order to derive realistic scenarios for the symmetry breaking, one should eliminate such terms. To achieve this, we can impose invariance under an additional discrete symmetry

$$\Delta_L\longrightarrow\Delta_L\ ,\quad \Delta_R\longrightarrow-\Delta_R\ . \qquad (1.19)$$

Another important observation is that we should eliminate terms in the potential of the form

$$\mathrm{Tr}(\tilde{\Phi}^\dagger\Phi)+\mathrm{Tr}(\Phi^\dagger\tilde{\Phi})\ , \qquad (1.20)$$

in order to avoid problems with flavor changing neutral currents in phenomenologically natural scenarios. This can be performed if we require invariance under the additional discrete symmetry

$$\Phi\longrightarrow i\Phi\ . \qquad (1.21)$$

Taking into account all these requirements, we can write the most general form of the scalar Higgs potential [15]

$$V = V_\phi + V_\Delta + V_{\phi\Delta} \ , \tag{1.22}$$

where

$$\begin{aligned} V_\phi &= -\mu_1^2 \mathrm{Tr}\Phi^\dagger\Phi + \lambda_1(\mathrm{Tr}\Phi^\dagger\Phi)^2 + \lambda_2 \mathrm{Tr}\Phi^\dagger\Phi\Phi^\dagger\Phi \\ &\quad + \frac{1}{2}\lambda_3(\mathrm{Tr}\Phi^\dagger\tilde{\Phi} + \mathrm{Tr}\tilde{\Phi}^\dagger\Phi)^2 + \frac{1}{2}\lambda_4(\mathrm{Tr}\Phi^\dagger\tilde{\Phi} - \mathrm{Tr}\tilde{\Phi}^\dagger\Phi)^2 \\ &\quad + \lambda_5 \mathrm{Tr}\Phi^\dagger\Phi\tilde{\Phi}^\dagger\tilde{\Phi} + \frac{1}{2}\lambda_6(\mathrm{Tr}\Phi^\dagger\tilde{\Phi}\Phi^\dagger\tilde{\Phi} + \mathrm{Tr}\tilde{\Phi}^\dagger\Phi\tilde{\Phi}^\dagger\Phi) \ , \end{aligned} \tag{1.23}$$

$$\begin{aligned} V_\Delta &= \rho_1[(\mathrm{Tr}\Delta_L^\dagger\Delta_L)^2 + (\mathrm{Tr}\Delta_R^\dagger\Delta_R)^2] \\ &\quad + \rho_2(\mathrm{Tr}\Delta_L^\dagger\Delta_L\Delta_L^\dagger\Delta_L + \mathrm{Tr}\Delta_R^\dagger\Delta_R\Delta_R^\dagger\Delta_R) \\ &\quad + \rho_3(\mathrm{Tr}\Delta_L^\dagger\Delta_L)(\mathrm{Tr}\Delta_R^\dagger\Delta_R) \\ &\quad + \rho_4(\mathrm{Tr}\Delta_L\Delta_L\mathrm{Tr}\Delta_R^\dagger\Delta_R^\dagger + \mathrm{Tr}\Delta_L^\dagger\Delta_L^\dagger\mathrm{Tr}\Delta_R\Delta_R) \ , \end{aligned} \tag{1.24}$$

$$\begin{aligned} V_{\phi\Delta} &= \alpha_1 \mathrm{Tr}\Phi^\dagger\Phi(\mathrm{Tr}\Delta_L^\dagger\Delta_L + \mathrm{Tr}\Delta_R^\dagger\Delta_R) \\ &\quad + \alpha_2(\mathrm{Tr}\Delta_L^\dagger\Phi\Phi^\dagger\Delta_L + \mathrm{Tr}\Delta_R^\dagger\Phi^\dagger\Phi\Delta_R) \\ &\quad + \alpha_2'(\mathrm{Tr}\Delta_L^\dagger\tilde{\Phi}\tilde{\Phi}^\dagger\Delta_L + \mathrm{Tr}\Delta_R^\dagger\tilde{\Phi}^\dagger\tilde{\Phi}\Delta_R) \ . \end{aligned} \tag{1.25}$$

In our investigations we can safely consider that the scalar potential conserves CP and take all occurring parameters to be real.

1.5 The pattern of symmetry breaking

Since we assume the weak interaction symmetry to be $SU(2)_L \otimes SU(2)_R \otimes U(1)_{B-L} \otimes P$, we can break it down to the $SU(2)_L \otimes U(1)_L$ model in two stages [16]:

$$\begin{aligned} SU(2)_L \otimes SU(2)_R \otimes U(1)_{B-L} \otimes P &\overset{M_P}{\to} SU(2)_L \otimes SU(2)_R \otimes U(1)_{B-L} \ , \\ SU(2)_L \otimes SU(2)_R \otimes U(1)_{B-L} &\overset{M_{W_R}}{\to} SU(2)_L \otimes U(1)_L \overset{M_{W_L}}{\to} U(1)_{em} \ . \end{aligned}$$

At the first stage only the parity symmetry is broken and weak gauge symmetry is unbroken, leaving the W_L and W_R massless, their masses arise at the subsequent stages of symmetry breaking. The parity breaking at the first stage would manifest itself as different gauge couplings $g_L \neq g_R$ at $\mu \gtrsim M_{W_R}$. Often the choice of Higgs multiplets breaks both parity and

$SU(2)_R$ at the same scale. In what follows we will assume this happening, *i.e.* $M_P = M_{W_R}$, which happens with the minimal choice of the Higgs multiplets in Sec. 1.3.

The original parity-conserving $SU(2)_L \otimes SU(2)_R \otimes U(1)_{B-L}$ symmetry of the theory is spontaneously broken by the vacuum expectation values of the Higgs fields. The most general form of v.e.v. of these fields consistent with electromagnetic invariance given by the gauge group $U(1)$ is

$$\langle \Delta_L \rangle = \begin{pmatrix} 0 & 0 \\ \frac{v_L}{\sqrt{2}} & 0 \end{pmatrix} , \tag{1.26}$$

$$\langle \Delta_R \rangle = \begin{pmatrix} 0 & 0 \\ \frac{v_R}{\sqrt{2}} & 0 \end{pmatrix} , \tag{1.27}$$

$$\langle \Phi \rangle = \begin{pmatrix} \frac{\kappa_1}{\sqrt{2}} & 0 \\ 0 & \frac{\kappa_2}{\sqrt{2}} \end{pmatrix} , \tag{1.28}$$

$$\langle \tilde{\Phi} \rangle = \begin{pmatrix} \frac{\kappa_2}{\sqrt{2}} & 0 \\ 0 & \frac{\kappa_1}{\sqrt{2}} \end{pmatrix} . \tag{1.29}$$

The parameters v_L, v_R, κ_1 and κ_2 above can be chosen to be real and non-negative. This means that only the real parts of the neutral fields can acquire vacuum expectation values and we can equivalently write the previous relations as

$$\langle \delta_L^0 \rangle = \frac{1}{\sqrt{2}} \langle \delta_L^{0r} \rangle = \frac{v_L}{\sqrt{2}} , \tag{1.30}$$

$$\langle \delta_R^0 \rangle = \frac{1}{\sqrt{2}} \langle \delta_R^{0r} \rangle = \frac{v_R}{\sqrt{2}} , \tag{1.31}$$

$$\langle \phi_1^0 \rangle = \frac{1}{\sqrt{2}} \langle \phi_1^{0r} \rangle = \frac{\kappa_1}{\sqrt{2}} , \tag{1.32}$$

$$\langle \phi_2^0 \rangle = \frac{1}{\sqrt{2}} \langle \phi_2^{0r} \rangle = \frac{\kappa_2}{\sqrt{2}} . \tag{1.33}$$

There are certain relationships between the parameters in the Higgs potential and the vacuum expectation values of the neutral fields. An important source for such correlations is the requirement that the scalar potential must have a minimum when evaluated in the vacuum state, where the neutral fields possess their vacuum expectation values. Necessary

conditions for this are the vanishing partial derivatives

$$\frac{\partial V}{\partial v_L} = \frac{\partial V}{\partial v_R} = \frac{\partial V}{\partial \kappa_1} = \frac{\partial V}{\partial \kappa_2} = 0 \ , \tag{1.34}$$

where the derivatives are evaluated in the vacuum state.

In order to illustrate this, we give a few details in what follows. The scalar potential evaluated in the vacuum state has the value

$$\begin{aligned} V_{vacuum} \ = \ & -\frac{1}{2}\mu_1^2(\kappa_1^2+\kappa_2^2) - \frac{1}{2}\mu_2^2(v_L^2+v_R^2) + \frac{1}{4}\lambda_1(\kappa_1^2+\kappa_2^2)^2 \\ & + \frac{1}{4}\lambda_2(\kappa_1^4+\kappa_2^4) + \frac{1}{2}(4\lambda_3+\lambda_5+\lambda_6)\kappa_1^2\kappa_2^2 \\ & + \frac{1}{4}(\rho_1+\rho_2)(v_L^2+v_R^2) + \frac{1}{4}\rho_3 v_L^2 v_R^2 \\ & + \frac{1}{4}[\alpha_1(\kappa_1^2+\kappa_2^2) + \alpha_2\kappa_2^2 + \alpha_2'\kappa_1^2](v_L^2+v_R^2) \ . \end{aligned} \tag{1.35}$$

Taking the derivative with respect to $v_{L,R}$ and subtracting the two resulting equations we get the condition

$$\rho_{dif}(v_R^2 - v_L^2) = 0 \ , \tag{1.36}$$

where ρ_{dif} denotes the combination

$$\rho_{dif} \equiv \rho_3 - 2(\rho_1+\rho_2) \ . \tag{1.37}$$

Using the same strategy considering the derivatives with respect to $\kappa_{1,2}$ we are led to

$$\Sigma\lambda(\kappa_1^2 - \kappa_2^2) = \Delta\alpha(v_L^2+v_R^2) \ , \tag{1.38}$$

where we have defined

$$\Sigma\lambda \equiv \lambda_2 - (4\lambda_3+\lambda_5+\lambda_6) \ ; \quad \Delta\alpha \equiv \frac{\alpha_2 - \alpha_2'}{2} \ . \tag{1.39}$$

Above we considered all the parameters v_L, v_R, κ_1 and κ_2 non-vanishing. A short glimpse at the expression of the potential in (1.35) convinces us that the necessary minimization condition is satisfied alternatively when any of the before-mentioned parameters vanishes.

Actually, vanishing parameters are somewhat more preferred in what we should call "realistic" symmetry breaking scenarios. This choice could eliminate some of the constraints imposed on the scalar field couplings and the vacuum expectation values, escaping

the necessity of highly correlated values, which is a more natural behavior for a model constructed on fairly general principles.

The different vacuum expectation value scenarios will not be discussed here, but we can make some general comments. First of all, it appears natural to have a non-vanishing value for v_R, because this value sets the scale for the right-handed weak interactions which restore the left-right symmetry. In a different line of reasoning, without restricting generality we can alway suppose $\kappa_1 \geq \kappa_2$, however with both κ_1 and κ_2 nonzero the light neutral Higgs boson will have strong FCNC coupling and its existence is phenomenologically not allowed.

These remarks lead us to devote our further investigations to the situation when $v_R, \kappa_1 \neq 0$, $\kappa_2 = 0$. It is preferred that we also have $v_L = 0$, eliminating in such way one more correlation among the coupling constants, however we should point out that the phenomenology of the model is more realistic when the coupling constants are approximately satisfying the before-mentioned relation. In other words, non-vanishing v_L requires $\rho_{dif} = 0$ in (1.36), while $v_L = 0$ offers the best results provided ρ_{dif} is small.

1.6 Gauge boson masses

The interaction between the Higgs fields and the gauge bosons originates in the Lagrangian

$$\mathcal{L}_H = \mathrm{Tr}(D_\mu \Phi)^\dagger (D^\mu \Phi) + \mathrm{Tr}(D_\mu \Delta_L)^\dagger (D^\mu \Delta_L) + \mathrm{Tr}(D_\mu \Delta_R)^\dagger (D^\mu \Delta_R) \ , \tag{1.40}$$

where the covariant derivatives for the different Higgs multiplets are given by the expressions

$$D_\mu \Phi = \partial_\mu \Phi + \frac{1}{2} ig \left(\vec{\tau} \vec{W}_{L\mu} \Phi - \Phi \vec{\tau} \vec{W}_{R\mu} \right) + ig' B_\mu S \Phi \ , \tag{1.41}$$

$$D_\mu \Delta_L = \partial_\mu \Delta_L + \frac{1}{2} ig \left(\vec{\tau} \vec{W}_{L\mu} \Delta_L - \Delta_L \vec{\tau} \vec{W}_{L\mu} \right) + ig' B_\mu S \Delta_L \ , \tag{1.42}$$

$$D_\mu \Delta_R = \partial_\mu \Delta_R + \frac{1}{2} ig \left(\vec{\tau} \vec{W}_{R\mu} \Delta_R - \Delta_R \vec{\tau} \vec{W}_{R\mu} \right) + ig' B_\mu S \Delta_R \ , \tag{1.43}$$

$\vec{\tau}$ being the usual 2×2 Pauli matrices.

During the symmetry breaking, out of the 20 real degrees of freedom present in the scalar sector, 6 will be absorbed in giving mass to the gauge bosons of the theory, the

charged $W_L^{\pm}$ and $W_R^{\pm}$ and the neutral Z_1 and Z_2. The photon field A will remain massless, as expected.

1.6.1 Charged sector

The mass term for the charged gauge bosons arises from the following interactions with the scalar fields:

$$\Phi : \frac{1}{2}g^2 \times \left[\Phi^\dagger \begin{pmatrix} 0 & W_L^{+\mu} \\ W_L^{-\mu} & 0 \end{pmatrix} - \begin{pmatrix} 0 & W_R^{+\mu} \\ W_R^{-\mu} & 0 \end{pmatrix} \Phi^\dagger\right] \times \left[\begin{pmatrix} 0 & W_{L\mu}^{-} \\ W_{L\mu}^{+} & 0 \end{pmatrix} \Phi - \Phi \begin{pmatrix} 0 & W_{R\mu}^{-} \\ W_{R\mu}^{+} & 0 \end{pmatrix}\right] , \tag{1.44}$$

$$\Delta_L : \frac{1}{2}g^2 \times \left[\Delta_L^\dagger \begin{pmatrix} 0 & W_L^{+\mu} \\ W_L^{-\mu} & 0 \end{pmatrix} - \begin{pmatrix} 0 & W_L^{+\mu} \\ W_L^{-\mu} & 0 \end{pmatrix} \Delta_L^\dagger\right] \times \left[\begin{pmatrix} 0 & W_{L\mu}^{-} \\ W_{L\mu}^{+} & 0 \end{pmatrix} \Delta_L - \Delta_L \begin{pmatrix} 0 & W_{L\mu}^{-} \\ W_{L\mu}^{+} & 0 \end{pmatrix}\right] , \tag{1.45}$$

$$\Delta_R : \frac{1}{2}g^2 \times \left[\Delta_R^\dagger \begin{pmatrix} 0 & W_R^{+\mu} \\ W_R^{-\mu} & 0 \end{pmatrix} - \begin{pmatrix} 0 & W_R^{+\mu} \\ W_R^{-\mu} & 0 \end{pmatrix} \Delta_R^\dagger\right] \times \left[\begin{pmatrix} 0 & W_{R\mu}^{-} \\ W_{R\mu}^{+} & 0 \end{pmatrix} \Delta_R - \Delta_R \begin{pmatrix} 0 & W_{R\mu}^{-} \\ W_{R\mu}^{+} & 0 \end{pmatrix}\right] . \tag{1.46}$$

In the above expressions we have denoted

$$W_{L,R}^{+} = \frac{W_{L,R}^1 - iW_{L,R}^2}{\sqrt{2}} \; ; \quad W_{L,R}^{-} = \frac{W_{L,R}^1 + iW_{L,R}^2}{\sqrt{2}} \; . \tag{1.47}$$

The actual mass terms in the Lagrangian arise from the non-vanishing vacuum expectation values (1.26, 1.27, 1.28), and for the charged gauge bosons they take the form

$$\begin{aligned} -\mathcal{L}_{mass}^W &= \frac{1}{4}g^2(v_L^2 + \frac{\kappa_1^2+\kappa_2^2}{2})W_L^{+\mu}W_{L\mu}^{+} + \frac{1}{4}g^2(v_R^2 + \frac{\kappa_1^2+\kappa_2^2}{2})W_R^{+\mu}W_{R\mu}^{+} \\ &\quad -\frac{1}{4}g^2\kappa_1\kappa_2(W_L^{+\mu}W_{R\mu}^{+} + W_R^{+\mu}W_{L\mu}^{+}) + H.c. \; , \end{aligned} \tag{1.48}$$

or in a matrix notation

$$-\mathcal{L}_{mass}^W = \frac{1}{2}g^2 \left(W_L^{+\mu}, W_R^{+\mu}\right) \mathcal{M}_W \begin{pmatrix} W_{L\mu}^{+} \\ W_{R\mu}^{+} \end{pmatrix} + H.c. \; , \tag{1.49}$$

with the charged gauge boson mass matrix

$$\mathcal{M}_W = \frac{1}{2}\begin{pmatrix} v_L^2 + \frac{\kappa_1^2+\kappa_2^2}{2} & -\kappa_1\kappa_2 \\ -\kappa_1\kappa_2 & v_R^2 + \frac{\kappa_1^2+\kappa_2^2}{2} \end{pmatrix} . \tag{1.50}$$

The mass eigenstates of the gauge bosons, W_1^+ and W_2^+ can be obtained by applying a 2-dimensional rotation on the initial weak eigenstates

$$\begin{pmatrix} W_{1\mu}^+ \\ W_{2\mu}^+ \end{pmatrix} = \begin{pmatrix} \cos\xi & \sin\xi \\ -\sin\xi & \cos\xi \end{pmatrix} \begin{pmatrix} W_{L\mu}^+ \\ W_{R\mu}^+ \end{pmatrix} . \tag{1.51}$$

One can find the corresponding angle ξ for this rotation demanding that the mass matrix of the new fields,

$$\hat{\mathcal{M}}_W = \begin{pmatrix} \cos\xi & \sin\xi \\ -\sin\xi & \cos\xi \end{pmatrix} \mathcal{M}_W \begin{pmatrix} \cos\xi & -\sin\xi \\ \sin\xi & \cos\xi \end{pmatrix} , \tag{1.52}$$

be diagonal. We can easily see that this condition can be written as

$$\hat{\mathcal{M}}_{W12} = \hat{\mathcal{M}}_{W21} = 0 , \tag{1.53}$$

or explicitly

$$(v_R^2 - v_L^2)\sin\xi\cos\xi - \kappa_1\kappa_2(\cos^2\xi - \sin^2\xi) = 0 . \tag{1.54}$$

Finally we find that the mixing angle between the weak eigenstates in the physical fields is given by the relation

$$\tan 2\xi = \frac{2\kappa_1\kappa_2}{v_R^2 - v_L^2} . \tag{1.55}$$

At this point we should recall the discussion in Sec. 1.5 about realistic symmetry breaking scenarios. There it was established that a vanishing vacuum expectation value κ_2 is preferred in order to have an acceptable model. This condition actually translates into the fact that there is no mixing at all among the left- and right-handed charged gauge bosons, and in the following we should disregard the possibility of its occurrence. Eq. (1.55) also tells us that even in the most general model the mixing between the charged weak eigenstates is small enough not to be taken into account, a direct consequence of the natural scales for the different vacuum expectation values.

From the matrix relation in Eq. (1.52) we can finally read off the expression for the charged W_L and W_R bosons (having convinced ourselves that there can be only a very

small mixing among the left- and right-handed fields, we can use the same name as before for the weak eigenstates) in the general case

$$M_L^2 = \frac{1}{4}g^2(2v_L^2 + \kappa_1^2 + \kappa_2^2 - 2\kappa_1\kappa_2 \sin 2\xi) \ , \tag{1.56}$$

$$M_R^2 = \frac{1}{4}g^2(2v_R^2 + \kappa_1^2 + \kappa_2^2 - 2\kappa_1\kappa_2 \sin 2\xi) \ , \tag{1.57}$$

or, taking into account our interest in realistic models of the left-right symmetric interaction,

$$M_L^2 = \frac{1}{4}g^2(2v_L^2 + \kappa_1^2) \ , \tag{1.58}$$

$$M_R^2 = \frac{1}{4}g^2(2v_R^2 + \kappa_1^2) \ . \tag{1.59}$$

1.6.2 Neutral sector

The mass term for the neutral gauge bosons arises from the following interactions with the scalar fields:

$$\Phi : \frac{1}{4}g^2 \times \left[\Phi^\dagger \begin{pmatrix} W_L^{3\mu} & 0 \\ 0 & -W_L^{3\mu} \end{pmatrix} - \begin{pmatrix} W_R^{3\mu} & 0 \\ 0 & -W_R^{3\mu} \end{pmatrix} \Phi^\dagger\right] \times \left[\begin{pmatrix} W_{L\mu}^{3} & 0 \\ 0 & -W_{L\mu}^{3} \end{pmatrix} \Phi - \Phi \begin{pmatrix} W_{R\mu}^{3} & 0 \\ 0 & -W_{R\mu}^{3} \end{pmatrix}\right] \ , \tag{1.60}$$

$$\Delta_L : \frac{1}{4}g^2 \times \left\{\left[\Delta_L^\dagger \begin{pmatrix} W_L^{3\mu} & 0 \\ 0 & -W_L^{3\mu} \end{pmatrix} - \begin{pmatrix} W_L^{3\mu} & 0 \\ 0 & -W_L^{3\mu} \end{pmatrix} \Delta_L^\dagger\right] + 2\frac{g'}{g}\Delta_L^\dagger B^\mu\right\} \times \left\{\left[\begin{pmatrix} W_{L\mu}^{3} & 0 \\ 0 & -W_{L\mu}^{3} \end{pmatrix} \Delta_L - \Delta_L \begin{pmatrix} W_{L\mu}^{3} & 0 \\ 0 & -W_{L\mu}^{3} \end{pmatrix}\right] + 2\frac{g'}{g}\Delta_L B_\mu\right\} \ , \tag{1.61}$$

$$\Delta_R : \frac{1}{4}g^2 \times \left\{\left[\Delta_R^\dagger \begin{pmatrix} W_R^{3\mu} & 0 \\ 0 & -W_R^{3\mu} \end{pmatrix} - \begin{pmatrix} W_R^{3\mu} & 0 \\ 0 & -W_R^{3\mu} \end{pmatrix} \Delta_R^\dagger\right] + 2\frac{g'}{g}\Delta_R^\dagger B^\mu\right\} \times \left\{\left[\begin{pmatrix} W_{R\mu}^{3} & 0 \\ 0 & -W_{R\mu}^{3} \end{pmatrix} \Delta_R - \Delta_R \begin{pmatrix} W_{R\mu}^{3} & 0 \\ 0 & -W_{R\mu}^{3} \end{pmatrix}\right] + 2\frac{g'}{g}\Delta_R B_\mu\right\} \ . \tag{1.62}$$

Using the vacuum expectation values given in Eqs. (1.26–1.28), we obtain the following mass term for the neutral gauge bosons in the Lagrangian:

$$\begin{aligned} -\mathcal{L}^{Z}_{mass} &= \frac{1}{8}g^2(\kappa_1^2+\kappa_2^2+4v_L^2)W_L^{3\mu}W^3_{L\mu}+\frac{1}{8}g^2(\kappa_1^2+\kappa_2^2+4v_R^2)W_R^{3\mu}W^3_{R\mu}+ \\ &\frac{1}{2}g'^2(v_L^2+v_R^2)B^\mu B_\mu-\frac{1}{8}g^2(\kappa_1^2+\kappa_2^2)(W_L^{3\mu}W^3_{R\mu}+W_R^{3\mu}W^3_{L\mu}) \\ &-\frac{1}{2}gg'v_L^2(W_L^{3\mu}B_\mu+B^\mu W^3_{L\mu})-\frac{1}{2}gg'v_R^2(W_R^{3\mu}B_\mu+B^\mu W^3_{R\mu})\ , \end{aligned} \tag{1.63}$$

or in an equivalent matrix notation,

$$-\mathcal{L}^{Z}_{mass}=\frac{1}{2}g^2\left(W_L^{3\mu},W_R^{3\mu},B^\mu\right)\mathcal{M}_Z\begin{pmatrix}W^3_{L\mu}\\W^3_{R\mu}\\B_\mu\end{pmatrix}\ , \tag{1.64}$$

where the neutral boson mass matrix is

$$\mathcal{M}_Z=g^2\begin{pmatrix}\frac{\kappa_1^2+\kappa_2^2}{4}+v_L^2 & -\frac{\kappa_1^2+\kappa_2^2}{4} & -\frac{g'}{g}v_L^2\\ -\frac{\kappa_1^2+\kappa_2^2}{4} & \frac{\kappa_1^2+\kappa_2^2}{4}+v_R^2 & -\frac{g'}{g}v_L^2\\ -\frac{g'}{g}v_L^2 & -\frac{g'}{g}v_R^2 & \frac{g'^2}{g^2}(v_L^2+v_R^2)\end{pmatrix}\ . \tag{1.65}$$

The physical fields can be obtained by applying an orthogonal transformation to the initial neutral weak eigenstates

$$\begin{pmatrix}A^\mu\\Z_1^\mu\\Z_2^\mu\end{pmatrix}=U_Z\begin{pmatrix}W_L^{3\mu}\\W_R^{3\mu}\\B^\mu\end{pmatrix}\ , \tag{1.66}$$

where U_Z is a 3×3 orthogonal matrix to be determined.

Even before having the exact expression for the matrix U_Z we can make some preliminary remarks. First, the left-right symmetry which constrained the coupling constants g_L and g_R to be equal, imposes that W_L and W_R can be present in the photon field only in the linear combination W_L+W_R. This allows us to write the electromagnetic field as

$$A^\mu=\sin\theta_W(W_L^{3\mu}+W_R^{3\mu})+(\cos 2\theta_W)^{1/2}B^\mu\ . \tag{1.67}$$

Because A^μ couples to the electromagnetic current and the strength of this coupling is given by the electric charge, we immediately see that θ_W satisfies the same relation as the well-known Weinberg angle of the $SU(2)_L\otimes U(1)_Y$ model,

$$\sin\theta_W=\frac{e}{g}\ , \tag{1.68}$$

with e being the elementary electric charge.

We can write one more analogous relation,

$$(\cos 2\theta_W)^{1/2} = \frac{e}{g'} \ , \tag{1.69}$$

and finally arrive at the expression of the Weinberg angle in the left-right symmetric model,

$$\tan\theta_W = \frac{g'}{\sqrt{g^2+g'^2}} \ . \tag{1.70}$$

The second remark is that it is natural to suppose that the heavy neutral gauge boson Z_2 doesn't mix with the light gauge sector and in consequence it can be written as

$$Z_2^\mu = b_2 W_R^{3\mu} + c_2 B^\mu \ , \tag{1.71}$$

with b_2 and c_2 two real coefficients with $b_2^2 + c_2^2 = 1$.

The third remark is similar to the second one and consist in the requirement that the mass term of the light neutral gauge boson, written as

$$Z_1^\mu = a_1 W_L^{3\mu} + b_1 W_R^{3\mu} + c_1 B^\mu \ ; \qquad a_1^2 + b_1^2 + c_1^2 = 1 \ , \tag{1.72}$$

receives no contribution from the heavy mass scale v_R.

The orthogonality of the U_Z matrix then provides us with the corresponding values of the mixing coefficients a_1,b_1, c_1, b_2 and c_2, and we can list the expressions for the physical mass eigenstates in the neutral sector:

$$\begin{aligned} A^\mu &= \sin\theta_W (W_L^{3\mu} + W_R^{3\mu}) + (\cos 2\theta)^{1/2} B^\mu \ , \\ Z_1^\mu &= \cos\theta_W W_L^{3\mu} - \sin\theta_W \tan\theta_W W_R^{3\mu} - \tan\theta_W (\cos 2\theta_W)^{1/2} B^\mu \ , \\ Z_2^\mu &= \frac{(\cos 2\theta_W)^{1/2}}{\cos\theta_W} W_R^{3\mu} - \tan\theta_W B^\mu \ . \end{aligned} \tag{1.73}$$

One can immediately check that the above expression for the neutral gauge boson mixing matrix U_Z indeed provides the physical fields, keeps the photon field massless ($m_A = 0$) and assures for the massive bosons

$$M_{Z_1}^2 = \frac{1}{4}\frac{g^2}{\cos^2\theta_W}(\kappa_1^2 + \kappa_2^2 + 4v_L^2) \ , \tag{1.74}$$

$$M_{Z_2}^2 = \frac{1}{4} g^2 \sin^2\theta_W \tan^2\theta_W (\kappa_1^2 + \kappa_2^2) + g'^2 \tan^2\theta_W v_L + (g^2 + g'^2) v_R^2 \ . \tag{1.75}$$

In realistic models, with negligible W_L–W_R mixing, our final result for these masses can be written as

$$M_{Z_1}^2 = \frac{1}{4}\frac{g^2}{\cos^2\theta_W}(\kappa_1^2 + 4v_L^2) \ , \tag{1.76}$$

$$M_{Z_2}^2 \simeq (g^2 + g'^2)v_R^2 \ . \tag{1.77}$$

Comparing Eq. (1.58) and (1.76) one can see that the well-known prediction of the Standard Model at tree level $M_{W_L}^2 = M_{Z_1}^2 \cos^2\theta_W$ is preserved to the lowest order. It gets corrections of order v_L^2/κ_1^2, but these corrections will be small. Actually, writing the tree-level ρ_W parameter as

$$\rho_W = \frac{M_{W_L}^2}{\cos^2\theta_W M_{Z_1}^2} = \frac{\kappa_1^2 + 2v_L^2}{\kappa_1^2 + 4v_L^2} \ , \tag{1.78}$$

we can readily impose some experimental constraints, noting that $|1-\rho_W| \lesssim 0.01$, implying

$$v_L \lesssim 0.07\kappa_1 \ . \tag{1.79}$$

1.7 The Higgs spectrum

The spectrum of the Higgs bosons present in the theory can be studied starting from the general expression of the quartic potential (1.22), replacing the fields which develop vacuum expectation values with their corresponding shift from this value, namely

$$\delta_L^{0r} \longrightarrow \delta_L^{0r} + v_L \ , \tag{1.80}$$

$$\delta_R^{0r} \longrightarrow \delta_R^{0r} + v_R \ , \tag{1.81}$$

$$\phi_1^{0r} \longrightarrow \phi_1^{0r} + \kappa_1 \ , \tag{1.82}$$

$$\phi_2^{0r} \longrightarrow \phi_2^{0r} + \kappa_2 \ . \tag{1.83}$$

In the subsequent analysis we will dedicate ourselves to the phenomenologically realistic scenarios and will neglect terms of order v_L/v_R while retaining terms of relative order v_L/κ_1 and κ_1/v_R, considering an overall vanishing κ_2.

Since both v_R and κ_1 must be nonzero, we can give the nontrivial conditions from Eq. (1.34) resulting from the derivative conditions in these two variables. These two conditions can be written as

$$\mu_1^2 = (\lambda_\Sigma - \Sigma\lambda)\kappa_2^2 + \frac{1}{2}\alpha'_\Sigma(v_l^2 + v_R^2) + \lambda_\Sigma\kappa_1^2 \ , \tag{1.84}$$

for the κ_1 derivative and

$$\mu_2^2 = \frac{1}{2}(\rho_{dif} + 2\rho_\Sigma)v_L^2 + \rho_\Sigma v_R^2 + \frac{1}{2}(\alpha_\Sigma \kappa_2^2 + \alpha'_\Sigma \kappa_1^2) \ , \tag{1.85}$$

from the v_R derivative. In addition to Eq. (1.37) and (1.39) we used the following notations for the different parameter combinations:

$$\begin{aligned} \lambda_\Sigma &\equiv \lambda_1 + \lambda_2 \ , \\ \rho_\Sigma &\equiv \rho_1 + \rho_2 \ , \\ \alpha_\Sigma &\equiv \alpha_1 + \alpha_2 \ , \quad \alpha'_\Sigma \equiv \alpha_1 + \alpha'_2 \ . \end{aligned} \tag{1.86}$$

1.7.1 The neutral scalar fields

The mass term for the real parts of the neutral Higgs fields is characterized by the 4×4 mass matrix $\mathcal{M}_{0r}^2$ which can be explicitly written in a ϕ_1^{0r}-ϕ_2^{0r}-δ_R^{0r}-δ_L^{0r} basis as

$$\mathcal{M}_{0r}^2 = \begin{pmatrix} 2\kappa_1^2\lambda_\Sigma & 2\kappa_1\kappa_2(\lambda_\Sigma - \Sigma\lambda) & v_R\kappa_1\alpha'_\Sigma & v_L\kappa_1\alpha'_\Sigma \\ 2\kappa_1\kappa_2(\lambda_\Sigma - \Sigma\lambda) & 2\kappa_2^2\lambda_\Sigma + \Delta_{22} & v_R\kappa_2\alpha_\Sigma & v_L\kappa_2\alpha_\Sigma \\ v_R\kappa_1\alpha'_\Sigma & v_R\kappa_2\alpha_\Sigma & 2v_R^2\rho_\Sigma & v_L v_R(2\rho_\Sigma + \rho_{dif}) \\ v_L\kappa_1\alpha'_\Sigma & v_L\kappa_2\alpha_\Sigma & v_L v_R(2\rho_\Sigma + \rho_{dif}) & 2v_L^2\rho_\Sigma + \frac{1}{2}(v_R^2 - v_L^2)\rho_{dif} \end{pmatrix} \ , \tag{1.87}$$

where we defined

$$\Delta_{22} = \Delta\alpha(v_L^2 + v_R^2) - (\kappa_1^2 - \kappa_2^2)\Sigma\lambda \ . \tag{1.88}$$

Neglecting terms with relative order of v_L/v_R and setting $\kappa_2 = 0$, this matrix simplifies to

$$\mathcal{M}_{0r}^2 = \begin{pmatrix} 2\kappa_1^2\lambda_\Sigma & 0 & v_R\kappa_1\alpha'_\Sigma & 0 \\ 0 & \Delta\alpha v_R^2 - \kappa_1^2\Sigma\lambda & 0 & 0 \\ v_R\kappa_1\alpha'_\Sigma & 0 & 2v_R^2\rho_\Sigma & 0 \\ 0 & 0 & 0 & \frac{1}{2}v_R^2\rho_{dif} \end{pmatrix} \ . \tag{1.89}$$

In this approximation one can immediately see that ϕ_2^{0r} and δ_L^{0r} are pure mass eigenstates, with the corresponding masses

$$m^2_{\phi_2^{0r}} = \Delta\alpha v_R^2 - \kappa_1^2\Sigma\lambda \ , \tag{1.90}$$

$$m^2_{\delta_L^{0r}} = \frac{1}{2}\rho_{dif}v_R^2 \ . \tag{1.91}$$

The other two states mix together, yielding the mass eigenstates

$$\begin{aligned} h^0 &= \cos\alpha\phi_1^{0r} - \sin\alpha\delta_R^{0r} \ , \\ H^0 &= \sin\alpha\phi_2^{0r} + \cos\alpha\delta_R^{0r} \ , \end{aligned} \tag{1.92}$$

where the mixing angle α is given by the expression similar to that in Eq. (1.55),

$$\tan 2\alpha = \frac{v_R\kappa_1\alpha'_\Sigma}{v_R^2\rho_\Sigma - \kappa_1^2\lambda_\Sigma} \ . \tag{1.93}$$

For a very heavy right handed mass scale it is reasonable to consider $v_R\rho_\Sigma \gg \kappa_1\alpha'_\Sigma$ and then we arrive at the expressions for the masses which read

$$m^2_{H^0} = 2v_R\rho_\Sigma^2 - 2\kappa_1^2\lambda_\Sigma + \kappa_1^2\frac{\alpha'^2_\Sigma}{\rho_\Sigma} \ , \tag{1.94}$$

$$m^2_{h^0} = \kappa_1^2\left(2\lambda_\Sigma - \frac{\alpha'^2_\Sigma}{2\rho_\Sigma}\right) \ , \tag{1.95}$$

and the mixing angle α between ϕ_2^{0r} and δ_L^{0r} is small.

1.7.2 The neutral pseudo-scalar fields

For the imaginary part of the neutral Higgs fields the 4×4 mass matrix has a much more simplified form in the ϕ_1^{0i}-ϕ_2^{0i}-δ_R^{0i}-δ_L^{0i} basis, namely

$$\mathcal{M}^2_{0i} = \begin{pmatrix} 0 & 0 & 0 & 0 \\ 0 & \Delta\alpha(v_L^2+v_R^2) + \Sigma'\lambda\kappa_1^2 & 0 & 0 \\ 0 & 0 & 0 & 0 \\ 0 & 0 & 0 & \frac{1}{2}\rho_{dif}v_R^2 \end{pmatrix} \ , \tag{1.96}$$

where we defined the parameter

$$\Sigma'\lambda \equiv \lambda_5 - \lambda_2 - 4\lambda_4 - \lambda_6 \ . \tag{1.97}$$

The physical pseudo-scalar particles are pure ϕ_2^{0i} and δ_L^{0i} states with the corresponding masses (neglecting terms of order v_L/v_R)

$$m^2_{\phi_2^{0i}} = \Delta\alpha v_R^2 + \kappa_1^2\Sigma'\lambda \ , \tag{1.98}$$

$$m^2_{\delta_L^{0i}} = \frac{1}{2}\rho_{dif}v_R^2 \ . \tag{1.99}$$

The ϕ_1^{0i} and δ_R^{0i} fields combine in forming the two neutral Goldstone bosons absorbed by Z_1 and Z_2.

1.7.3 The singly charged scalar fields

The four singly charged Higgs fields mix together in the mass term through the following mixing matrix (given in the ϕ_1^+-ϕ_2^+-δ_R^+-δ_L^+ basis):

$$\mathcal{M}_+^2 = \begin{pmatrix} \Delta\alpha v_R^2 & 0 & \frac{\Delta\alpha}{\sqrt{2}} v_R\kappa_1 & 0 \\ 0 & \Delta\alpha v_L^2 & 0 & \frac{\Delta\alpha}{\sqrt{2}} v_L\kappa_1 \\ \frac{\Delta\alpha}{\sqrt{2}} v_R\kappa_1 & 0 & \frac{\Delta\alpha}{2}\kappa_1^2 & 0 \\ 0 & \frac{\Delta\alpha}{\sqrt{2}} v_L\kappa_1 & 0 & \frac{\rho_{dif}}{2}(v_R^2 - v_L^2) + \frac{\Delta\alpha}{2}\kappa_1^2 \end{pmatrix} . \tag{1.100}$$

One can immediately see that given $\kappa_2 = 0$, ϕ_1^+ mixes only with δ_R^+ and in the same manner ϕ_2^+ mixes only with δ_L^+. We should recall also the discussion in Sec. 1.5 where we have seen that realistic vacuum expectation value scenarios required $v_L = 0$ and ρ_{dif} adjustable, but preferably small or $v_L \neq 0$ and $\rho_{dif} = 0$. In the formulas listed below both of these possibilities are contained.

The mass matrix $\mathcal{M}_+^2$ has two vanishing eigenvalues, corresponding to the two charged Goldstone boson states absorbed by the W_L^+ and W_R^+. The simply charged physical Higgs fields will then be the orthogonal combinations

$$h^+ = \frac{\phi_1^+ + \frac{\kappa_1}{\sqrt{2}v_R}\delta_R^+}{\left(1 + \frac{\kappa_1^2}{2v_R^2}\right)^{1/2}} , \tag{1.101}$$

$$\tilde{\delta}_L^+ = \frac{\delta_L^+ + \frac{\sqrt{2}v_L}{\kappa_1}\phi_2^+}{\left(1 + \frac{2v_L^2}{\kappa_1^2}\right)^{1/2}} , \tag{1.102}$$

having the corresponding masses

$$m_{h^+}^2 = \Delta\alpha(v_R^2 + \frac{1}{2}\kappa_1^2) , \tag{1.103}$$

$$m_{\delta_L^+}^2 = \frac{1}{2}\rho_{dif} + \frac{1}{2}\Delta\alpha(\kappa_1^2 + 2v_L^2) . \tag{1.104}$$

1.7.4 The doubly charged scalar fields

Since there are only two doubly charged Higgs fields, their mass matrix will be 2×2 and will be expressed in the δ_R^{++}–δ_L^{++} basis as

$$\mathcal{M}_{++}^2 = \begin{pmatrix} -\rho_2 v_R^2 + \Delta\alpha\kappa_1^2 & 2\rho_4 v_L v_R \\ 2\rho_4 v_L v_R & -\rho_2 v_L^2 + \frac{1}{2}\rho_{dif} v_R^2 + \Delta\alpha\kappa_1^2 \end{pmatrix} . \tag{1.105}$$

Neglecting again terms of relative order v_L/v_R we can see that δ_R^{++} and δ_L^{++} are pure mass eigenstates with the corresponding masses

$$m_{\delta_R^{++}} = -\rho_2 v_R^2 + \Delta\alpha\kappa_1^2 , \tag{1.106}$$

$$m_{\delta_L^{++}} = \frac{1}{2}\rho_{dif} v_R^2 - \rho_2 v_L^2 + \Delta\alpha\kappa_1^2 . \tag{1.107}$$

A consequence is that for $v_L \neq 0$ the mass of δ_L^{++} does not receive any contribution from the heavy mass scale v_R, whereas for $v_L = 0$ it can only be light if ρ_{dif} is small.

1.8 The unphysical Goldstone bosons

Working in a general R_ξ gauge leads to the presence of unphysical particles in the theory, the Goldstone bosons. For our further investigations only the Goldstone bosons associated to the charged gauge bosons are of interest, so we will give only their expressions.

The scalar G_L^+ associated to W_L^+ turns out to be a pure Φ_2^+ state in the case $v_L = 0$. The situation of the G_R^+ associated to W_R^+ is a little bit more complex. In principle G_R^+ and the charged Higgs field h^+ will be given by a mixing between the weak eigenstates ϕ_1^+ and δ_R^+:

$$\begin{pmatrix} h^+ \\ G_R^+ \end{pmatrix} = \begin{pmatrix} c_\beta & s_\beta \\ -s_\beta & c_\beta \end{pmatrix} \begin{pmatrix} \phi_1^+ \\ \delta_R^+ \end{pmatrix} , \tag{1.108}$$

where the sine of the mixing angle is expressed via the different vacuum expectation values as

$$s_\beta = \frac{\kappa_1}{(\kappa_1^2 + 2v_R^2)^{1/2}} = \frac{M_L}{M_R} . \tag{1.109}$$

One can see that Eq. (1.101) is obtained from here also, and we can give the similar expression for G_R^+:

$$G_R^+ = \frac{\frac{\kappa_1}{\sqrt{2}v_R}\phi_1^+ - \delta_R^+}{\left(1+\frac{\kappa_1^2}{2v_R^2}\right)^{1/2}} \ . \tag{1.110}$$

1.9 Fermion masses

The Yukawa interaction of the lepton and quark fields has the expression

$$\begin{aligned} -\mathcal{L}_{\mathcal{Y}} &= h_1\bar{L}'_L\Phi L'_R + h_2\bar{L}'_L\tilde{\Phi}L'_R + h_3\bar{Q}'_L\Phi Q'_R + h_4\bar{Q}'_L\tilde{\Phi}Q'_R \\ &\quad + ih_5\left(L'^T_L C\tau_2\Delta_L L'_L + L'^T_R C\tau_2\Delta_R L'_R\right) + H.c. \ . \end{aligned} \tag{1.111}$$

In the above expression C is the charge conjugation matrix and τ_2 is the corresponding Pauli matrix

$$\tau_2 = \begin{pmatrix} 0 & -i \\ i & 0 \end{pmatrix} \ . \tag{1.112}$$

Only the neutrino fields in the leptonic doublets can develop a Majorana mass term. The expression of this mass term has the form

$$-\mathcal{L}^{\nu}_{Maj} = \sum_{i,j}^{n_G} h_{ij}\left(\bar{\nu'}^C_{Li}v_L\nu_{Lj} + \bar{\nu'}^C_{Ri}v_R\nu_{Rj}\right) \ . \tag{1.113}$$

An important observation is in order at this moment. In the framework of realistic vacuum expectation value scenarios $v_L = 0$, which means that only the right-handed neutrinos will develop Majorana mass. As we will see in the next chapter, such a pattern is preferred in order to have heavy neutrinos as light as 100 GeV in the theory.

1.10 Interactions of the Higgs scalars

In the previous sections it has been shown that the left-right symmetric model based on the $SU(2)_L \otimes SU(2)_R \otimes U(1)_{B-L}$ gauge group has a much more complex Higgs sector compared to the Standard Model. The presence of the supplementary scalars makes the description of different processes more involved, however their interactions are easily derived using the

properties of the model. In this section we will summarize these interactions, listing the corresponding terms from the Lagrangian. The Feynman rules can then be easily read off these expressions, and their diagrammatic representation will be provided in the Appendix.

1.10.1 The flavor-changing scalars $\phi_2^{0r,i}$

In contrast with the Standard Model, flavor-changing interactions are present in the theory already at tree level, through the neutral $\Phi_2^{0r,i}$ particles. Their coupling to the charged leptons is given by the Lagrangian

$$\begin{aligned}\mathcal{L}_{int}^{\phi_2^0,l} = & - \frac{g_w}{2M_L}\sum_{\alpha=1}^{2n_G}\phi_2^{0r}\bar{l}_1\left[B_{l_1\alpha}^L B_{l_2\alpha}^{R*} m_{n_\alpha}\mathrm{P}_R + B_{l_1\alpha}^R B_{l_2\alpha}^{L*} m_{n_\alpha}\mathrm{P}_L\right] l_2 \\ & - \frac{ig_w}{2M_L}\sum_{\alpha=1}^{2n_G}\phi_2^{0i}\bar{l}_1\left[B_{l_1\alpha}^L B_{l_2\alpha}^{R*} m_{n_\alpha}\mathrm{P}_R - B_{l_1\alpha}^R B_{l_2\alpha}^{L*} m_{n_\alpha}\mathrm{P}_L\right] l_2 \ , \end{aligned} \tag{1.114}$$

where B^L and B^R are the leptonic mixing matrices, to be discussed in more detail in Chapter 2, P_L and P_R being the left- and right-handed projectors.

The similar expression for quarks is obtained by introducing the corresponding V^L and V^R mixing matrices, which diagonalize the quark mass matrix and lead to the mass eigenstates.

The initial Lagrangian also leads to the observation that there is no $\phi_2^0 - W_L^+ - W_L^-$, respectively $\phi_2^0 - W_R^+ - W_R^-$ vertex in the theory. However, the coupling to charged gauge bosons with different chirality is possible, and it is given by

$$\mathcal{L}_{int}^{\phi_2^0 - W_L - W_R} = g_w M_L\left(\phi_2^{0r} W_{R\mu}^- W_L^{+\mu} + i\phi_2^{0i} W_{R\mu}^- W_L^{+\mu}\right) + H.c. \tag{1.115}$$

Following this result, there will exist vertices containing one or two Goldstone bosons:

$$\mathcal{L}_{int}^{\phi_2^0 - G_L - W_R} = \frac{ig_w}{\sqrt{2}} W_{R\mu}^-\left(\partial^\mu\phi_2^0 G_L^+ - \phi_2^0\partial^\mu G_L^+\right) + H.c. \ , \tag{1.116}$$

$$\mathcal{L}_{int}^{\phi_2^0 - W_L - G_R} = \frac{ig_w}{\sqrt{2}} s_\beta W_{L\mu}^-\left(\partial^\mu\phi_2^{0*} G_R^+ - \phi_2^{0*}\partial^\mu G_R^+\right) + H.c. \ , \tag{1.117}$$

$$\mathcal{L}_{int}^{\phi_2^0 - G_L - G_R} = \frac{g_w}{2M_R}\left(m_{\phi_2^{0r}}^2\phi_2^{0r} G_L^+ G_R^- + im_{\phi_2^{0i}}^2\phi_2^{0i} G_L^+ G_R^-\right) + H.c. \tag{1.118}$$

Also, from the underlying symmetry it follows that there will be no $\phi_2^0 - h^+ - W_R^-$ vertex, the corresponding coupling with the left-handed gauge sector reading as

$$\mathcal{L}_{int}^{\phi_2^0 - W_L - h} = \frac{ig_w}{\sqrt{2}} c_\beta\left(\phi_2^0\partial^\mu h^- W_{L\mu}^+ - \partial^\mu\phi_2^0 h^- W_{L\mu}^+\right) + H.c. \ , \tag{1.119}$$

$$\mathcal{L}_{int}^{\phi_2^0-G_L-h} = \frac{g_w}{2M_L}c_\beta\left[\left(m_h^2-m_{\phi_2^{0r}}^2\right)\phi_2^{0r}+i\left(m_h^2-m_{\phi_2^{0i}}^2\right)\phi_2^{0i}\right]G_L^+h^- + H.c.\ . \tag{1.120}$$

The vertex $\phi_2^0-h^+-h^-$ will vanish as well, and with this we exhausted the possible interactions of the flavor changing Higgs scalars which could present interest for our further investigations.

1.10.2 The charged Higgs scalars $h^\pm$

The vertices containing $h^\pm$ were partly described in the previous subsection. As we have no interest in our work in the neutral gauge boson couplings, these will be omitted. This means that the only supplementary interaction is that with the fermions. The Lagrangian describing the interaction with leptons has the expression

$$\mathcal{L}_{int}^h = \frac{g_w}{\sqrt{2}M_L}c_\beta h^-\bar{l}\sum_{\alpha,\beta=1}^{2n_G}\left[B_{l\alpha}^R m_l \mathrm{P}_R - B_{l\beta}^R\left(\delta_{\alpha\beta}-\frac{C_{\beta\alpha}^{R*}}{c_\beta^2}\right)m_{n_\beta}\mathrm{P}_L\right]n_\alpha + H.c.\ , \tag{1.121}$$

$C_{\alpha\beta}^R$ being the neutrino mixing matrix, to be introduced in the next chapter.

Chapter 2

Neutrino masses and mixing

Since their existence was postulated by Pauli [17], the neutrinos continued to be regarded by many as somewhat "mysterious" particles. The main reason for this was that until now the masses of these particles escaped experimental measurements. Although initially there were introduced as truly massless particles, the later point of view was that a relatively small mass for the three known neutrinos, the electron-neutrino (ν_e), the muon-neutrino (ν_μ) and the tau-neutrino (ν_τ) would be consistent with all experimental data. In the light of recent experimental results [3–6] one can safely conclude that this insight proved to be correct.

There was no a priori theoretical reason for the masslessness of the neutrinos. As neutral fermions, one should have expected that their mass would originate in the same way as for the other observed fermions (leptons and quarks). In the Standard Model of particle interaction however the neutrino masses vanished due to the fact that only the left-handed components of the different neutrino fields were given physical existence. In principle the same considerations assured the existence of parity violation in particle interactions.

In this chapter we will try to present some minimal differences compared to the Standard Model regarding the neutrino masses. All this attempt is justified by the belief that the Standard Model is not the ultimate description of the basic particle interactions, but merely an effective theory with its applicability limited to our present experimental boundaries in reaching higher energies in our experiments. As the present model accommodates astonishingly well most of the available experimental data, it is reasonable to expect that at

energies not much higher than the currently available ones, but reachable in the foreseeable future, the differences compared to the Standard Model will be small. This is the main reason for restricting ourselves only to minimal extensions of the present model.

Among the various scenarios describing the origin of neutrino masses, the "see-saw" mechanism, conceived within the framework of $SO(10)$ or left-right symmetric models turned out to be the most attractive [18]. If this mechanism is really the one chosen by nature, then heavy Majorana neutrinos, N, may manifest themselves in L-violating processes at high-energy ee [19–21], ep [22], and pp colliders [23–27], in possible lepton-flavor-violating decays of the Z [28] and Higgs particles (H) [29,30] or through universality-breaking effects in leptonic diagonal Z-boson decays [31]. Their existence may also influence [32–34] a number of electroweak oblique parameters given in [35–38] or specific Higgs observables considered recently [39,40]. Finally, there are many other places scanned by exhaustive combined analysis of charged-current-universality effects in leptonic π decays, neutral-current interactions in neutrino-nucleon scatterings, τ-polarization asymmetries, neutrino-counting experiments at the CERN Large Electron Positron Collider (LEP), etc. [41–45], in which Majorana neutrinos could also manifest their presence. Another possible solution of the neutrino-mass problem has been contemplated in the framework of heterotic superstring models [46–48] or certain scenarios of $SO(10)$ models [49].

2.1 Neutrinos in the $SU(2)_L \otimes U(1)_Y$ model

First we will concern ourselves with the $SU(2)_L \otimes U(1)_Y$ gauge group. This group is the same as that of the Standard Model, compared to which the only difference we consider is the existence of the right-handed neutrino fields. Analogously to the Standard Model, we consider that fermions acquire their mass during the spontaneous symmetry breaking of the local $SU(2)_L \otimes U(1)_Y$ symmetry down to the $U(1)_{em}$ symmetry of electromagnetism. The relevant mass term in the Lagrangian will contain a supplementary Majorana mass term compared to the expression for the charged fermions. Following [25] this term can be written as

$$-\mathcal{L}_m^{\nu} = \bar{\nu}_{R_i}^0 m_{D_{ij}}^{\dagger} \nu_{L_j}^0 + \bar{\nu}_{L_i}^0 m_{D_{ij}} \nu_{R_j}^0 + \frac{1}{2} \bar{\nu}_{R_i}^{0C} m_{M_{ij}} \nu_{R_j}^0 + \frac{1}{2} \bar{\nu}_{R_i}^0 m_{M_{ij}}^{\dagger} \nu_{R_j}^{0C} \ , \tag{2.1}$$

where the indices i and j take the values $i, j = 1..n_G$, n_G being the number of neutrino generations present in the theory. The left- and right-handed Weyl spinors which describe the neutrino field were denoted with ν_L^0 and ν_R^0, m_D and m_M being the Dirac, respectively Majorana mass matrices (of dimension $n_G \times n_G$). This is the most general form compatible with invariance under $SU(2)_L \otimes U(1)_Y$ gauge transformations.

The previous mass Lagrangian can be expressed through the Majorana fields defined as

$$\begin{aligned} f &= \nu_L^0 + (\nu_L^0)^C \ , \\ F &= \nu_R^0 + (\nu_R^0)^C \ . \end{aligned} \tag{2.2}$$

Using this definition we get

$$-\mathcal{L}_m^\nu = \frac{1}{2} \left(\bar{f}_L, \bar{F}_L\right)_\alpha M_{\alpha\beta}^\nu \begin{pmatrix} f_R \\ F_R \end{pmatrix}_\beta + H.c. \ , \tag{2.3}$$

with the corresponding matrix

$$M^\nu = \begin{pmatrix} 0 & m_D \\ m_D^T & m_M \end{pmatrix} \ . \tag{2.4}$$

The fact that M^ν is generally a complex symmetric matrix (with $M^\nu = M^{\nu T}$) follows directly from the general properties of Majorana fields.

One can diagonalize the matrix M^ν with a $2n_G \times 2n_G$ unitary matrix U^νas follows:

$$U^{\nu T} M^\nu U^\nu = \hat{M}^\nu \ . \tag{2.5}$$

While diagonalizing M^ν, the Majorana fields are subjected themselves to the transformations

$$\begin{pmatrix} f_R \\ F_R \end{pmatrix} = U^\nu \begin{pmatrix} \nu_R \\ N_R \end{pmatrix} \ , \tag{2.6}$$

$$\begin{pmatrix} f_L \\ F_L \end{pmatrix} = U^{\nu *} \begin{pmatrix} \nu_L \\ N_L \end{pmatrix} \ . \tag{2.7}$$

After the diagonalization of M^ν and the corresponding transformation of the Majorana fields we obtain n_G light neutrino mass eigenstates (ν_i) and n_G heavy neutrino mass eigenstates (N_i). Using these fields one can write the interaction between the Majorana neutrinos and the gauge, respectively Higgs bosons in terms of mass eigenstates:

$$\mathcal{L}^W_{int} = \frac{g_w}{\sqrt{2}} W^{-\mu} \left[\bar{l}_i \gamma_\mu \mathrm{P}_L B_{l_i \nu_j} \nu_j + \bar{l}_i \gamma_\mu \mathrm{P}_L B_{l_i N_j} N_j \right] + H.c. \ , \tag{2.8}$$

where $l_i, i = 1..n_G$ denote the corresponding charged lepton fields, and the left handed projector P_L is defined as

$$\mathrm{P}_L = \frac{1-\gamma_5}{2} \ . \tag{2.9}$$

This is the expression we will use from now on in our work, for completeness however let us list the other expressions also:

$$\begin{aligned}
\mathcal{L}^Z_{int} = & - \frac{g_w}{4\cos\theta_W} Z^{0\mu} \left[\bar{\nu}_i \gamma_\mu \left[i\mathrm{Im}(C_{\nu_i\nu_j}) - \gamma_5 \mathrm{Re}(C_{\nu_i\nu_j}) \right] \nu_j \right. \\
& + \left(\bar{\nu}_i \gamma_\mu \left[i\mathrm{Im}(C_{\nu_i N_j}) - \gamma_5 \mathrm{Re}(C_{\nu_i N_j}) \right] N_j + H.c \right) \\
& + \left. \bar{N}_i \gamma_\mu \left[i\mathrm{Im}(C_{N_i N_j}) - \gamma_5 \mathrm{Re}(C_{N_i N_j}) \right] N_j \right] \ , \qquad (2.10) \\
\mathcal{L}^H_{int} = & - \frac{g_w}{4M_W} H^0 \left[\bar{\nu}_i \left[(m_{\nu_i} + m_{\nu_j}) \mathrm{Re}(C_{\nu_i\nu_j}) \right. \right. \\
& + \left. i\gamma_5 (m_{\nu_j} - m_{\nu_i}) \mathrm{Im}(C_{\nu_i\nu_j}) \right] \nu_j \\
& + 2\bar{\nu}_i \left[(m_{\nu_i} + m_{N_j}) \mathrm{Re}(C_{\nu_i N_j}) \right. \\
& + \left. i\gamma_5 (m_{N_j} - m_{\nu_i}) \mathrm{Im}(C_{\nu_i N_j}) \right] N_j \\
& + \bar{N}_i \left[(m_{N_i} + m_{N_j}) \mathrm{Re}(C_{N_i N_j}) \right. \\
& + \left. \left. i\gamma_5 (m_{N_j} - m_{N_i}) \mathrm{Im}(C_{N_i N_j}) \right] N_j \right] \ . \qquad (2.11)
\end{aligned}$$

The B and C matrices in the above expressions are obtained from the matrix U^ν, and they are defined in accordance with the expressions below:

$$B_{l_i\alpha} = \sum_{k=1}^{n_G} V^l_{ik} U^{\nu *}_{k\alpha} \ \text{ with } \ \alpha = 1, ..., 2n_G \ \text{ and } \ i = 1, ..., n_G \ , \tag{2.12}$$

$$C_{\alpha\beta} = \sum_{k=1}^{n_G} U^\nu_{k\alpha} U^{\nu *}_{k\beta} \ \text{ with } \ \alpha, \beta = 1, ..., 2n_G \ . \tag{2.13}$$

In these definitions V^l is the corresponding Kobayashi-Maskawa mixing matrix for the leptonic sector.

In the equations 2.12 and 2.13 one must note that the indices α and β refer to the light neutrino fields ν_α or ν_β when $\alpha, \beta = 1, ..., n_G$ and to the heavy neutrino fields $N_{\alpha - n_G}$ and $N_{\beta - n_G}$ when $\alpha, \beta = n_G + 1, ..., 2n_G$.

In order to calculate different processes one usually fixes a definite gauge for the theory. In general, a renormalizable R_ξ gauge will contain the unphysical Goldstone bosons, so it is of interest to give their interactions with the leptonic sector as well (in fact, our interest is restricted to the charged Goldstone particles $G^\pm$):

$$\begin{aligned} \mathcal{L}_{int}^{G^\mp} = & - \frac{g_w}{\sqrt{2}} G^- \left[\bar{l}_i \left[m_{l_i} B_{l_i \nu_j} \mathrm{P}_L - B_{l_i \nu_j} m_{\nu_j} \mathrm{P}_R \right] \nu_j \right. \\ & + \left. \bar{l}_i \left[m_{l_i} B_{l_i N_j} \mathrm{P}_L - B_{l_i N_j} m_{\nu_j} \mathrm{P}_R \right] N_j \right] + H.c. \ , \end{aligned} \tag{2.14}$$

with

$$\mathrm{P}_R = \frac{1 + \gamma_5}{2} \ . \tag{2.15}$$

2.2 Expressing the neutrino masses

The considerations presented in the previous section have treated the neutrinos as nonzero mass particles and therefore they are fairly general in nature. In practice, it is known that the light neutrinos have a very small mass compared to other particles. For this reason it is of interest to investigate models which assure such values for the masses. We can note that a light neutrino becomes massless at the tree level if the condition

$$\sum_{\alpha=1}^{2n_G} M_{\beta\alpha}^\nu U_{\alpha i}^\nu = 0 \quad \text{for each} \quad \beta = 1, ..., 2n_G \tag{2.16}$$

is satisfied. In the equation above i denotes the corresponding massless neutrino, so one can have $i = 1, ..., n_G$.

When all light neutrinos ν_i are massless, one can easily see that all the couplings in the Lagrangians proportional to m_{ν_i} disappear. However, about the structure of M^ν allowed by the masslessness condition (refmassless) one can have definite predictions only in the context of certain models. A two-generation model with $n_G = 2$ will be briefly discussed in the next section.

To get a better feeling of the relative sizes of the resulting expressions for the neutrino masses one can expand the unitary matrix U^ν in a power series of the matrix parameter $\xi = m_D m_M^{-1}$ following [51],[22], including the constraint $\xi_{ij} < 1$. Up to third order of ξ, U^ν can be written as

$$U^\nu = \begin{pmatrix} 1 - \frac{\xi^* \xi^T}{2} & \xi^* \left(1 - \frac{\xi^T \xi^*}{2}\right) J \\ -\xi^T \left(1 - \frac{\xi^* \xi^T}{2}\right) & \left(1 - \frac{\xi^T \xi^*}{2}\right) J \end{pmatrix} + \mathcal{O}(\xi^4) \ . \tag{2.17}$$

In the above expression J is a $n_G \times n_G$ diagonal unitary matrix, having as elements ± 1 and $\pm i$, and it guarantees that all the nonzero mass eigenvalues turn out to be positive.

With this expansion one can give the resulting neutrino masses up to next to leading order in ξ:

$$m_\nu = m_D \xi^T = \xi m_D^T = 0 \ , \tag{2.18}$$

$$m_N = J m_M \left[1 + \frac{1}{2 m_M} \left(\xi^\dagger m_D + m_D^T \xi^*\right) + \mathcal{O}(\xi^3)\right] J \ . \tag{2.19}$$

In this approximation one can obtain also the expressions of the mixing matrices B and C:

$$B_{l_i \nu_j} = \left[V^l \left(1 - \frac{\xi \xi^\dagger}{2}\right)\right]_{l_i \nu_j} \ , \quad B_{l_i N_j} = \left[V^l \xi \left(1 - \frac{\xi^\dagger \xi}{2}\right) J^*\right]_{l_i N_j} \ , \tag{2.20}$$

$$C_{\nu_i \nu_j} = \left(1 - \xi \xi^\dagger\right)_{\nu_i \nu_j} \ , \quad C_{\nu_i N_j} = \left[\xi \left(1 - \xi^\dagger \xi\right) J^*\right]_{\nu_i N_j} \ , \tag{2.21}$$

$$C_{N_i N_j} = \left(J \xi^\dagger \xi J^*\right)_{N_i N_j} \ . \tag{2.22}$$

A global analysis of the mixing parameters ξ_{ij} based on charged-current universality, neutral current effects and other experimental constraints has been performed in [52]. It has been shown that these parameters have maximal values of order 0.1 – 0.2, the larger bound being safely applicable to the e–τ, μ–τ . The larger mixings seem to be preferred by some neutrino-mass schemes [53–55] for resolving the solar neutrino problem through the MSW mechanism [56–59]. The heavy neutrinos with large mixings, on the other hand, must be heavier than the Z^0 boson, since otherwise they could have already been produced in Z^0 decays at LEP.

2.3 The model with two generations ($n_G = 2$)

In this section we consider the case of two massless neutrinos present in the theory. The matrices m_D and m_M have the general form, as parameterized in [60],

$$m_D = \begin{pmatrix} a & b \\ c & d \end{pmatrix} , \tag{2.23}$$

$$m_M = \begin{pmatrix} A & 0 \\ 0 & B \end{pmatrix} , \tag{2.24}$$

where m_D is a general complex matrix and m_M can be chosen to be real. In order to have two massless neutrinos, the conditions

$$\prod_{i=1}^{4} m_i^2 = \det(M^\nu M^{\nu\dagger}) = 0 , \tag{2.25}$$

$$\begin{aligned} \sum_{1<j<k}^{4} m_i^2 m_j^2 m_k^2 &= \frac{1}{6}\left[\mathrm{Tr}^3(M^\nu M^{\nu\dagger}) + 2\mathrm{Tr}(M^\nu M^{\nu\dagger})^3 \right. \\ &\quad \left. -3\mathrm{Tr}(M^\nu M^{\nu\dagger})\mathrm{Tr}(M^\nu M^{\nu\dagger})^2\right] = 0 , \end{aligned} \tag{2.26}$$

must be satisfied. From the first one we can immediately obtain the constraint

$$\det m_D = 0 . \tag{2.27}$$

Without loss of generality we can assume that $a \neq 0$, so we have

$$d = \frac{bc}{a} , \quad B = -\frac{b^2}{a^2} A . \tag{2.28}$$

It turns out that the parameters a, b, c, d should be either purely real or purely imaginary numbers. For example, taking them real, the masses of the heavy neutrinos turn out to be

$$\begin{aligned} m_{N_1} &= \frac{A}{2}\left[1 - \frac{b^2}{a^2} + \left(1 + \frac{b^2}{a^2}\right)\sqrt{1 + \frac{4a^2}{a^2+b^2}\left(1 + \frac{c^2}{a^2}\right)\frac{a^2}{A^2}}\right] \\ &= A + \mathcal{O}(\frac{1}{A}) , \\ m_{N_2} &= -\frac{A}{2}\left[1 - \frac{b^2}{a^2} - \left(1 + \frac{b^2}{a^2}\right)\sqrt{1 + \frac{4a^2}{a^2+b^2}\left(1 + \frac{c^2}{a^2}\right)\frac{a^2}{A^2}}\right] \\ &= \frac{b^2}{a^2} A + \mathcal{O}(\frac{1}{A}) . \end{aligned} \tag{2.29}$$

In this scheme we obtain the matrix J as being

$$J = \begin{pmatrix} 1 & 0 \\ 0 & i \end{pmatrix} . \tag{2.30}$$

From these results one can immediately draw some conclusions. We notice that even in the case $a = b = c$, we have $B = -A$, which means that models with family independent mixings can naturally account for massless neutrinos already at tree level. A more careful analysis actually shows that in order to achieve this goal, one has to assume that the Dirac mass terms are described by a universal Yukawa coupling a and the two right-handed eigenstates $\nu^0_{R_{1,2}}$ possess opposite CP quantum numbers. Such patterns with "democratic"-type mixing between quark families have also been proposed [61,62] in order to explain the structure of the usual Cabbibo-Kobayashi-Maskawa mixing matrix.

To our present knowledge, the "see-saw" mechanism [18,63] is the only scheme which naturally generates small, non-vanishing neutrino masses. According to this mechanism, the Majorana mass terms ($m_M \sim A \sim m_N$) in Eq. (2.24) can be regarded as remnant parts of a more fundamental theory. Such theories could be the left-right symmetric models [2], grand unified (GUT) models (e.g. $SO(10)$ [64]), or superstring models with an E_6 symmetry [46]. In all these models it is possible to have TeV-mass scales determined by the breaking mechanism itself, as the symmetry of the original gauge group breaks spontaneously down to $SU(2)_L \otimes U(1)_Y$. If the Dirac mass term m_D is of the order of a typical charged-lepton or quark mass, as dictated by GUT relations [65], and the Majorana-mass scale m_M is sufficiently large, one can obtain a very light neutrino with $m_\nu \simeq m_D^2/m_M$, and for the heavy neutrino $m_N \simeq m_M$. Thus, in order to have $m_{\nu_i} \lesssim 1 - 10$ eV for $m_D \approx 1$ GeV through the see-saw mechanism, one must require that very heavy neutrinos with masses $m_{N_i} \gtrsim 10^7 - 10^8$ GeV are present. It turned out, however, that in a two generational model small neutrino masses can be naturally induced by radiative corrections with $m_{N_i} \sim 100$ GeV and $\xi_{ij} \sim 0.1$.

2.4 Neutrinos in the $SU(2)_L \otimes SU(2)_R \otimes U(1)_{B-L}$ model

Left-right symmetric models based on the gauge group $SU(2)_L \otimes SU(2)_R \otimes U(1)_{B-L}$ were motivated from the fact that the spontaneous breakdown of gauge and discrete symmetries

can be accomplished on the same footing. Such models can naturally arise from $SO(10)$ grand unified theories via the breaking pattern

$$\begin{aligned} SO(10) &\rightarrow SU(4)_{PS} \otimes SU(2)_L \otimes SU(2)_R \\ &\rightarrow SU(3)_c \otimes SU(2)_L \otimes SU(2)_R \otimes U(1)_{B-L} \rightarrow SM \ . \end{aligned} \tag{2.31}$$

The assignment of quantum numbers to leptons under the gauge group $SU(2)_L \otimes SU(2)_R \otimes U(1)_{B-L}$ is arranged as follows:

$$L'_L = \begin{pmatrix} \nu'_l \\ l' \end{pmatrix}_L : (0, 1/2, -1) \ , \tag{2.32}$$

$$L'_R = \begin{pmatrix} \nu'_l \\ l' \end{pmatrix}_R : (1/2, 0, -1) \ , \tag{2.33}$$

where the prime superscript of the leptonic fields simply denotes the weak eigenstates.

In a minimal left-right symmetric model baryon-lepton number $(B - L)$ violating operators are allowed in the Yukawa sector. Such $(B - L)$ violating interactions are introduced by certain Higgs multiplets ($\Delta_{L,R}$ as we have seen in Chapter 1) and give rise to a Majorana mass term $m_{M_{ij}}$ in the following way:

$$\mathcal{L}_{int}^{B-L} = -\sum_{i,j=1}^{n_G} \frac{\sqrt{2} m_{M_{ij}}}{2 v_R} \left(h_{ij} \bar{L}'^C_{L_i} \varepsilon_{ij} \Delta_L L'_{L_j} + \bar{L}'^C_{R_i} \varepsilon_{ij} \Delta_R L'_{R_j} \right) + H.c. \tag{2.34}$$

Here, ε_{ij} is the usual Levi-Civita tensor and the parameters $h_{ij} = 1$ if the left-right symmetry is explicitly imposed. A phenomenological analysis of μ and τ decays shows that $h_{ij} \ll 1$ [15]. In the equation above v_R is the vacuum expectation value of Δ_R and it sets the mass of the right-handed gauge bosons.

In the case when the vacuum expectation values of the symmetry-breaking Higgs scalars satisfy certain natural scenarios, the neutrino mass matrix takes the general see-saw-type form, as in Sec. 2.1. The mass matrix M^ν can be diagonalized in the same manner as presented there. The interaction of the leptons with the right-handed $W_R^\mp$ and the corresponding Goldstone bosons $G_R^\mp$ can be written as

$$\mathcal{L}_{int}^{W_R} = -\frac{g_w}{\sqrt{2}} W_R^{-\mu} B_{l\alpha}^R \bar{l} \gamma_\mu \mathrm{P}_R n_\alpha + H.c. \ , \tag{2.35}$$

$$\mathcal{L}_{int}^{G_R} = -\frac{g_w}{\sqrt{2} M_L} s_\beta G_R^- B_{l\alpha}^R \bar{l} \left(m_l \mathrm{P}_R - m_{n_\alpha} \mathrm{P}_L \right) n_\alpha + H.c. \tag{2.36}$$

Here l and n_α are the mass eigenstates of the charged and neutral leptons, respectively, and the parameter s_β is defined via the masses of the W_L and W_R as being $s_\beta^2 = M_L^2/M_R^2$. One can write the expressions of the right-handed neutrino mixing matrices similar to Eq. (2.12) and (2.13):

$$B^R_{l_i\alpha} = \sum_{k=n_G+1}^{2n_G} V^{lR}_{ik} U^{\nu}_{k\alpha} \quad \text{with} \quad \alpha = 1, ..., 2n_G \quad \text{and} \quad i = 1, ..., n_G \ , \tag{2.37}$$

$$C^R_{\alpha\beta} = \sum_{k=n_G+1}^{2n_G} U^{\nu *}_{k\alpha} U^{\nu}_{k\beta} \quad \text{with} \quad \alpha, \beta = 1, ..., 2n_G \ . \tag{2.38}$$

One can easily conclude that the matrices B^L and C^L correspond to those discussed in Sec. 2.1.

The flavor-mixing matrices B^L and C^L satisfy a number of identities, which are derived by using the information of $SU(2)_L \otimes U(1)_Y$ invariance of the Yukawa interaction $\mathcal{L}^{\nu}_m$. These identities, forced by the renormalizability of the inter family see-saw-type model, are listed below [25,28–30,50]:

$$\sum_{\alpha=1}^{2n_G} B^L_{l_i\alpha} B^{L*}_{l_j\alpha} = \delta_{l_i l_j} \quad \text{with} \quad i, j = 1, ..., n_G \ , \tag{2.39}$$

$$\sum_{k=1}^{n_G} B^L_{l_k\alpha} B^{L*}_{l_k\beta} = C^L_{\alpha\beta} \quad \text{with} \quad \alpha, \beta = 1, ..., 2n_G \ , \tag{2.40}$$

$$\sum_{\gamma=1}^{2n_G} C^L_{\alpha\gamma} C^{L*}_{\beta\gamma} = C^L_{\alpha\beta} \quad \text{with} \quad \alpha \ , \beta = 1, ..., 2n_G. \tag{2.41}$$

$$\sum_{\beta=1}^{2n_G} B^L_{l_k\beta} C^L_{\beta\alpha} = B^L_{l_k\alpha} \ , \tag{2.42}$$

$$\sum_{\alpha=1}^{2n_G} m_\alpha C^L_{\beta\alpha} C^L_{\gamma\alpha} = 0 \ , \tag{2.43}$$

$$\sum_{\alpha=1}^{2n_G} m_\alpha B^L_{l_k\alpha} C^{L*}_{\alpha\beta} = 0 \ , \tag{2.44}$$

$$\sum_{\alpha=1}^{2n_G} m_\alpha B^L_{l_{k1}\alpha} B^L_{l_{k2}\alpha} = 0 \ . \tag{2.45}$$

In addition, the existence of the right-handed mixing matrices leads to the following additional identities:

$$\sum_{\alpha=1}^{2n_G} B^L_{l_1\alpha} B^R_{l_2\alpha} = 0 \ , \tag{2.46}$$

$$\sum_{k=1}^{n_G} B^{R*}_{l_k\alpha} B^R_{l_l\beta} = C^R_{\alpha\beta} \ , \tag{2.47}$$

$$C^{L*}_{\alpha\beta} + C^R_{\alpha\beta} = \delta_{\alpha\beta} \ . \tag{2.48}$$

In a two generation mixing model one can use these relations to obtain compact expressions for the corresponding matrix elements. These turn out to be

$$B^L_{lN_1} = \frac{\rho^{1/4} s^{\nu_l}_L}{\sqrt{1+\rho^{1/2}}} \ , \quad B^L_{lN_2} = \frac{i s^{\nu_l}_L}{\sqrt{1+\rho^{1/2}}} \ , \tag{2.49}$$

where $\rho = m^2_{N_2}/m^2_{N_1} (\geq 1)$ is the mass ratio of the two heavy neutrinos present in the model, and $s^{\nu_l}_L$ is the lepton number violating mixing defined as

$$(s^{\nu_l}_L)^2 \equiv \sum_{\alpha=n_G+1}^{2n_G} \mid B^L_{l\alpha} \mid^2 \simeq \left(m^\dagger_D \frac{1}{m^2_M} m_D \right)_{ll} \ . \tag{2.50}$$

Furthermore,

$$C^L_{N_1N_1} = \frac{\rho^{1/2}}{1+\rho^{1/2}} \sum_{i=1}^{n_G} (s^{\nu_i}_L)^2 \ , \tag{2.51}$$

$$C^L_{N_2N_2} = \frac{1}{1+\rho^{1/2}} \sum_{i=1}^{n_G} (s^{\nu_i}_L)^2 \ , \tag{2.52}$$

$$C^L_{N_1N_2} = -C^L_{N_2N_1} = \frac{i\rho^{1/4}}{1+\rho^{1/2}} \sum_{i=1}^{n_G} (s^{\nu_i}_L)^2 \ . \tag{2.53}$$

Similar, but somewhat more involved expressions can be written for the corresponding matrix elements of B^R and C^R. The important feature to be noticed here is that the leptonic sector of the two generation model depends only on five parameters: the masses of the two heavy neutrinos m_{N_1} and m_{N_2} (or equivalently m_{N_1} and ρ), the mixing angles $(s^{\nu_i}_L)^2$, which are constrained by low-energy data, and an unconstrained Cabbibo-type angle θ_R entering the expressions for B^R and C^R.

Having made these remarks about the neutrino masses, we will assume in what follows that the see-saw-type scenario with two heavy neutrinos is in effect.

Chapter 3

$K_L \to e\mu$ in the Standard Model with heavy neutrinos

The Standard Model of particle interactions based on the invariance under $SU(2)_L$ isospin and $U(1)_Y$ hypercharge gauge transformations provides a sufficiently accurate description of the subatomic particles to incorporate all the presently available experimental data. One of the basic characteristics of this model is that the separate leptonic quantum numbers are conserved to all orders of perturbation theory. If the Standard Model is considered as an effective theory, the low-energy limit of a more fundamental theory (*e.g.*, superstrings or grand unified theories), one may then have to worry about large flavor-changing-neutral current (FCNC) effects that could violate experimental data. Among the possible FCNC decays forbidden in the SM, the decay $K_L \to e\mu$ can play a central role either to constrain or establish new physics beyond the Standard Model. This process is interesting because it involves both the quark (hadronic) and the leptonic sector of the given model via flavor changing interactions.

From a theoretical point of view one can distinguish two mechanisms by which the decay $K_L \to e\mu$ can occur in extensions of the Standard Model. First, one can consider new lepton-flavor-violating interactions. $K_L \to e\mu$ has been studied in models based on technicolor [66], supersymmetry [68], compositeness [69,70], horizontal symmetry [71], extended scalar sectors [72], exotic leptoquarks [73] or superstrings [74]. An alternative approach is to consider non-vanishing and non-degenerate neutrino masses within the Standard Model

and minimal extensions of it, such as the $SU(2)_L \otimes SU(2)_R \otimes U(1)_{B-L}$ model.

The latter approach was adopted in [75,76], where the effect of Dirac neutrino masses in the above mentioned models was studied. Taking into account the stringent upper limits on the masses of the three observed neutrinos, the $K_L \to e\mu$ rate turns out to be unmeasurably small unless a fourth family with significant mixings with the ν_e and ν_μ is postulated. However, such a model is highly unnatural and can only be obtained by an extreme fine-tuning of the Yukawa couplings.

It was argued in the literature that extensions of the Standard Model containing more than one neutral isosinglet can dramatically relax the severe constraints on the mixings between light and heavy neutrinos [49,46,60,21,25], which are dictated by usual see-saw scenarios [18]. Such models with enhanced light-heavy neutrino mixings are also associated with large Dirac mass terms in the general neutrino mass matrix [25]. As an immediate phenomenological consequence, non-decoupling virtual effects originating from heavy neutrinos can considerably enhance the decay rates $H \to l\bar{l}'$ [29], $Z \to l\bar{l}'$ [28], $\tau \to eee$ [50], and the values of other observables [31] to an experimentally accessible level.

In this chapter we will see how the presence of the heavy neutrinos enhances the branching ratio for the rare decay $K_L \to e\mu$, due to non-decoupling effects arising from chirality difference between left-handed and right-handed couplings. The anticipated result may be related to the observation made by Paschos in [66] for the $K_L - K_S$ mass difference in the context of left-right symmetric models. The treatment will bear close resemblance to the one presented in [67], but in the present work a more detailed discussion will be carried out.

3.1 The process $K_L \to e\mu$

In order to briefly describe the electroweak sector of the SM with one right-handed neutrino per family, we will adopt the notations given in Chapter 2, inspired by [25]. To be specific, we will first consider an $SU(2)_L \otimes U(1)_Y$ symmetric model with n_G generations of charged leptons l_i ($i = 1, \ldots, n_G$) and light (heavy) Majorana neutrinos ν_α (N_α). The charged-

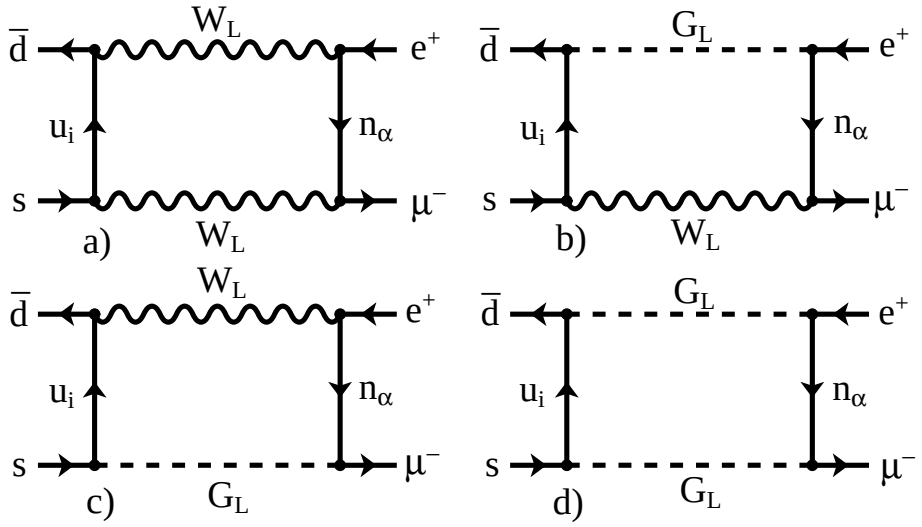

Figure 3.1: Feynman diagrams contributing to $K_L \to e\mu$ in Majorana neutrino models relying on the gauge groups $SU(2)_L \otimes U(1)_Y$ in the Feynman–'t Hooft gauge

current interaction of this model is then governed by the Lagrangian given in Eq. (2.8)

$$\mathcal{L}_{int}^{W} = -\frac{g_w}{\sqrt{2}} W^{-\mu} \sum_{i=1}^{n_G} \sum_{\alpha=1}^{2n_G} \bar{l}_i \gamma_\mu P_L B_{l_i\alpha}^{L} n_\alpha + H.c. \,, \tag{3.1}$$

where g_w is the $SU(2)_L$ weak coupling constant, $P_L(P_R) = (1 - (+)\gamma_5)/2$, and B^L is an $n_G \times 2n_G$ matrix obeying a number of useful identities given in Eq. (2.39–2.45).

In Eq. (3.1), we have collectively defined the mass eigenstates of the light and heavy neutrinos as follows: $n_\alpha \equiv \nu_\alpha$ for $\alpha = 1, \ldots, n_G$ and $n_\alpha \equiv N_{\alpha - n_G}$ for $\alpha = n_G + 1, \ldots, 2n_G$.

In the model under consideration, there are no tree level FCNC interactions in the theory, which means that the decay $K_L \to e\mu$ can occur only at the 1-loop level, induced by the diagrams shown in Fig. 3.1. In Fig. 3.1, the field G_L describes the would-be Goldstone boson in the Feynman–'t Hooft gauge, which is related to the longitudinal polarization of the W_L boson in the unitary gauge. In the applicable limit of vanishing external momenta, the amplitude of the decay process $K_L \to e\mu$ takes the general form

$$A \;=\; \left(\frac{g_w}{\sqrt{2}}\right)^4 \langle 0|\bar{d}\gamma_\kappa \mathrm{P}_L s|\bar{K}^0\rangle \bar{u}_\mu \gamma^\kappa \mathrm{P}_L v_e \frac{1}{(4\pi)^2} \frac{1}{M_L^2} \times$$

$$\times \sum_{u_i=u,c,t} V_{id}^{L*} V_{is}^{L} \sum_{\alpha=1}^{2n_G} B_{\mu\alpha}^{L} B_{e\alpha}^{L*} I(\lambda_i, \lambda_\alpha) \ , \tag{3.2}$$

where $\lambda_\alpha = m_{n_\alpha}^2/M_W^2$, $\lambda_i = m_{u_i}^2/M_L^2$, V^L is the usual Cabbibo-Kobayashi-Maskawa (CKM) matrix, and the loop function I is obtained from the Feynman graphs in Fig. 3.1 [78]. The function I is analytically given by the relation

$$I(\lambda_i, \lambda_\alpha) = \left(1 + \frac{1}{4}\lambda_i\lambda_\alpha\right) I_1(\lambda_i, \lambda_\alpha) + 2\lambda_i\lambda_\alpha I_2(\lambda_i, \lambda_\alpha) \ , \tag{3.3}$$

where the corresponding box functions I_1 and I_2 are defined by the loop integrals

$$I_1(\lambda_i, \lambda_i) = \frac{1}{i}(4\pi)^2 M_L^2 \int \frac{d^4k}{(2\pi)^4} \frac{k^2}{(k^2 - m_{u_i}^2)(k^2 - m_{n_\alpha}^2)(k^2 - M_L^2)^2} \ , \tag{3.4}$$

$$I_2(\lambda_i, \lambda_i) = \frac{1}{i}(4\pi)^2 M_L^4 \int \frac{d^4k}{(2\pi)^4} \frac{1}{(k^2 - m_{u_i}^2)(k^2 - m_{n_\alpha}^2)(k^2 - M_L^2)^2} \ , \tag{3.5}$$

leading to the expressions

$$\begin{aligned} I_1(\lambda_i, \lambda_\alpha) &= \left[\frac{\lambda_i^2 \ln\lambda_i}{(\lambda_\alpha - \lambda_i)(1-\lambda_i)^2} + \frac{\lambda_\alpha^2 \ln\lambda_\alpha}{(\lambda_i - \lambda_\alpha)(1-\lambda_\alpha)^2}\right. \\ &\quad \left. - \frac{1}{(1-\lambda_i)(1-\lambda_\alpha)}\right] \ , \end{aligned} \tag{3.6}$$

$$\begin{aligned} I_2(\lambda_i, \lambda_\alpha) &= -\left[\frac{\lambda_i \ln\lambda_i}{(\lambda_\alpha - \lambda_i)(1-\lambda_i)^2} + \frac{\lambda_\alpha \ln\lambda_\alpha}{(\lambda_i - \lambda_\alpha)(1-\lambda_\alpha)^2}\right. \\ &\quad \left. + \frac{1}{(1-\lambda_i)(1-\lambda_\alpha)}\right] \ . \end{aligned} \tag{3.7}$$

Tracing back the origin of these functions to the corresponding Feynman diagrams, we can immediately see that the diagram *d*) in Fig. 3.1, with the non-physical would-be Goldstone bosons in the loop, contributes significantly more to the decay amplitude in the Feynman–'t Hooft gauge than the diagram containing the physical particles. The reason for this is the presence of the large neutrino mass in the coupling to the leptons. These large neutrino masses will be responsible for the non-decoupling effects revealed in this decay.

3.2 The reduced amplitude $\tilde{A}$

Following closely Ref. [79], we define a reduced amplitude $\tilde{A}$ through the expression

$$A = \left(\frac{g_w}{\sqrt{2}}\right)^4 \langle 0|\bar{d}\gamma_\kappa \mathrm{P}_L s|\bar{K}^0\rangle \bar{u}_\mu \gamma^\kappa \mathrm{P}_L v_e \frac{1}{(4\pi)^2} \frac{1}{M_W^2} \tilde{A} \ , \tag{3.8}$$

where

$$\tilde{A} = \sum_{i=u,c,t} V_{id}^* V_{is} \sum_{\alpha=1}^{2n_G} B_{\mu\alpha}^L B_{e\alpha}^{L*} I(\lambda_i, \lambda_\alpha) \ . \tag{3.9}$$

The advantage of this definition is that $\tilde{A}$ is a dimensionless quantity carrying the whole electroweak physics.

As we have seen in Eq. (2.39), the matrix B^L obeys a generalized GIM identity [80]

$$\sum_{\alpha=1}^{2n_G} B_{l_1\alpha}^L B_{l_2\alpha}^{L*} = \delta_{l_1 l_2} \ , \tag{3.10}$$

similar to the known one satisfied by the CKM matrix V^L. A double GIM mechanism is then operative both for the intermediate u-type quarks and neutral leptons, which allows us to rewrite Eq. (3.9) as

$$\tilde{A} = \sum_{i=u,c,t} V_{id}^* V_{is} \sum_{\alpha=1}^{2n_G} B_{\mu\alpha}^L B_{e\alpha}^{L*} \left[I(\lambda_i, \lambda_\alpha) - I(0, \lambda_\alpha) - I(\lambda_i, 0) + I(0,0) \right] \ . \tag{3.11}$$

The pseudounitarity relation (2.39) allows us to finally express $\tilde{A}$ in a simplified manner as

$$\tilde{A} = \sum_{i=c,t} V_{id}^* V_{is} \sum_{\alpha=n_G+1}^{2n_G} B_{\mu\alpha}^L B_{e\alpha}^{L*} E(\lambda_i, \lambda_\alpha) \ , \tag{3.12}$$

with

$$\begin{aligned} E(\lambda_i, \lambda_\alpha) \ &= \ \lambda_i \lambda_\alpha \left\{ -\frac{3}{4} \frac{1}{(1-\lambda_i)(1-\lambda_\alpha)} \right. \\ &+ \left[\frac{1}{4} - \frac{3}{2} \frac{1}{\lambda_i - 1} - \frac{3}{4} \frac{1}{(\lambda_i - 1)^2} \right] \frac{\ln \lambda_i}{\lambda_i - \lambda_\alpha} \\ &+ \left. \left[\frac{1}{4} - \frac{3}{2} \frac{1}{\lambda_\alpha - 1} - \frac{3}{4} \frac{1}{(\lambda_\alpha - 1)^2} \right] \frac{\ln \lambda_\alpha}{\lambda_\alpha - \lambda_i} \right\} \ . \end{aligned} \tag{3.13}$$

In Eq. (3.12), we have considered that the up quark u and the light neutrinos ν_e, ν_μ and ν_τ are massless. Only the virtual c and t quarks, and the n_G heavy Majorana neutrinos will then contribute to $\tilde{A}$. Using the double GIM reduced form for the loop function given in Eq. (3.13) guarantees that the amplitude is not proportional to small differences of large numbers.

For definite results, we have restricted ourselves to a model with $n_G = 2$ (neglecting mixings due to ν_τ), where the mixings B_{lN_α} and the two heavy neutrino masses, m_{N_1} and

m_{N_2}, satisfy the relation [28]

$$B^L_{lN_2} B^{L*}_{l'N_2} = \frac{m_{N_1}}{m_{N_2}} B^L_{lN_1} B^{L*}_{l'N_1} \ . \tag{3.14}$$

The branching ratio for $K_L \to e\mu$ may conveniently be calculated by using isospin invariance relations between the decay amplitudes of $\bar{K}^0 \to \mu^- e^+$ and $K^- \to \mu^- \nu_\alpha$. Setting $m_e = 0$ relative to m_μ in the phase space factors, one finds

$$B(K_L \to e\mu) = 4.1 \times 10^{-4} \left| \tilde{A} \right|^2 \ . \tag{3.15}$$

3.3 Phenomenological aspects

The process $K_L \to e\mu$ can not be considered independently from the other low energy processes which involve the same leptonic mixing matrix B^L. Experimental bounds coming from the non-observation of the decay $\mu \to e\gamma$ will constrain the parameter space of our theory and impose severe limits on the decay $K_L \to e\mu$.

The decay width for $\mu \to e\gamma$ is given by the expression

$$\Gamma(\mu^- \to e^- \gamma) = \frac{\alpha_{em} G_F^2 m_\mu^5}{2^{11} \pi^4} \mid F_\gamma \mid^2 \ , \tag{3.16}$$

with the corresponding electromagnetic fine structure constant $\alpha_{em} \approx \frac{1}{137}$ and Fermi constant $G_F = \frac{\alpha_{em}}{\sqrt{2} \sin^2 \theta_W M_L^2}$. In Majorana neutrino models, the transition amplitude F_γ can be expressed as

$$F_\gamma = \sum_{\alpha=1}^{2n_G} B^L_{\mu\alpha} B^{L*}_{e\alpha} F(\lambda_\alpha) \ , \tag{3.17}$$

and after taking into account the GIM-mechanism for the neutrinos, for the branching ratio of $\mu \to e\gamma$, defined as $B(\mu \to e\gamma) = \frac{\Gamma(\mu^- \to e^- \gamma)}{\Gamma(\mu^- \to e^- \bar{\nu}_e \nu_\mu)}$, we obtain in the model with two generations the expression

$$B(\mu \to e\gamma) = \frac{6\alpha_{em}}{\pi} \Big| \sum_{\alpha=1,2} B^L_{\mu N_\alpha} B^{L*}_{eN_\alpha} F(\lambda_\alpha) \Big|^2 \ , \tag{3.18}$$

where the loop function F calculated in [78,81] is given by

$$F(\lambda_\alpha) = \frac{2\lambda_\alpha^3 + 5\lambda_\alpha^2 - \lambda_\alpha}{4(1-\lambda_\alpha)^3} + \frac{3\lambda_\alpha^3 \ln \lambda_\alpha}{2(1-\lambda_\alpha)^4} \ . \tag{3.19}$$

The present experimental upper limit $B(\mu \to e\gamma) < 1.2 \times 10^{-11}$ together with Eqs. (3.14) and (3.18) can be used to obtain combined constraints on the mixings B_{lN_α} and heavy neutrino masses. These constraints are quite useful in order to individually evaluate the contribution of the charm and top quark to $B(K_L \to e\mu)$. In our numerical analysis, we have used the maximally allowed values $V_{td} = 0.018$ and $V_{ts} = 0.054$, and the central value for the top-quark $m_t = 175$ GeV as reported by the CDF collaboration [82].

Contrary to [83] where only one heavy neutrino family with mass not much heavier than M_W was considered, we find that the charm-quark contribution is negligible and only top-quark loop effects are of interest here for heavy neutrino masses larger than 150 GeV.

Of course, the mass of the heavy neutrinos should not exceed an upper limit that invalidates perturbative unitarity. This mass limit is qualitatively estimated to be no bigger than 50 TeV [25]. The condition for preserving perturbative unitarity can be suggestively imposed as the requirement that the total decay width of the heavy neutrinos should not exceed one half the mass of the heavy neutrino,

$$\frac{\Gamma_{N_j}}{m_{N_j}} \leq \frac{1}{2} \; . \tag{3.20}$$

The total decay width of the heavy neutrino will be given by summing up the partial decay rates corresponding to the different allowed decay modes:

$$\begin{aligned} \Gamma_{N_i} &= \sum_l \left(\Gamma(N_j \to l^+ W^-) + \Gamma(N_j \to l^- W^+) \right) \\ &+ \sum_\nu \left(\Gamma(N_j \to \nu Z^0) + \Gamma(N_j \to \nu H^0) \right) \; . \end{aligned} \tag{3.21}$$

For the case $m_{N_j} \gg M_W, M_Z, M_H$, we obtain for the total decay width

$$\Gamma_{N_j} = \frac{\alpha_W}{16 M_L^2} m_{N_j}^3 \left(2 \sum_l \mid B_{lN_j}^L \mid^2 + 2 \sum_\nu \mid C_{\nu N_j} \mid^2 \right) . \tag{3.22}$$

In our model with two right-handed ν_R and three left-handed ν_L neutrino fields, and using the expressions given in Eqs. (2.49–2.53), one can arrive starting from Eq. (3.20) at the inequalities

$$m_{N_1} \leq M_W \sqrt{\frac{2(1+\rho^{-1/2})}{\alpha_W} \left[(s_L^{\nu_e})^2 + (s_L^{\nu_\mu})^2 + (s_L^{\nu_\tau})^2 \right]} \equiv m_{N_1}^{max} \; , \tag{3.23}$$

$$m_{N_2} \leq \rho^{1/4} m_{N_1}^{max} \; . \tag{3.24}$$

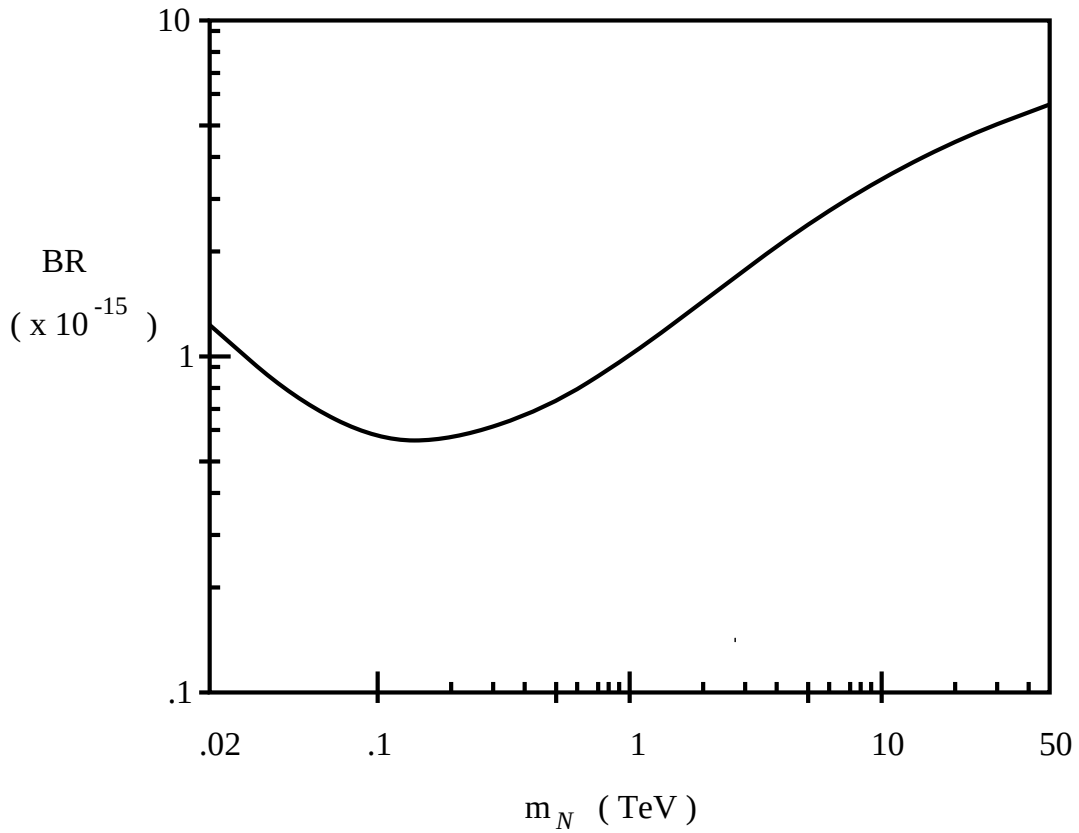

Figure 3.2: $B(K_L \to e\mu)$ as a function of the heavy neutrino mass m_N in the SM with right-handed neutrinos ($m_N \simeq m_{N_1} \simeq m_{N_2},\ m_t = 175$ GeV).

Choosing ρ and m_{N_1} as free parameters, the two inequalities (3.23) and (3.24) can be combined in a single relation

$$m_{N_1}^2 \leq \frac{2M_W^2}{\alpha_W} \frac{1-\rho^{-1/2}}{\rho^{1/2}} \left[(s_L^{\nu_e})^2 + (s_L^{\nu_\mu})^2 + (s_L^{\nu_\tau})^2 \right]^{-1} \ , \quad \rho \geq 1 \ . \tag{3.25}$$

In our process only the heavy neutrino mixings with the electrons and muons are relevant and we can safely consider $(s_L^{\nu_\tau})^2 = 0$ in the previous condition. From Fig. 3.2, we see that the branching ratio takes the maximum value $B(K_L \to e\mu) = 5.5 \times 10^{-15}$, which is still rather far from the present experimental sensitivity $B(K_L \to e\mu) < 4.7 \times 10^{-12}$ at 90% C.L. [84]. In Fig. 3.2, we have further assumed that the two heavy neutrinos, N_1 and N_2, have about the same mass m_N. Nevertheless, in Fig. 3.3 we have plotted the dependence of the branching ratio as a function of the value $\rho = m_{N_2}/m_{N_1}$ for selected values of m_{N_1}. The solid curve in Fig. 3.3 determines an upper limit of the allowed region for $B(K_L \to e\mu)$

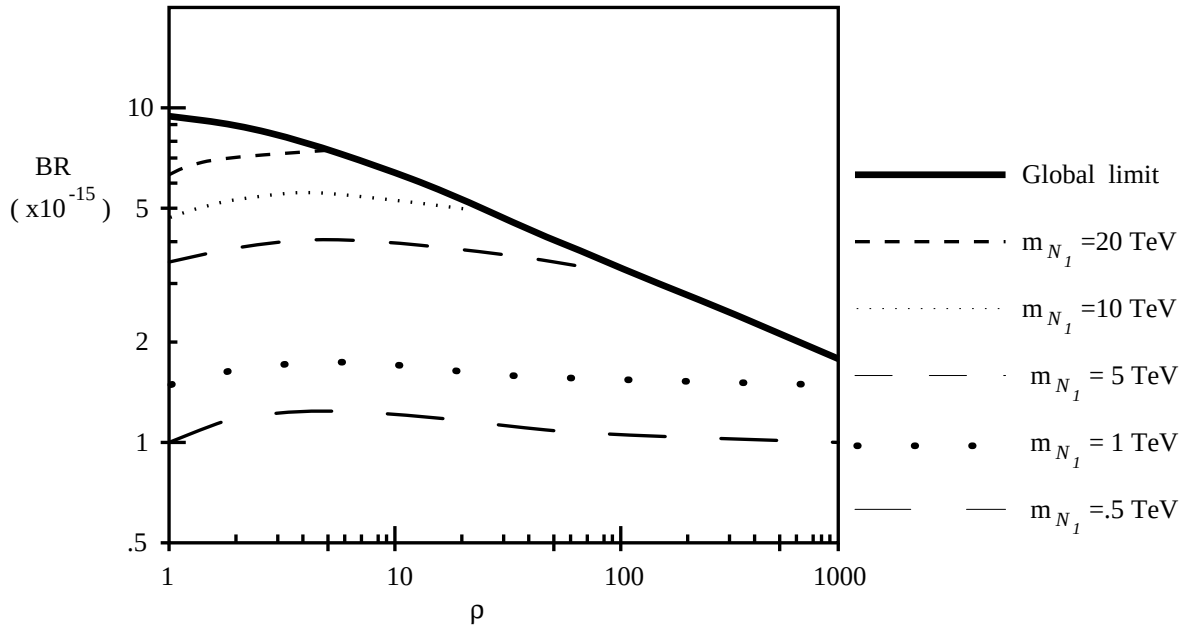

Figure 3.3: $B(K_L \to e\mu)$ versus $\rho = m_{N_2}/m_{N_1}$ in the $SU(2)_L \otimes U(1)_Y$ model with neutral singlets.

by taking into account the combined constraints arising from the neutrino mixings $B^L_{lN_\alpha}$ and the validity of perturbative unitarity.

One of the novelties found investigating the decay $K_L \to \mu e$ in the Standard Model with right-handed neutrinos is the dominance of the contribution of the virtual top-quark over the contribution of the virtual charm-quark. In the literature it was repeatedly argued, that the charm-quark contribution is the relevant one to the process described by the box diagrams in Fig. 3.1.

There were many reasons to promote this point of view. One of them was the smallness of the mixing between the top-quark and the d-, respectively s-quark compared to the same mixings with the charm-quark. The measure of this smallness is given by the ratio between the corresponding products of Cabbibo-Kobayashi-Maskawa matrix elements,

$$\frac{\mid V^{L*}_{td} V_{ts} \mid}{\mid V^{L*}_{cd} V_{cs} \mid} \simeq 3.2 \times 10^{-3} \ , \tag{3.26}$$

using the allowed values [84] $\mid V^L_{cd} \mid \simeq 0.224$, $\mid V^L_{cs} \mid \simeq 0.975$, $\mid V^L_{td} \mid \simeq 0.014$ and $\mid V^L_{ts} \mid \simeq 0.044$. Based on this, the authors of [83] considered the relation for the branching ratio given in Eq. (3.15), using the definition of the reduced amplitude in Eq. (3.9), as being bounded from

above by the limiting case $V_{td}^{L*}V_{ts}^{L} \to 0$. Computing then the charm-quark contribution, an upper limit of 2×10^{-16} for $B(K_L \to e\mu)$ was obtained. This result is actually consistent with the result presented in our work, with the necessary remark that this is not the dominant contribution to be considered.

The very heavy top quark is another reason why its contribution becomes dominant due to the non-decoupling effects. This argument is based mainly on the evolution of the direct experimental limit on the top-quark mass over the years. One can see the influence of this limit in a previous study of $K_L \to e\mu$ [79]. There the authors argue that the contribution of the top-quark to the decay amplitude can be at most of the same order of magnitude as the contribution of the charm-quark. To substantiate this, it is correctly stated that for light neutrinos the top-quark contribution is negligible, for heavy neutrinos the relation between the two different contributions is qualitatively estimated as being

$$\left| \frac{\tilde{A}_{(\text{top})}}{\tilde{A}_{(\text{charm})}} \right| \sim \sin^4\theta_C (m_t/m_c)^2 \sim (m_t/20m_c)^2 \ , \tag{3.27}$$

where θ_C is the Cabbibo mixing angle ($\sin\theta_C \simeq 0.223$). Using $m_c = 1.35$ GeV for the charm-quark mass, it turns out that the relation above provides a ratio of the order of unity using the experimental limit considered in [79], namely $m_t > 55$ GeV. However, using the presently accepted value of 180 GeV for the top mass, we obtain a ratio of ≈ 40, which means again that the top-quark contribution will be overwhelming.

Using the doubly GIM reduced loop function for $\tilde{A}$ in Eq. (3.12), in Fig. 3.3 we represented both the top- and the charm-quark contributions to the decay rate $B(K_L \to e\mu)$. From this plot one can see that for the heavy neutrino mass below $m_N \sim 50$ GeV the charm contribution dominates, as correctly stated in [79]. However, when the heavy neutrino mass increases, the non-decoupling effects associated with them start to dominate, and for $m_N \approx 150$ GeV the top contribution will be an order of magnitude greater than the corresponding charm contribution.

We stress again that the dominance of the top quark in this decay was previously overlooked in the literature. A closer investigation of Fig. 3.3 reveals that the curve representing the contribution of the charm-quark to the decay rate for the various heavy neutrino masses m_N is actually identical to the curve presented in Fig. 2. of Ref. [83]. However, this contribution is only the smaller part of the story, the more interesting part is the one

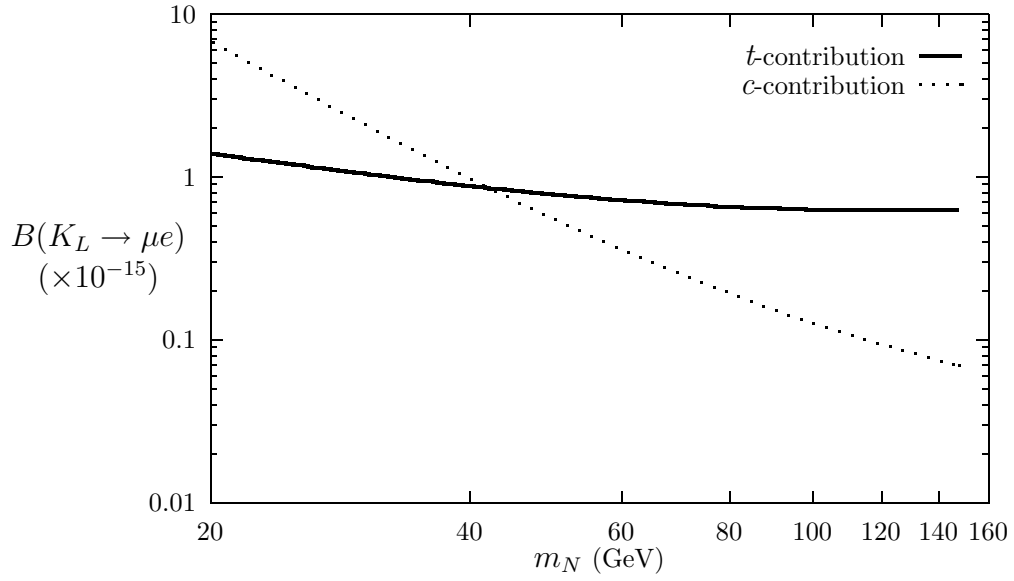

Figure 3.4: Top- and charm-quark contribution to $B(K_L \to e\mu)$ for increasing heavy neutrino mass m_N

corresponding to the top-quark. The interest is motivated basically by the fact that this contribution is the dominant one, however it is of interest to point out the non-decoupling behavior reflected in the *increase* of the branching ratio with the increase of the mass of the heavy neutrino, as one can see in Fig. 3.2. To the contrary of this behavior, the charm-quark contribution displays a monotonous decrease when one goes to regions with more massive heavy neutrinos.

We argued that the heavy top mass plays an important role in giving the dominant contribution to the process under scrutiny. The most relevant aspect is that nature seemed to prefer a top quark significantly heavier than the W and Z bosons. This property is sufficient to place the virtual top quarks to the origin of the decay $K_L \to e\mu$. In the given range, however, the exact value of m_t does not have a critical influence on the decay rate. This question was quantitatively studied giving m_t values in the range $\sim$ 140–200 GeV, and the results are displayed in Fig. 3.3. Although the increase of the branching ratio with the increasing of the top quark mass is obvious, it is also clear that this increase is not at all dramatic, and in no way could lead to observable rates for $K_L \to e\mu$ within the boundaries of the present model.

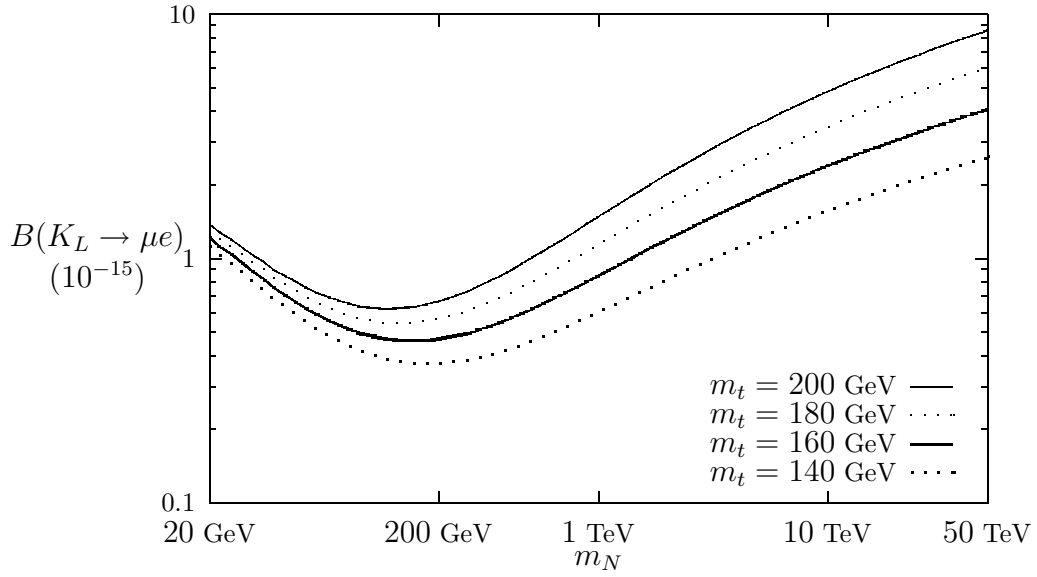

Figure 3.5: The effect of the top mass on the decay rate $B(K_L \to e\mu)$

The main conclusion of this chapter is that the $SU(2)_L \otimes U(1)_Y$ model can not accommodate branching ratios comparable with the existing experimental limit for the process $K_L \to e\mu$, even in the presence of supplementary right-handed neutrinos compared to the Standard Model. However, the presence of non-decoupling effects characteristic to the heavy neutrinos in the model presented led to a value of the branching ratio higher than the one obtained in previous works presented in the literature. An important source for this enhancement proved to be the very heavy top-quark mass.

Presuming that the rare decay $K_L \to e\mu$ will be detected in the foreseeable future with a branching ratio not very far below the present experimental limit, it is absolutely necessary to adopt a different model to provide a theoretical understanding of such a result. In this work we have chosen a left-right symmetric model based on the gauge group $SU(2)_L \otimes SU(2)_L U(1)_{B-L}$ to carry out our calculation. This model constitutes a more complex extension of the Standard Model, with a much richer particle content. In the following chapter we will see that due to the presence of the right-handed gauge interaction the non-decoupling effects are amplified, the model representing a possible framework to provide an observable branching ratio for $K_L \to e\mu$.

Chapter 4

$K_L \to e\mu$ in the left-right symmetric model

We have seen in the previous chapter that the Standard Model based on the $SU(2)_L \otimes U(1)_Y$ gauge group can not provide an observable branching ratio for the process $K_L \to e\mu$, even in the presence of heavy right-handed neutrinos in the model. One can understand this result as a consequence of the severe constraints imposed on the mixings in the leptonic sector by other low energy processes, in particular the non-observation of the radiative muon decay $\mu \to e\gamma$. It is therefore unavoidable to consider interactions beyond the scope of the Standard Model in order to be able to accommodate an eventual evidence for $K_L \to e\mu$ with a branching ratio not far below the present experimental limit.

In this work we have chosen a general left-right symmetric model based on the gauge group $SU(2)_L \otimes SU(2)_R \otimes U(1)_{B-L}$. The main characteristics of this model were presented in Chapter 1. We recall here that this model predicts two charged gauge bosons W_L and W_R, which are generally not mass eigenstates, but the relevant mixing angle is proportional to the vacuum expectation value (v_L) of the left-handed Higgs triplet Δ_L with quantum numbers $(0, 1, 2)$. For simplicity, we will work out the realistic scenario of the vacuum expectation values stressed in Chapter 1, which actually corresponds to the case (d) of Ref. [15], in which $v_L = 0$. In this case, the W_L and W_R bosons become mass eigenstates with masses $M_L = M_W$ and M_R, respectively. As a general feature of the extensions to the Standard Model, in the left-right symmetric model flavor-changing neutral scalar fields

will be also present. They were identified in Chapter 1 as the fields ϕ_2^{0r} and ϕ_2^{0i}. The mass of these particles must be heavy enough to evade the constraints on the flavor-changing neutral current (FCNC) effects.

As a direct consequence of the FCNC couplings of the Higgs particles to the fermions, in the $SU(2)_L \otimes SU(2)_R \otimes U(1)_{B-L}$ model the process $K_L \to e\mu$ can appear already at tree level, and not only at the level of loop contributions. As we will see however, the tree level contribution is suppressed by the heavy Higgs masses, and the one-loop graphs become dominant. It will turn out, that there are graphs at the one-loop level which do not vanish in the infinite Higgs mass limit $m_\phi \to \infty$ and which can produce branching ratios for $K_L \to e\mu$ of the same order of magnitude as the present experimental limit. Given the perspectives of the new experimental facilities, and particularly the measurements at DAPHNE, it is realistic to expect that the statistics needed for improved results will be achieved and that evidence could be found for decays with branching ratios not much below the presently excluded values.

We will start our discussion with considerations about the hadronic matrix elements relevant to our process. Here we will make use of the PCAC theorem to relate the different matrix elements in order to present the results corresponding to different diagrams in a similar way. Then we will discuss briefly the tree level process via flavor changing neutral Higgs particles. As the tree level contribution is suppressed by the mass of these Higgs particles, we will evaluate the one-loop contributions to this process. In order to do this, we will take into account all relevant diagrams, which will have additional right-handed charged gauge bosons ($W_R^\pm$) and additional charged Higgs bosons $h^\pm$ present on the internal lines, compared to the $SU(2)_L \otimes U(1)_Y$ model where only the left-handed charged gauge bosons ($W_L^\pm$) were relevant. Following other works [79] we will evaluate first the relevant box-type diagrams in the Feynman–'t Hooft gauge. We will show how chirality changing diagrams lead to results for the branching ratio $B(K_L \to e\mu)$ comparable with the present experimental limit. Then we will dedicate a chapter to questions regarding gauge invariance and renormalization, and will evaluate the contribution of the gauge complements to the corresponding box diagrams in the Feynman–'t Hooft gauge. The results first obtained in [85] are presented providing a few more details.

4.1 Hadronic matrix elements for $K_L \to e\mu$

In Chapter 3 we introduced the reduced amplitude $\tilde{A}$ for the process $K_L \to e\mu$ through the defining relation given in Eq. (3.8)

$$A = \left(\frac{g_w}{\sqrt{2}}\right)^4 \langle 0|\bar{d}\gamma_\kappa \mathrm{P}_L s|\bar{K}^0\rangle \bar{u}_\mu \gamma^\kappa \mathrm{P}_L v_e \frac{1}{(4\pi)^2}\frac{1}{M_W^2}\tilde{A} \ .$$

The term $\langle 0|\bar{d}\gamma_\kappa \mathrm{P}_L s|\bar{K}^0\rangle \bar{u}_\mu \gamma^\kappa \mathrm{P}_L v_e$ arose from the Lorentz structure present in the expressions for the diagrams given in Fig. 3.1. Adopting the $SU(2)_L \otimes SU(2)_R \otimes U(1)_{B-L}$ model we will encounter various Lorentz structures as we have new interactions present in the theory. The left-handed gauge interaction will have a right-handed counterpart and flavor changing scalar interactions will also be present. It is mandatory then to relate the different hadronic matrix elements if we intend to express our results in an unambiguous way.

In order to relate the different matrix elements we will make use of the ideas of the extended PCAC ("partially conserved axial-vector current") hypothesis, outlined in the following.

In the limit $m_u = m_d = m_s = 0$ the Lagrangian of full QCD can be written in the form

$$\mathcal{L}_{QCD} = \mathcal{L}_{\text{chiral}} - (m_u \bar{u}u + m_d \bar{d}d + m_s \bar{s}s) + \mathcal{L}_{cbt} \ , \tag{4.1}$$

where $\mathcal{L}_{cbt}$ contains terms pertaining only to the quarks c, b and t, and the chiral Lagrangian is expressed as

$$\mathcal{L}_{\text{chiral}} = -\frac{1}{4}G_a^{\mu\nu}G_{a\mu\nu} + \bar{\psi}i\not{D}\psi \ . \tag{4.2}$$

In this expression $G_a^{\mu\nu}$ is the gluon field tensor, the light quarks forming a triplet

$$\psi = \begin{pmatrix} u \\ d \\ s \end{pmatrix} \ , \tag{4.3}$$

and the color indices have been suppressed.

$\mathcal{L}_{\text{chiral}}$ is invariant under the following global symmetry transformations:

$$\begin{aligned} SU(3)_V &: \ \psi \to e^{-i\lambda_a\omega_a/2}\psi \ , \\ U(1)_V &: \ \psi \to e^{-i\alpha}\psi \ , \end{aligned}$$

$$\begin{aligned} SU(3)_A &: \psi \to e^{-i\gamma_5 \lambda_a \theta_a/2}\psi \ , \\ U(1)_A &: \psi \to e^{-i\gamma_5 \beta}\psi, \end{aligned} \tag{4.4}$$

where ω_a, θ_a, α and β are arbitrary real constants, and λ_a stand for the usual Gell-Mann matrices. The subscripts V and A stand respectively for "vector" and "axial-vector". The corresponding Noether currents are respectively

$$\begin{aligned} J^k_\mu &= \bar{\psi}\gamma_\mu \lambda_k \psi \ \ (k = \overline{1,8}) \ \ \text{(isospin current)} \ , \\ j_\mu &= \bar{\psi}\gamma_\mu \psi \ \ \text{(baryonic current)} \ , \\ J^k_{5\mu} &= \bar{\psi}\gamma_\mu \gamma_5 \lambda_k \psi \ \ (k = \overline{1,8}) \ , \\ j_{5\mu} &= \bar{\psi}\gamma_\mu \gamma_5 \psi \ . \end{aligned} \tag{4.5}$$

The baryonic current is conserved even in the perturbed system defined by $\mathcal{L}_{QCD}$. The $SU(3)$ flavor isospin is conserved as long as $m_u = m_d = m_s$. The axial-vector currents are conserved only in the chiral symmetric limit apart from possible anomalies, not discussed here.

These symmetries manifest themselves differently in nature. $SU(3)_V$ is realized directly in the well-known "eight-fold way" suggested by Gell-Mann, i.e. hadrons fall into easy recognizable flavor multiplets. $U(1)_V$ is manifested directly as baryon number conservation in the strong interactions.

On the other hand, a direct manifestation of $SU(3)_A$ would require that each flavor multiplet be accompanied by a mirror multiplet of the same mass, but with opposite parity. There is no hint for this in the hadronic spectrum. For example, there is not even an approximate mirror image of the nucleon iso-doublet. Assuming that the real world is well approximated by the chiral symmetric limit, we must conclude that $SU(3)_A$ is spontaneously broken. This calls for pseudoscalar Goldstone bosons, which we can identify with the "unperturbed" light pseudoscalar mesons. The physical mesons then correspond to the perturbed states of the Goldstone bosons, whose masses come from m_u, m_d and m_s.

Having made these remarks, we can proceed to express the different hadronic matrix elements. As we are interested in particular in the neutral kaon, we can write, using Lorentz invariance and flavor isospin conservation, the only non-vanishing matrix element for the axial-vector current

$$\langle 0|J^{\bar{K}^0}_{5\mu}(x)|\bar{K}^0(p)\rangle = i f_K p_\mu e^{-ip\cdot x} \ , \tag{4.6}$$

where f_K is the kaon decay constant, p_μ is the kaon 4-momentum and the corresponding axial-vector current has the expression

$$J_{5\mu}^{\bar{K}^0}(x) = \bar{d}(x)\gamma^\mu\gamma_5 s(x) \ . \tag{4.7}$$

We can immediately obtain

$$\langle 0|\partial^\mu J_{5\mu}^{\bar{K}^0}(x)|\bar{K}^0(p)\rangle = f_K m_K^2 e^{-ip\cdot x} \ . \tag{4.8}$$

This is consistent with the view that the kaon is a Goldstone boson in the chiral limit, for $\partial_\mu J_{5\mu}^{\bar{K}^0} = 0$ implies $m_K = 0$.

We can define

$$\phi^{\bar{K}^0} \equiv \frac{1}{m_K^2 f_K}\partial^\mu J_{5\mu}^{\bar{K}^0}(x) \ . \tag{4.9}$$

Then

$$\langle 0|\phi^{\bar{K}^0}(x)|\bar{K}^0(p)\rangle = e^{-ip\cdot x} \ . \tag{4.10}$$

Thus, $\phi^{\bar{K}^0}(x)$ can be used as a kaon field operator. It is composed of quark operators, reflecting the bound-state nature of the kaon. The whole content of PCAC is a rule for using $\phi^{\bar{K}^0}(x)$ in the chiral limit ($m_K \to 0$).

Using Eq. (4.7) for the expression of the axial-vector current, we can evaluate the kaon field operator as being

$$\phi^{\bar{K}^0}(x) = \frac{1}{m_K^2 f_K}\left(\bar{d}(x)\overleftarrow{\not\partial}\gamma_5 s(x) - \bar{d}(x)\gamma_5\not\partial s(x)\right) \ . \tag{4.11}$$

Using the equations of motion

$$(i\not\partial - m_s)\, s(x) = 0 \ ; \quad \bar{d}(x)(i\overleftarrow{\not\partial} + m_d) = 0 \ , \tag{4.12}$$

we can write

$$\phi^{\bar{K}^0}(x) = \frac{i(m_d + m_s)}{m_K^2 f_K}\bar{d}(x)\gamma_5 s(x) \ . \tag{4.13}$$

The expression above supplies us with the result for the matrix element $\langle 0|\bar{d}(x)\gamma_5 s(x)|\bar{K}^0(p)\rangle$:

$$\langle 0|\bar{d}(x)\gamma_5 s(x)|\bar{K}^0(p)\rangle = \frac{m_K^2 f_K}{i(m_d + m_s)}e^{-ip\cdot x} \ . \tag{4.14}$$

With this result we can continue to evaluate also matrix elements of different Lorentz structure. In our work it will be important to have the matrix elements with a rank 2 tensor structure. Parity conservation implies that only the $\langle 0|\bar{d}\gamma^\kappa\gamma^\sigma\gamma_5 s|\bar{K}^0\rangle$ matrix element will be non-vanishing. Furthermore, Lorentz invariance implies that this matrix element should be constructed from the only available 4-vector p_μ of the kaon momentum. This means that the matrix element will not have an antisymmetric component in κ and σ, and the symmetric part then can be written using the well-known anticommutation relations of the Dirac γ-matrices

$$\langle 0|\bar{d}\gamma^\kappa\gamma^\sigma\gamma_5 s|\bar{K}^0\rangle = g^{\kappa\sigma}\langle 0|\bar{d}\gamma_5 s|\bar{K}^0\rangle \ . \tag{4.15}$$

In the study of the decay $K_L \to e\mu$ expressions containing the hadronic matrix elements *and* the leptonic spinors appear in the decay amplitude. To evaluate them, we can remark that

$$\langle 0|\bar{d}\gamma^\kappa\gamma_5 s|\bar{K}^0\rangle \bar{u}_\mu(p_\mu)\gamma_\kappa\gamma_5 v_e(p_e) = if_K e^{-ip\cdot x} p^\kappa \bar{u}_\mu(p_\mu)\gamma_\kappa\gamma_5 v_e(p_e) \ . \tag{4.16}$$

As a consequence of momentum conservation, we will have $p = p_\mu + p_e$ and we can take advantage of the equations of motion for the leptonic spinors in the momentum space

$$\bar{u}_\mu(p_\mu)(\not{p}_\mu - m_\mu) = 0 \ ; \quad (\not{p}_e + m_e)v_e(p_e) = 0 \ , \tag{4.17}$$

writing

$$p^\kappa \bar{u}_\mu(p_\mu)\gamma_\kappa\gamma_5 v_e(p_e) = (m_\mu + m_e)\bar{u}_\mu(p_\mu)\gamma_5 v_e(p_e) \ . \tag{4.18}$$

Finally we can write our result as

$$\langle 0|\bar{d}\gamma^\kappa\gamma_5 s|\bar{K}^0\rangle \bar{u}_\mu(p_\mu)\gamma_\kappa\gamma_5 v_e(p_e) = if_K e^{-ip\cdot x}(m_\mu + m_e)\bar{u}_\mu(p_\mu)\gamma_5 v_e(p_e) \ . \tag{4.19}$$

In the decay amplitude for $K_L \to e\mu$ we will encounter the following expressions (in the following we neglect the electron mass compared to that of the muon as $m_e \ll m_\mu$):

$$\langle 0|\bar{d}\gamma^\kappa \mathrm{P}_L s|\bar{K}^0\rangle \bar{u}_\mu(p_\mu)\gamma_\kappa \mathrm{P}_L v_e(p_e) = -\frac{1}{2} if_K m_\mu e^{-ip\cdot x}\bar{u}_\mu(p_\mu)\mathrm{P}_L v_e(p_e) \ . \tag{4.20}$$

Similarly,

$$\langle 0|\bar{d}\gamma^\kappa\gamma^\sigma \mathrm{P}_R s|\bar{K}^0\rangle \bar{u}_\mu(p_\mu)\gamma_\kappa \mathrm{P}_L v_e(p_e) = \frac{1}{2}\frac{m_K^2 f_K}{i(m_d + m_s)} e^{-ip\cdot x} 4\bar{u}_\mu(p_\mu)\mathrm{P}_L v_e(p_e) \ , \tag{4.21}$$

where we used for the Dirac γ matrices

$$g^{\kappa\sigma}\gamma_\kappa\gamma_\sigma = \gamma^\kappa\gamma_\kappa = 4 \ . \tag{4.22}$$

Now we can evaluate the hadronic enhancement factor η used in Eq. (16) of Ref. [67] that results from the different type of operator describing the kaon-to-vacuum matrix element and is defined as

$$\eta \equiv \frac{\langle 0|\bar{d}\gamma^\sigma\gamma^\kappa \mathrm{P}_R s|\bar{K}^0\rangle \bar{u}_\mu \gamma_\sigma \gamma_\kappa \mathrm{P}_L v_e}{\langle 0|\bar{d}\gamma^\alpha \mathrm{P}_L s|\bar{K}^0\rangle \bar{u}_\mu \gamma_\alpha \mathrm{P}_L v_e} \ . \tag{4.23}$$

Using the expressions given in Eq. (4.20) and (4.21) we obtain for this factor

$$\eta = \frac{4M_K^2}{(m_s + m_d)m_\mu} \simeq 50 \ , \tag{4.24}$$

and one can readily see that the kaon decay constant f_K does not actually appear in the final expression.

Taking into account also Eq. (4.14) we can define a second hadronic enhancement factor η' as

$$\eta' \equiv \frac{\langle 0|\bar{d}\mathrm{P}_R s|\bar{K}^0\rangle \bar{u}_\mu \mathrm{P}_L v_e}{\langle 0|\bar{d}\gamma^\alpha \mathrm{P}_L s|\bar{K}^0\rangle \bar{u}_\mu \gamma_\alpha \mathrm{P}_L v_e} \ , \tag{4.25}$$

and we can write it as

$$\eta' = \frac{M_K^2}{(m_s + m_d)m_\mu} = \frac{\eta}{4} \ . \tag{4.26}$$

The two hadronic enhancement factors defined in Eqs. (4.23) and (4.25) (and, as we have seen their expressions, actually the factor η suffices) allow us to express *all* decay amplitudes in the decay $K_L \to e\mu$ relative to the common factor of the external particles encountered in the case of the $SU(2)_L \otimes U(1)_Y$ model, namely $\langle 0|\bar{d}\gamma_\kappa \mathrm{P}_L s|\bar{K}^0\rangle \bar{u}_\mu \gamma^\kappa \mathrm{P}_L v_e$. The strong feature of this procedure is that we can take the advantage of expressing the branching ratio $B(K_L \to e\mu)$ by using isospin invariance relations between the decay amplitudes of $\bar{K}^0 \to \mu^- e^+$ and $K^- \to \mu^- \nu_\alpha$, as done in Chapter 3, being able to use also the very simple relation given in Eq. (3.15).

The ideas of the extended PCAC used in this section are based mainly on the $SU(3)$ flavor symmetry. One can do a similar discussion for the matrix elements of the pion, and then one has to rely only on the $SU(2)$ isospin symmetry (the "usual" PCAC treatment), which is much less broken in nature, and as a consequence the results obtained are much more exact. For our purposes, however, the analysis performed here provides an acceptable result with a sufficient degree of precision.

4.2 $K_L \to e\mu$ at tree level

In the left-right symmetric model chosen by us based on the gauge group $SU(2)_L \otimes SU(2)_R \otimes U(1)_{B-L}$ the process $K_L \to e\mu$ can occur already at tree level. The reason for this are the neutral scalars with flavor-changing couplings to fermions present in the theory. We have seen in Chapter 1 that these Higgs scalars arise from the much more involved symmetry-breaking sector of the theory. If in the case of the Standard Model a single Higgs doublet suffices to break the $SU(2)_L \otimes U(1)_Y$ symmetry, in the left-right symmetric model one has to consider 20 real degrees of freedom (grouped in one bi-doublet and two triplets of different chirality) in order to provide a minimal, but still general pattern[†] for the symmetry breaking. The flavor-changing neutral scalars arise from that neutral component of the Higgs bidoublet which does not develop a vacuum expectation value in the scenarios labeled as "realistic" in Chapter 1, in our convention these are the physically distinct ϕ_2^{0r} and ϕ_2^{0i} fields with their corresponding masses given in Eqs. (1.90) and (1.98)

$$\begin{aligned} m^2_{\phi_2^{0r}} &= \Delta\alpha v_R^2 - \kappa_1^2 \Sigma\lambda \ , \\ m^2_{\phi_2^{0i}} &= \Delta\alpha v_R^2 + \kappa_1^2 \Sigma'\lambda \ . \end{aligned}$$

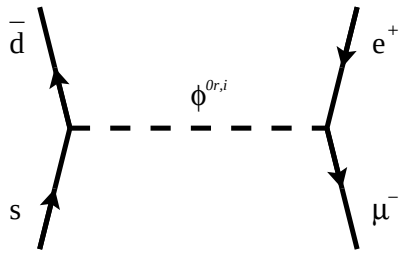

Figure 4.1: Tree level graph for the decay $K_L \to e\mu$

The Feynman diagram corresponding to the tree level $K_L \to e\mu$ decay is depicted in Fig. 4.1. The corresponding decay amplitude can be written as

$$A_{\text{tree}} = \left(\frac{g_w}{\sqrt{2}}\right)^4 \langle 0|\bar{d}\gamma_\kappa \mathrm{P}_L s|\bar{K}^0\rangle \bar{u}_\mu \gamma^\kappa \mathrm{P}_L v_e \frac{1}{(4\pi)^2}\frac{1}{M_W^2}\tilde{A}_{\text{tree}} \ . \tag{4.27}$$

[†]The given pattern is the minimal one which exhibits the general left-right nature of the original symmetry.

Of course, this expression should not be misleading, as the process is naturally only of order $(g_w)^2$, writing it forcing an explicit $(g_w)^4$ serves only the goal of an easier comparison with the result in the $SU(2)_L \otimes U(1)_Y$ model and a more straightforward numerical evaluation. A compensating $\left(\frac{1}{g_w}\right)^2$ factor then should be included in the expression of $\tilde{A}_{\text{tree}}$. Using the Feynman rules given in Appendix A. the dominant contribution to the reduced amplitude corresponding to the exchange of ϕ_2^{0r} at tree level is

$$\tilde{A}^r_{\text{tree}} = -i \left(\frac{4\pi}{g_w}\right)^2 \eta' \sum_{i=c,t} \sum_{\alpha=1}^{2n_G} \frac{(\lambda_i \lambda_\alpha)^{1/2}}{\lambda_{\phi^r}} V^{L*}_{id} V^R_{is} B^L_{\mu\alpha} B^{R*}_{e\alpha} \ , \tag{4.28}$$

where the contribution of the u-quark has been neglected due to its very small mass and $\lambda_{\phi^r} = m^2_{\phi_2^{0r}}/M_L^2$.

The flavor-changing coupling of ϕ_2^{0r} to the d-type quarks and the charged lepton is proportional to the mass of the different u-type quarks and neutrinos, respectively. The factor of proportionality is given by the corresponding left- and right-handed mixing matrices both in the quark and the leptonic sector.

To determine the dominant contribution, we used the maximally allowed values for the Kobayashi-Maskawa matrix elements of the top quark, $V^L_{td} = 0.015$ and $V^L_{ts} = 0.048$, and take the values $V^L_{cd} = 0.220$ and $V^L_{cs} = 0.975$ for the corresponding matrix elements of the charm quark. Taking the masses $m_c = 1.35$ GeV and $m_t = 180$ GeV we obtain

$$\lambda_t = 5.03 \qquad \lambda_t^{1/2} V^L_{td} = 0.034 \qquad \lambda_t^{1/2} V^L_{ts} = 0.108 \tag{4.29}$$

$$\lambda_c = 2.8 \cdot 10^{-4} \quad \lambda_c^{1/2} V^L_{cd} = 3.7 \cdot 10^{-3} \quad \lambda_c^{1/2} V^L_{cs} = 0.016 \ . \tag{4.30}$$

If we work in a non-explicitly left-right symmetric model, the right-handed quark mixing matrix elements can evade some constraints and can be taken close to unity. In this case it is clear that the dominant contribution comes from those parts of the flavor-changing coupling to the quarks which are proportional to the top-quark mass.

The non-observation of the decay $\mu \to e\gamma$ imposes a constraint on the leptonic mixing matrix elements, which will obey the relation

$$\left| B^R_{\mu\alpha} B^L_{e\alpha} \right| \leq \frac{1.18 \cdot 10^{-4}}{\sqrt{\beta}} \ . \tag{4.31}$$

The physics contained in this relation is that the heavier the right-handed gauge boson W_R gets, the weaker the constraints on the right-handed leptonic mixings B^R become

(we should remember that the constraints on the left-handed mixings B^L are essentially independent of M_R).

Using the presently accepted experimental limit for $B(K_L \to e\mu) \leq 4.7 \cdot 10^{-12}$ we can try to impose constraints on the mass of the flavor changing Higgs scalar. In order to compare our result to other values given in the literature, we will consider the case of an explicitly left-right symmetric model with $V^L = V^R$. With the presumption that the flavor-changing scalars are nearly degenerate $m_{\phi^r} \simeq m_{\phi^i} \simeq m_\phi$ and considering typical values for the heavy neutrino mass $m_N = 10$ TeV and the right-handed gauge boson mass $M_R = 1$ TeV, we obtain

$$\lambda_\phi^2 \geq 4.5 \cdot 10^8 \left(\frac{V_{td}}{0.015}\right)^2 \left(\frac{V_{ts}}{0.048}\right)^2 \left(\frac{m_N}{10\ \text{TeV}}\right)^2 \left(\frac{M_R}{1\ \text{TeV}}\right)^2 \left(\frac{s^\nu}{0.01}\right)^2 . \tag{4.32}$$

This result allows us to impose a lower bound on the flavor-changing Higgs mass of $m_\phi \geq 12$ TeV. In fact we can display the dependence of this bound on the heavy neutrino mass m_N and the right-handed gauge boson mass M_R:

$$m_{\phi_2^{0r}} \geq 12 \left(\frac{V_{td}}{0.015}\right)^{1/2} \left(\frac{V_{ts}}{0.048}\right)^{1/2} \left(\frac{m_N}{10\ \text{TeV}}\right)^{1/2} \left(\frac{M_R}{1\ \text{TeV}}\right)^{1/2} \left(\frac{s^\nu}{0.01}\right)^{1/2} \text{TeV} . \tag{4.33}$$

In is interesting to note here that this bound on m_ϕ is much more constraining that the one resulting from the observed $K_L - K_S$ mass difference. The authors of Ref. [86] argue that using the vacuum-insertion method to calculate the $K^0 - \bar{K}^0$ transition-matrix element of the $(\bar{d}\gamma_5 s)(\bar{d}\gamma_5 s)$ operator in a diagram similar to that presented in Fig. 4.1, the smallness of the $K_L - K_S$ mass difference will set a lower bound on the exchanged flavor-changing Higgs mass of

$$m_\phi > 8.5\ \text{TeV} . \tag{4.34}$$

We must stress, however, that the bound on m_ϕ derived from $K_L \to e\mu$ is just an approximate one, as we based our estimates on maximally allowed values of the mixing parameters. A lighter flavor changing neutral Higgs particle could be easily accommodated in the theory by smaller values for these mixings. This being said, we will take more seriously the bound derived from the observed $K_L - K_S$ mass difference.

There is, however, no physical reason why the flavor changing Higgses should not be considerably heavier than their lower bound. For $m_\phi \sim 20$ TeV the allowed branching

ratio is already suppressed by two additional orders of magnitude, decreasing to a value of $\sim 10^{-13}$.

Our main conclusion at this point is that the decay $K_L \to e\mu$ is not the right place to look in order to place a lower bound on the masses of the participating Higgs scalars, as more reliable constraints exist from the smallness of the $K_L - K_S$ mass difference. As heavy scalars are not at all excluded from the theory (we must be aware that even the formal limit $m_\phi \to \infty$ makes sense) one can conclude that one loop corrections can play an important role in the description of $K_L \to e\mu$. In what follows we will turn our attention to such contributions.

4.3 $K_L \to e\mu$ at one loop level

In Chapter 3 the branching ratio of the decay $K_L \to e\mu$ was calculated in the Standard Model with heavy neutrinos. There the process could occur only at the one-loop level through the non-vanishing mixings between the leptons. In the left-right symmetric model the decay can take place already at tree level, but as we have seen in the previous section, the heavy flavor-changing neutral Higgs particles suppress the branching ratio by orders of magnitude below the present experimental limit. It is of interest therefore to study the one-loop contributions also in the left-right symmetric model.

The theory based on the $SU(2)_L \otimes SU(2)_R \otimes U(1)_{B-L}$ gauge group has new, right-handed gauge interactions and an extended Higgs sector, correspondingly there will be an increased number of one-loop diagrams contributing to $K_L \to e\mu$. In order to keep track of all possible diagrams it is convenient to place them in distinct groups and to study them separately. Our choice is to study gauge independent sets of diagrams. In the following we will display these sets in the unitary gauge (i.e. only the diagrams with physical particles).

The diagrams in the group A. are displayed in Fig. 4.2. One can immediately recognize that diagram (a) corresponds to the one present in the Standard Model. Diagram (b) can be obtained from (a) simply replacing everywhere $W_L^\pm$ with $W_R^\pm$ and it is a direct consequence of the left-right symmetry. Finally diagram (c) arises due to the presence of the charged Higgs scalars $h^\pm$ in the theory.

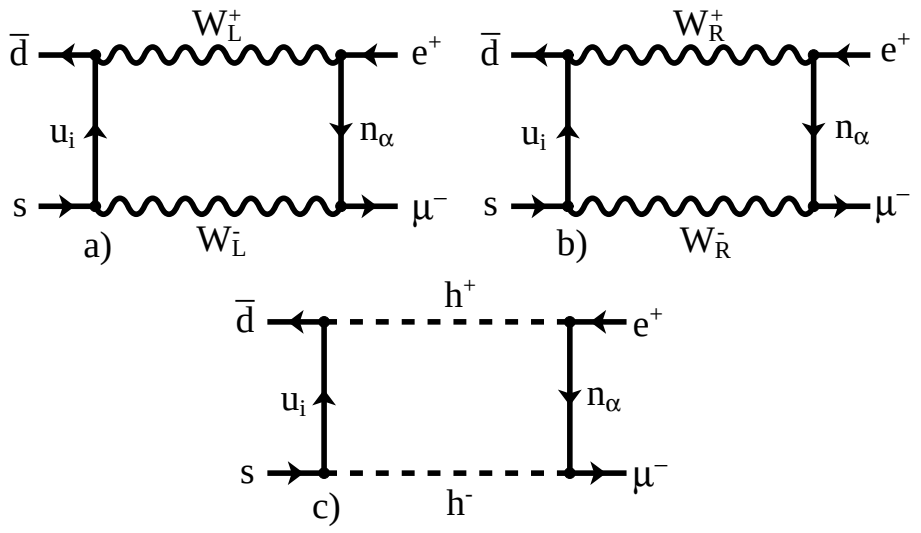

Figure 4.2: Gauge invariant set of diagrams contributing to $K_L \to e\mu$ in the $SU(2)_L \otimes SU(2)_R \otimes U(1)_{B-L}$ model. Group A.

The diagrams in group A. are gauge independent by themselves. The physical reason for this is that diagram (a) represents a physical quantity and it gives the decay amplitude in the limit $M_R \to \infty$. That diagram (b) is gauge invariant follows then from the left-right symmetry. Finally, diagram (c) has no gauge dependence at all.

On a different line of reasoning, in a renormalizable R_ξ gauge one always has the freedom to choose different gauge parameters ξ_L and ξ_R for the left- and right-handed gauge bosons. Diagrams (a) and (b) will then involve propagators with different gauge parameters, i.e. unrelated to each other. As these are the only diagrams with two W-s with the same chirality, their final gauge independence follows.

In Fig. 4.3 a second set of diagrams is displayed. These diagrams contain two charged gauge bosons of different chirality in the internal lines. This group has actually two symmetrical subsets, obtained simply by interchanging $W_L \longleftrightarrow W_R$.

Group B. tells us a little bit more about the complexity of the model. Besides the usual box-diagrams (a and b) there will be vertex-type diagrams (c–f) and self-energy type diagrams (g and h). The latter two arise from the non-vanishing $\phi_2^0 - W_L - W_R$ coupling[†].

[†]There is no $\phi_2^0 - W_L - W_L$ or $\phi_2^0 - W_R - W_R$ coupling in the theory

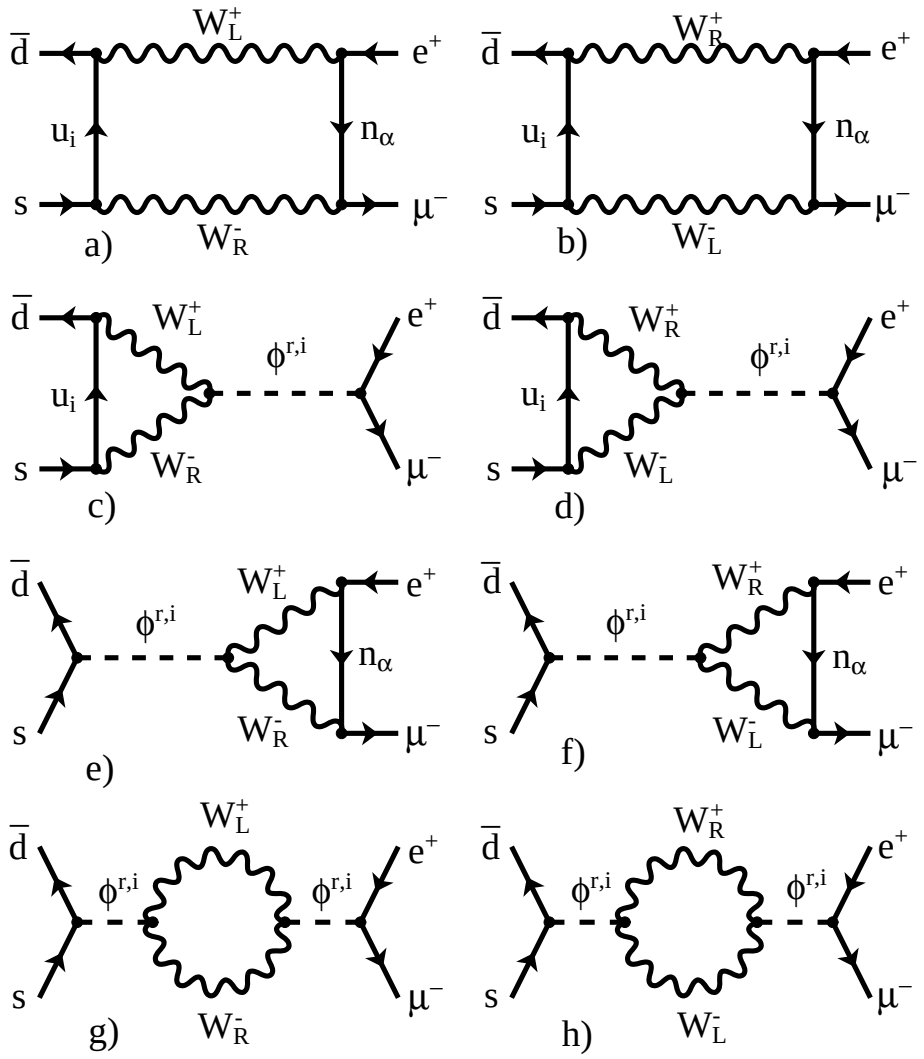

Figure 4.3: Gauge invariant set of diagrams contributing to $K_L \to e\mu$ in the $SU(2)_L \otimes SU(2)_R \otimes U(1)_{B-L}$ model. Group B.

Diagrams (c–h) of group B. are divergent, as they represent contributions to the vertex- and neutral Higgs self-energy counterterms in the theory. This means that we will need to go through a renormalization procedure in order to obtain finite results. The most interesting feature is that this renormalization procedure is needed also to show that group B. is actually a gauge invariant subset of diagrams. If the gauge invariance of group A. was more or less a trivial problem, in this case one could worry about the diagrams (c–h), which contain the flavor-changing neutral Higgs bosons not present in the box-graphs (a) and (b). At the first glance one could think that the vertex- and self-energy type diagrams are suppressed by one, correspondingly two heavy scalar propagators and that they could not cancel the gauge dependence of the box graphs. However, in a renormalizable R_ξ gauge the coupling of the scalars to the left- and right-handed unphysical Goldstone bosons is itself proportional to m_ϕ^2, this coupling canceling in the $p = 0$ limit of the momentum transfer the suppression coming from the heavy propagators. The exact mechanism of the gauge cancelations will be outlined in the next chapter.

We have seen in the discussion of the first group of diagrams that one can freely choose independent gauge parameters ξ_L and ξ_R for the left- and right-handed gauge interactions in a general renormalizable gauge R_ξ. Then we can be sure that there will be no gauge-dependent contributions coming from other sets of diagrams depending on both ξ_L and ξ_R, as only the diagrams in group B. will have W_L and W_R appearing simultaneously.

Fig. 4.4 displays a set of diagrams specific to our left-right symmetric model. The box-diagrams of group A. with the identical gauge bosons as well as the entire set of diagrams in Fig. 4.3 are mandatory for all such models, as their presence is required by the existence of the W_L and W_R bosons. Diagrams with charged Higgs particles $h^\pm$ on the other hand are required by the particular pattern of the symmetry breaking in our case. The $SU(2)_L \otimes SU(2)_R \otimes U(1)_{B-L}$ symmetry can be broken with a simpler Higgs sector compared to the one presented in Chapter 1, so that no such charged scalars are present. Our realistic scenario however is much more consistent with the presence of heavy neutrinos in the theory.

Similarly to group B., the non-vanishing $\phi_2^0 - W_L - h$ coupling leads to the existence of the vertex- and self-energy type graphs (c–h). As a further similarity, our discussion in the previous case about divergences, renormalization and gauge independence stands valid

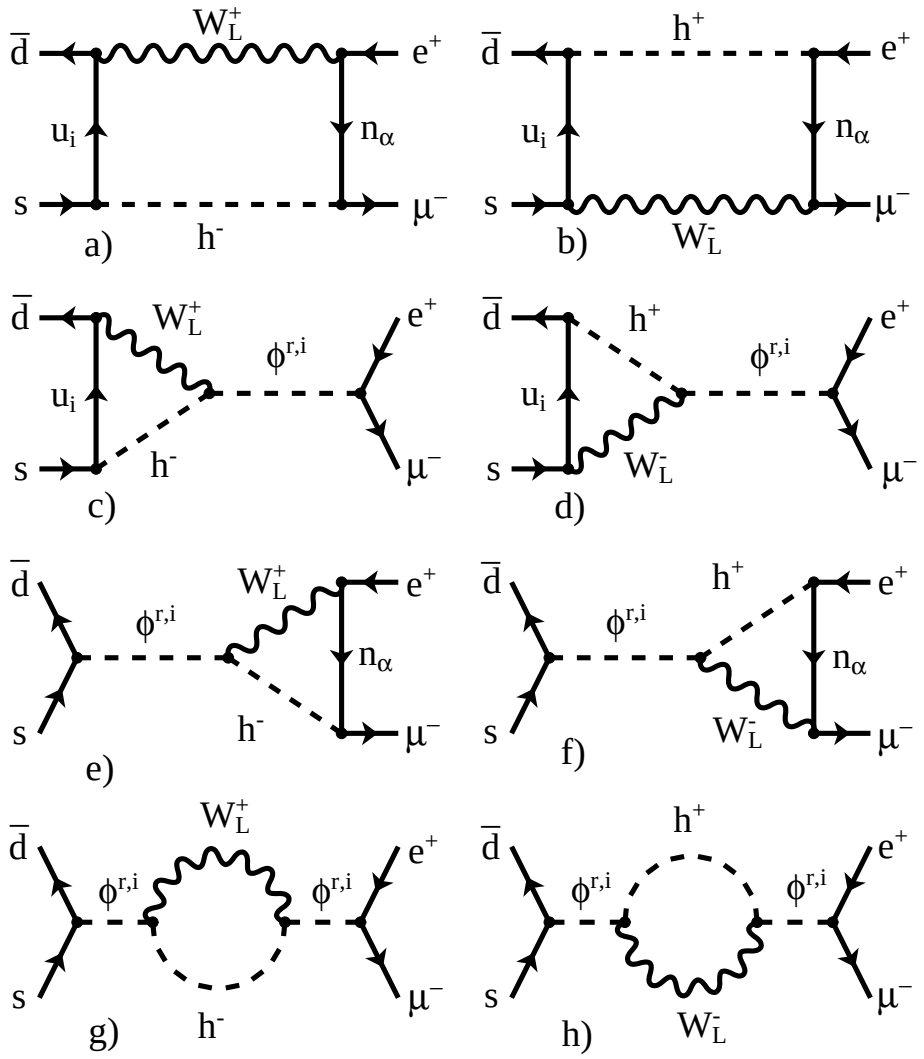

Figure 4.4: Gauge invariant set of diagrams contributing to $K_L \to e\mu$ in the $SU(2)_L \otimes SU(2)_R \otimes U(1)_{B-L}$ model. Group C.

in this case too. The only remark one should make is that the gauge cancelations in this case will turn out to be more cumbersome, mainly because the coupling to the unphysical Goldstone boson $\phi_2^0 - G_L - h$ will be proportional to $m_\phi^2 - m_h^2$ instead of m_ϕ^2, and the Higgs propagator will not disappear in the $p = 0$ momentum transfer limit. We will see however that with a proper renormalization procedure this inconvenience can be passed and the gauge invariance of this set of graphs can be proved.

It is again easy to convince ourselves that the gauge structure which appears in this group of diagrams can be cancelled only by diagrams with one internal W_L (because of the gauge parameter ξ_L) and an internal charged Higgs h (because of the m_h dependence). However, there are no other diagrams besides the ones depicted in Fig. 4.4.

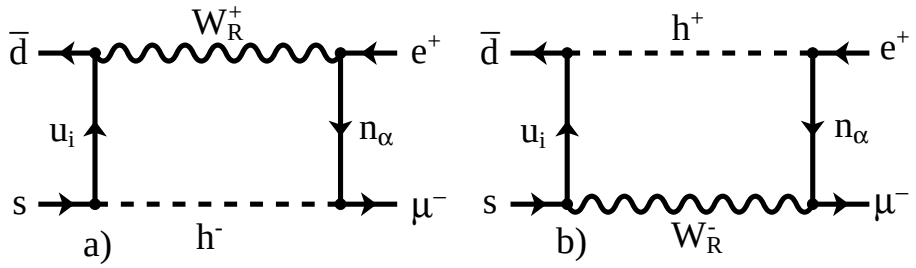

Figure 4.5: Gauge invariant set of diagrams contributing to $K_L \to e\mu$ in the $SU(2)_L \otimes SU(2)_R \otimes U(1)_{B-L}$ model. Group D.

The last type of diagrams considered will be those in Fig. 4.5. They correspond to the diagrams of group C., when one substitutes W_L with W_R. However, the coupling $\phi_2^0 - W_R - h$ vanishes in our model, which means that there will be no vertex- and self-energy type diagrams present in this group, only the finite box-graphs will contribute.

The graphs presented in Fig. 4.2–4.5 will give the leading contribution to one-loop level to $K_L \to e\mu$. We are aware of the fact that at one loop level there are also other possible graphs present. Fig. 4.6 shows some examples of them. Diagram (a) represents a tadpole contribution to the neutral Higgs mass counterterm. There are effectively hundreds of possible tadpole graphs in an arbitrary gauge. Strictly speaking these graphs should belong either to group B. or C. and then these would become gauge independent *before* renormalization. It is more convenient however to require gauge invariance *after*

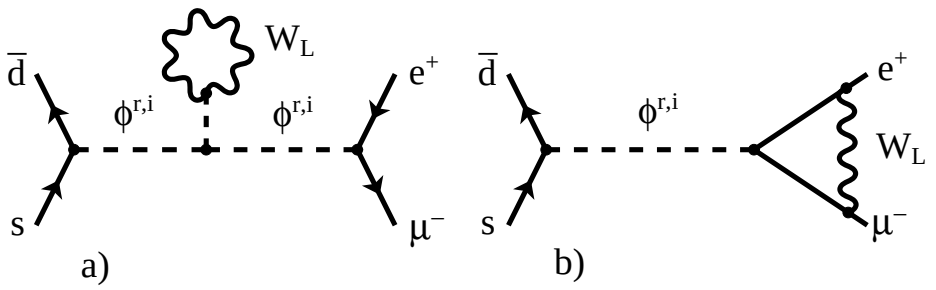

Figure 4.6: Additional one-loop diagrams: tadpoles (a) and corrections on external legs (b)

renormalization, as the momentum-independent tadpoles vanish during the corresponding subtractions. This means that one can forget the tadpoles from the very beginning.

Diagram (b) on the other hand is representative for radiative corrections applied on the external legs of the tree-level diagram. Beside the vertex corrections there exist also the fermion self-energies, not shown here. After proper renormalization these diagrams contribute only to the physical vertex coupling and the masses of the fermions respectively, and the corresponding diagrams will be suppressed by the heavy neutral Higgs mass.

One could also consider diagrams contributing to the neutral Higgs self-energy through fermionic loops. These diagrams are gauge independent by themselves, but they will also be suppressed by the heavy mass of the scalar, as the coupling to the fermions is proportional to the fermion masses.

At this point we have identified all possible one-loop contributions to $K_L \to e\mu$. The one-loop decay amplitude for the process will be given then by the sum of all relevant diagrams,

$$A_{\text{1-loop}} = \left(\frac{g_w}{\sqrt{2}}\right)^4 \langle 0|\bar{d}\gamma_\kappa \mathrm{P}_L s|\bar{K}^0\rangle \bar{u}_\mu \gamma^\kappa \mathrm{P}_L v_e \frac{1}{(4\pi)^2}\frac{1}{M_W^2}\tilde{A}_{\text{1-loop}} \ , \tag{4.35}$$

where the reduced 1-loop amplitude is

$$\tilde{A}_{\text{1-loop}} = \tilde{A}_A + \tilde{A}_B + \tilde{A}_C + \tilde{A}_D \ , \tag{4.36}$$

containing the corresponding contributions from the different groups of diagrams.

4.4 Box diagrams

In a general left-right symmetric model based on the gauge group $SU(2)_R \otimes SU(2)_L \otimes U(1)_{B-L}$ an enhancement for the process $K_L \to e\mu$ can be obtained compared to the Standard Model. In the literature usually the contribution of the box-graphs is evaluated [79], and then the contribution of the gauge complement graphs is estimated. In order to compare our results with the previously obtained ones, we will follow this procedure.

The advantage of this treatment is that the box diagrams are finite and one does not need to take into account any renormalization procedure. The diagrams can be evaluated in the Feynman–'t Hooft gauge. Compared to the diagrams depicted in the unitary gauge, diagrams with additional non-physical Goldstone bosons replacing the gauge bosons in the internal lines must be taken into account, which means that the number of diagrams will increase compared to the ones presented in Fig. 4.2–4.5, but with the advantage of an easier computation for the relevant loop functions.

4.4.1 Box diagrams. Group A.

The contributions to $\tilde{A}_A$ come from the three diagrams in Fig 4.2:

$$\tilde{A}_A = \tilde{A}_A^a + \tilde{A}_A^b + \tilde{A}_A^c \ . \tag{4.37}$$

$\tilde{A}_A^a$ corresponds to the amplitude evaluated in Chapter 3. In Eq. (3.12) we obtained the expression

$$\tilde{A}_A = \sum_{i=c,t} V_{id}^* V_{is} \sum_{\alpha=n_G+1}^{2n_G} B_{\mu\alpha}^L B_{e\alpha}^{L*} E(\lambda_i, \lambda_\alpha) \ ,$$

with

$$\begin{aligned} E(\lambda_i, \lambda_\alpha) \ &= \ \lambda_i \lambda_\alpha \left\{ -\frac{3}{4} \frac{1}{(1-\lambda_i)(1-\lambda_\alpha)} \right. \\ &+ \left[\frac{1}{4} - \frac{3}{2} \frac{1}{\lambda_i - 1} - \frac{3}{4} \frac{1}{(\lambda_i - 1)^2} \right] \frac{\ln \lambda_i}{\lambda_i - \lambda_\alpha} \\ &+ \left. \left[\frac{1}{4} - \frac{3}{2} \frac{1}{\lambda_\alpha - 1} - \frac{3}{4} \frac{1}{(\lambda_\alpha - 1)^2} \right] \frac{\ln \lambda_\alpha}{\lambda_\alpha - \lambda_i} \right\} \ . \end{aligned}$$

$\tilde{A}_A^b$ corresponds to the amplitude $\tilde{A}_{RR}$ given in Eq. (19) of Ref. [67], and it can be expressed in terms of the same loop function E as

$$\tilde{A}_A^b = \beta^2 \sum_{i=c,t} V_{id}^{R*} V_{is}^R \sum_{\alpha=n_G+1}^{2n_G} B_{\mu\alpha}^R B_{e\alpha}^{R*} E(\beta\lambda_i, \beta\lambda_\alpha) \ , \tag{4.38}$$

where we recall the definition $\beta = M_L^2/M_R^2$.

$\tilde{A}_A^c$ was previously not given in the literature and it can be written as

$$\begin{aligned} \tilde{A}_A^c &= \sum_{i=u,c,t} V_{id}^{R*} V_{is}^R \sum_{\alpha=n_G+1}^{2n_G} \sum_{\gamma=n_G+1}^{2n_G} \sum_{\delta=n_G+1}^{2n_G} B_{\mu\alpha}^R B_{e\alpha}^{R*} \lambda_i (\lambda_\gamma \lambda_\delta)^{1/2} \\ &\quad \times (s_\beta^2 \delta_{\gamma\alpha} - C_{\gamma\alpha}^L)(s_\beta^2 \delta_{\delta\alpha} - C_{\delta\alpha}^{L*}) I_A^c(\lambda_i, \lambda_\alpha, \lambda_h) \ , \end{aligned} \tag{4.39}$$

where we defined $\lambda_h = m_h^2/M_W^2$ and the loop integral I_A^c is

$$I_A^c(\lambda_i, \lambda_\alpha, \lambda_h) \stackrel{def}{=} \frac{1}{4} \frac{(4\pi)^2}{i} M_L^2 \int \frac{d^4k}{(2\pi)^4} \frac{k^2}{(k^2 - m_{u_i}^2)(k^2 - m_{n_\alpha}^2)(k^2 - m_h^2)^2} \ , \tag{4.40}$$

leading to

$$\begin{aligned} I_A^c(\lambda_i, \lambda_\alpha, \lambda_h) &= -\frac{1}{4} \left[\frac{\lambda_i^2 \ln \lambda_i}{(\lambda_i - \lambda_h)^2 (\lambda_i - \lambda_\alpha)} + \frac{\lambda_\alpha^2 \ln \lambda_\alpha}{(\lambda_\alpha - \lambda_h)^2 (\lambda_\alpha - \lambda_i)} \right. \\ &\quad + \frac{\lambda_h \ln \lambda_h}{(\lambda_h - \lambda_i)(\lambda_\alpha - \lambda_h)} \left(\frac{\lambda_i}{\lambda_h - \lambda_i} - \frac{\lambda_\alpha}{\lambda_\alpha - \lambda_h} \right) \\ &\quad \left. + \frac{\lambda_h}{(\lambda_h - \lambda_i)(\lambda_h - \lambda_\alpha)} \right] \ . \end{aligned} \tag{4.41}$$

We can apply the GIM mechanism to the amplitude given in Eq. (4.39). Then we can neglect the contribution of the internal u-quark, and write

$$\begin{aligned} \tilde{A}_A^c &= \sum_{i=c,t} V_{id}^{R*} V_{is}^R \sum_{\alpha=n_G+1}^{2n_G} \sum_{\gamma=n_G+1}^{2n_G} \sum_{\delta=n_G+1}^{2n_G} B_{\mu\alpha}^R B_{e\alpha}^{R*} \lambda_i^2 (\lambda_\gamma \lambda_\delta)^{1/2} \\ &\quad \times (s_\beta^2 \delta_{\gamma\alpha} - C_{\gamma\alpha}^L)(s_\beta^2 \delta_{\delta\alpha} - C_{\delta\alpha}^{L*}) E^h(\lambda_i, \lambda_\alpha, \lambda_h) \ , \end{aligned} \tag{4.42}$$

with the GIM-reduced loop function given by the relation

$$\begin{aligned} E^h(\lambda_i, \lambda_\alpha, \lambda_h) &= -\frac{1}{4} \left[\frac{\lambda_i \ln \lambda_i}{(\lambda_i - \lambda_h)^2 (\lambda_i - \lambda_\alpha)} + \frac{\lambda_\alpha \ln \lambda_\alpha}{(\lambda_\alpha - \lambda_h)^2 (\lambda_\alpha - \lambda_i)} \right. \\ &\quad + \frac{\ln \lambda_h}{(\lambda_h - \lambda_i)(\lambda_\alpha - \lambda_h)} \left(\frac{\lambda_h}{\lambda_h - \lambda_i} - \frac{\lambda_\alpha}{\lambda_\alpha - \lambda_h} \right) \\ &\quad \left. + \frac{1}{(\lambda_h - \lambda_i)(\lambda_h - \lambda_\alpha)} \right] \ . \end{aligned} \tag{4.43}$$

4.4.2 Box diagrams. Group B.

The box-graphs belonging to group B. are presented in diagrams (a) and (b) of Fig. 4.3. In consequence we can write

$$\tilde{A}_B = \tilde{A}_B^a + \tilde{A}_B^b \ . \tag{4.44}$$

In the Feynman–'t Hooft gauge the non-physical Goldstone bosons will also appear in the internal lines, increasing the number of diagrams to be considered. As group B. presents the richest gauge structure with both W_L and W_R involved, we present the box-graphs including the non-physical particles in Fig. 4.7.

Summing all the individual contributions we obtain:

$$\begin{aligned}
\tilde{A}_B^a &= \beta\eta \sum_{i=c,t} V_{id}^{L*} V_{is}^{R} \sum_{\alpha=n_G+1}^{2n_G} B_{\mu\alpha}^{R} B_{e\alpha}^{L*} (\lambda_i\lambda_\alpha)^{1/2} \\
&\quad \times \left[\left(1 + \frac{\beta\lambda_i\lambda_\alpha}{4} \right) J_1(\lambda_i, \lambda_\alpha, \beta) - \frac{1+\beta}{4} J_2(\lambda_i, \lambda_\alpha, \beta) \right] \ , \qquad (4.45) \\
\tilde{A}_B^b &= \beta\eta \sum_{i=c,t} V_{id}^{R*} V_{is}^{L} \sum_{\alpha=n_G+1}^{2n_G} B_{\mu\alpha}^{L} B_{e\alpha}^{R*} (\lambda_i\lambda_\alpha)^{1/2} \\
&\quad \times \left[\left(1 + \frac{\beta\lambda_i\lambda_\alpha}{4} \right) J_1(\lambda_i, \lambda_\alpha, \beta) - \frac{1+\beta}{4} J_2(\lambda_i, \lambda_\alpha, \beta) \right] \ . \qquad (4.46)
\end{aligned}$$

The box functions J_1 and J_2 are given by

$$\begin{aligned}
J_1(\lambda_i, \lambda_\alpha, \beta) &= \frac{\lambda_i \ln\lambda_i}{(1-\lambda_i)(1-\beta\lambda_i)(\lambda_\alpha-\lambda_i)} + \frac{\lambda_\alpha \ln\lambda_\alpha}{(1-\lambda_\alpha)(1-\beta\lambda_\alpha)(\lambda_i-\lambda_\alpha)} \\
&+ \frac{\beta \ln\beta}{(1-\beta)(1-\beta\lambda_i)(1-\beta\lambda_\alpha)} \ , \\
J_2(\lambda_i, \lambda_\alpha, \beta) &= \frac{\lambda_i^2 \ln\lambda_i}{(1-\lambda_i)(1-\beta\lambda_i)(\lambda_\alpha-\lambda_i)} + \frac{\lambda_\alpha^2 \ln\lambda_\alpha}{(1-\lambda_\alpha)(1-\beta\lambda_\alpha)(\lambda_i-\lambda_\alpha)} \\
&+ \frac{\ln\beta}{(1-\beta)(1-\beta\lambda_i)(1-\beta\lambda_\alpha)} \ . \qquad (4.47)
\end{aligned}$$

The resulting expression for $\tilde{A}_B$ corresponds to the expression given to $\tilde{A}_{LR}$ in Eq. (15) of Ref. [67], if one identifies the quantity $\beta_g = (g_R^2/g_L^2)M_L^2/M_R^2$ with β, which can be performed by choosing the coupling constants related to the gauge groups $SU(2)_L$ and $SU(2)_R$, $g_L = g_w$ and g_R respectively, to be equal, as it was done in Chapter 1. We can also see that the hadronic enhancement factor η introduced in Sec. 4.1 appears in the final expression. The main reason for this is the presence of the gauge interactions with mixed chirality.

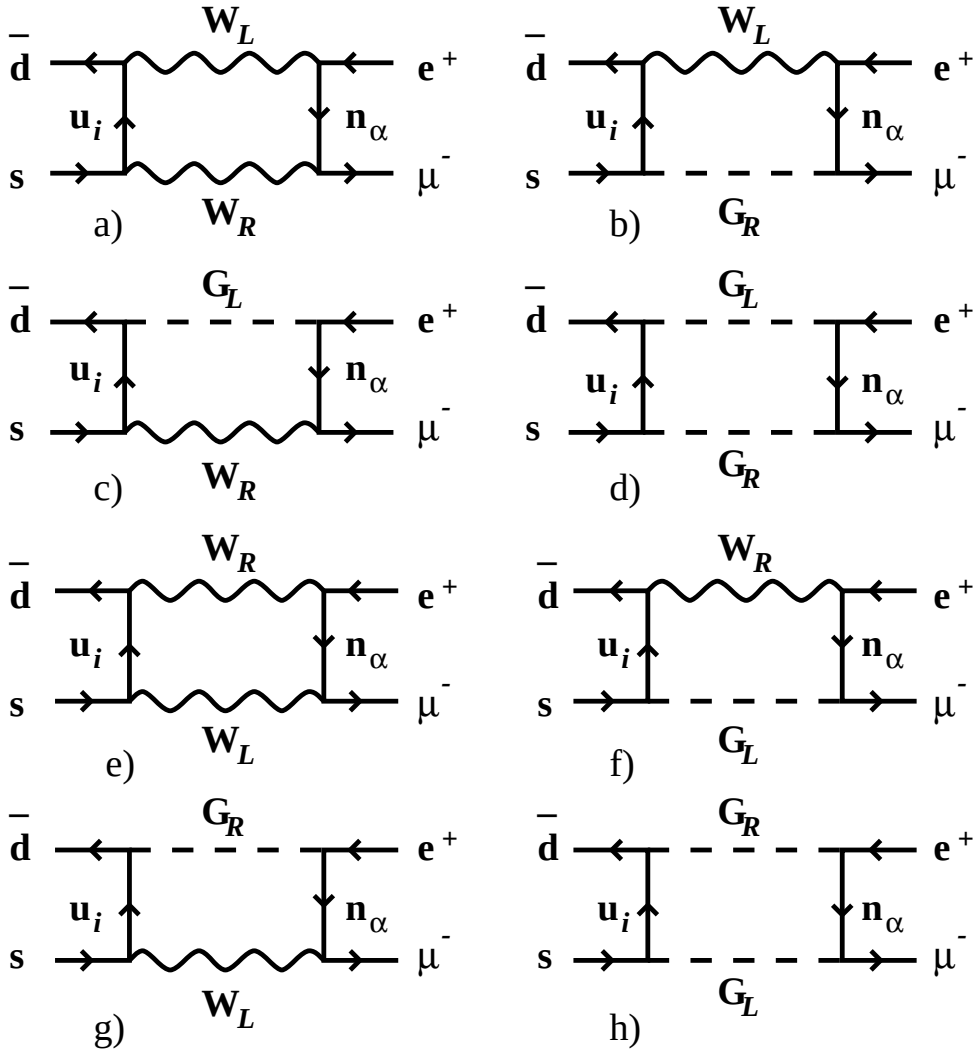

Figure 4.7: Box diagrams of group B. in the Feynman–'t Hooft gauge

4.4.3 Box diagrams. Group C.

Following our notation, we have

$$\tilde{A}_C = \tilde{A}_C^a + \tilde{A}_C^b \ . \tag{4.48}$$

The corresponding expressions for the two contributions are

$$\begin{aligned}
\tilde{A}_C^a &= \eta \sum_{i=c,t} V_{id}^{L*} V_{is}^R \sum_{\alpha=n_G+1}^{2n_G} \sum_{\gamma=n_G+1}^{2n_G} B_{\mu\gamma}^R B_{e\alpha}^{L*} (\lambda_i \lambda_\gamma)^{1/2} (s_\beta^2 \delta_{\gamma\alpha} - C_{\gamma\alpha}^L) \\
&\quad \times \left[I_1^C(\lambda_i, \lambda_\alpha, \lambda_h) - \frac{1}{4} \lambda_i \lambda_\alpha I_2^C(\lambda_i, \lambda_\alpha, \lambda_h) \right] \ , \qquad (4.49) \\
\tilde{A}_C^b &= \eta \sum_{i=c,t} V_{id}^{R*} V_{is}^L \sum_{\alpha=n_G+1}^{2n_G} \sum_{\gamma=n_G+1}^{2n_G} B_{\mu\alpha}^L B_{e\gamma}^{R*} (\lambda_i \lambda_\gamma)^{1/2} (s_\beta^2 \delta_{\gamma\alpha} - C_{\gamma\alpha}^{L*}) \\
&\quad \times \left[I_1^C(\lambda_i, \lambda_\alpha, \lambda_h) - \frac{1}{4} \lambda_i \lambda_\alpha I_2^C(\lambda_i, \lambda_\alpha, \lambda_h) \right] \ , \qquad (4.50)
\end{aligned}$$

where the loop integrals are defined as

$$I_1^C(\lambda_i, \lambda_\alpha, \lambda_h) \stackrel{def}{=} \frac{1}{4} \frac{(4\pi)^2}{i} M_L^2 \int \frac{d^4k}{(2\pi)^4} \frac{k^2}{(k^2 - m_{u_i}^2)(k^2 - m_{n_\alpha}^2)(k^2 - m_h^2)(k^2 - M_L^2)} \ , \tag{4.51}$$

$$I_2^C(\lambda_i, \lambda_\alpha, \lambda_h) \stackrel{def}{=} \frac{(4\pi)^2}{i} M_L^4 \int \frac{d^4k}{(2\pi)^4} \frac{1}{(k^2 - m_{u_i}^2)(k^2 - m_{n_\alpha}^2)(k^2 - m_h^2)(k^2 - M_L^2)} \ , \tag{4.52}$$

leading to the expressions

$$\begin{aligned}
I_1^C(\lambda_i, \lambda_\alpha, \lambda_h) &= -\frac{1}{4} \left[\frac{\lambda_i^2 \ln \lambda_i}{(\lambda_i - \lambda_h)(\lambda_i - 1)(\lambda_i - \lambda_\alpha)} + \frac{\lambda_\alpha^2 \ln \lambda_\alpha}{(\lambda_\alpha - \lambda_h)(\lambda_\alpha - 1)(\lambda_\alpha - \lambda_i)} \right. \\
&\quad \left. + \frac{\lambda_h^2 \ln \lambda_h}{(\lambda_h - 1)(\lambda_h - \lambda_i)(\lambda_h - \lambda_\alpha)} \right] \ , \qquad (4.53) \\
I_2^C(\lambda_i, \lambda_\alpha, \lambda_h) &= \frac{\lambda_i \ln \lambda_i}{(\lambda_i - \lambda_h)(\lambda_i - 1)(\lambda_i - \lambda_\alpha)} + \frac{\lambda_\alpha \ln \lambda_\alpha}{(\lambda_\alpha - \lambda_h)(\lambda_\alpha - 1)(\lambda_\alpha - \lambda_i)} \\
&\quad + \frac{\lambda_h \ln \lambda_h}{(\lambda_h - 1)(\lambda_h - \lambda_i)(\lambda_h - \lambda_\alpha)} \ . \qquad (4.54)
\end{aligned}$$

In Eqs. (4.49) and (4.50) we kept an explicit 1/4 factor in front of the second loop integral I_2^C in order to remember it originates from the hadronic enhancement factor $\eta' = \eta/4$.

4.4.4 Box diagrams. Group D.

The two box diagrams in Fig. 4.5 will give a total contribution

$$\tilde{A}_D = \tilde{A}_D^a + \tilde{A}_D^b \ . \tag{4.55}$$

For the individual diagrams we will obtain

$$\begin{aligned}\tilde{A}_D^a &= \sum_{i=c,t} V_{id}^{R*} V_{is}^R \sum_{\alpha=n_G+1}^{2n_G} \sum_{\gamma=n_G+1}^{2n_G} B_{\mu\gamma}^R B_{e\alpha}^{R*} \lambda_i (\lambda_\alpha \lambda_\gamma)^{1/2} (s_\beta^2 \delta_{\gamma\alpha} - C_{\gamma\alpha}^L) \\ &\quad \times [s_\beta^2 I_1^D(\lambda_i, \lambda_\alpha, \lambda_h) - I_2^D(\lambda_i, \lambda_\alpha, \lambda_h)] \ , \qquad (4.56) \\ \tilde{A}_D^b &= \sum_{i=c,t} V_{id}^{R*} V_{is}^R \sum_{\alpha=n_G+1}^{2n_G} \sum_{\gamma=n_G+1}^{2n_G} B_{\mu\alpha}^R B_{e\gamma}^{R*} \lambda_i (\lambda_\alpha \lambda_\gamma)^{1/2} (s_\beta^2 \delta_{\gamma\alpha} - C_{\gamma\alpha}^{L*}) \\ &\quad \times [s_\beta^2 I_1^D(\lambda_i, \lambda_\alpha, \lambda_h) - I_2^D(\lambda_i, \lambda_\alpha, \lambda_h)] \ , \qquad (4.57)\end{aligned}$$

with the loop integrals I_1^D and I_2^D defined as

$$\begin{aligned} I_1^D(\lambda_i, \lambda_\alpha, \lambda_h) &\stackrel{def}{=} \frac{(4\pi)^2}{4i} M_L^2 \int \frac{d^4k}{(2\pi)^2} \frac{k^2}{(k^2 - m_{u_i}^2)(k^2 - m_{n_\alpha}^2)(k^2 - m_h^2)(k^2 - M_R^2)} \ , \qquad (4.58) \\ I_2^D(\lambda_i, \lambda_\alpha, \lambda_h) &\stackrel{def}{=} \frac{(4\pi)^2}{i} M_L^4 \int \frac{d^4k}{(2\pi)^2} \frac{1}{(k^2 - m_{u_i}^2)(k^2 - m_{n_\alpha}^2)(k^2 - m_h^2)(k^2 - M_R^2)} \ , \qquad (4.59)\end{aligned}$$

where we have taken into account that $s_\beta^2 = \beta$.

From the definitions we can readily obtain the expressions of the loop integrals:

$$\begin{aligned} I_1^D(\lambda_i, \lambda_\alpha, \lambda_h) &= -\frac{\beta^2}{4} \left[\frac{\lambda_i^2 \ln \lambda_i}{(\lambda_i - \lambda_h)(\beta\lambda_i - 1)(\lambda_i - \lambda_\alpha)} + \frac{\lambda_\alpha^2 \ln \lambda_\alpha}{(\lambda_\alpha - \lambda_h)(\beta\lambda_\alpha - 1)(\lambda_\alpha - \lambda_i)} \right. \\ &\quad \left. + \frac{\lambda_h^2 \ln \lambda_h}{(\beta\lambda_h - 1)(\lambda_h - \lambda_i)(\lambda_h - \lambda_\alpha)} + \frac{\ln \beta}{(\beta\lambda_h - 1)(\beta\lambda_i - 1)(\beta\lambda_\alpha - 1)} \right] , \qquad (4.60) \\ I_2^D(\lambda_i, \lambda_\alpha, \lambda_h) &= \beta^2 \left[\frac{\lambda_i \ln \lambda_i}{(\lambda_i - \lambda_h)(\beta\lambda_i - 1)(\lambda_i - \lambda_\alpha)} + \frac{\lambda_\alpha \ln \lambda_\alpha}{(\lambda_\alpha - \lambda_h)(\beta\lambda_\alpha - 1)(\lambda_\alpha - \lambda_i)} \right. \\ &\quad \left. + \frac{\lambda_h \ln \lambda_h}{(\beta\lambda_h - 1)(\lambda_h - \lambda_i)(\lambda_h - \lambda_\alpha)} + \frac{\beta \ln \beta}{(\beta\lambda_h - 1)(\beta\lambda_i - 1)(\beta\lambda_\alpha - 1)} \right] . \qquad (4.61)\end{aligned}$$

At this point we have all the results relevant to the possible box-diagrams describing the decay $K_L \to e\mu$ in the left-right symmetric model. Some of these results were already presented in [67], others were obtained here for the first time. We stress again that all box graphs are finite and their contribution can be given analytically. With all these results at hand one can proceed to make numerical estimates for the branching ratio $B(K_L \to e\mu)$.

4.5 Phenomenological results derived from the box diagrams

Before evaluating the branching ratio $B(K_L \to e\mu)$ a few remarks are necessary. The first one concerns the mixing matrix elements which appear in the expressions for the decay amplitudes given in the previous section. In Sec. 3.3 the constrains imposed on B^L by other low-energy processes (in particular the decay $\mu \to e\gamma$) were discussed in some detail. In the left-right symmetric model the mixing matrix B^R is also present in the expression for the amplitude. Following a similar procedure to the one outlined in Sec. 3.3 in the case of B^L, we can extract constraints on B^R from the experimental limit of the decay $\mu \to e\gamma$ that can be mediated by right-handed currents. In particular, if the mixings $B^L_{\mu N_\alpha}$ are assumed to be extremely suppressed or vanish, then only W_R bosons can provide a nonzero value to the decay $\mu \to e\gamma$. In the presence of the right-handed currents, the transition amplitude F_γ given in Eq. (3.17) will have the expression

$$F_\gamma = \beta \sum_{\alpha=1}^{2n_G} B^R_{\mu\alpha} B^{R*}_{e\alpha} F(\lambda_\alpha) \ , \tag{4.62}$$

where the loop-function $F(\lambda_\alpha)$ has the same expression as the one displayed by Eq. (3.19).

The constraint imposed on B^R can be written then from the expression of the branching ratio

$$B(\mu \to e\gamma) = \beta \frac{6\alpha_{em}}{\pi} \Big| \sum_{\alpha=1,2} B^R_{\mu N_\alpha} B^{R*}_{eN_\alpha} F(\lambda_\alpha) \Big|^2 \ . \tag{4.63}$$

For neutrinos much heavier than W_L (i.e $\lambda_N \gg 1$) the loop function $F(\lambda_N)$ will have a constant value and can be factorized out of the summation. Considering the experimental upper limit $B(\mu \to e\gamma) < 1.2 \times 10^{-11}$ leads to the constraint

$$\Big| \sum_{\alpha=1,2} B^R_{\mu N_\alpha} B^{R*}_{eN_\alpha} \Big|^2 < \frac{2 \times 10^{-8}}{\beta} \ . \tag{4.64}$$

In our calculations we will evaluate only separate terms containing the combinations $B^R_{\mu N_\alpha} B^{L*}_{eN_\alpha}$ or $B^R_{\mu N_\alpha} B^{R*}_{eN_\alpha}$, applying the constraint on $\left|B^R\right|$ derived from Eq. (4.64), which is a rather conservative approach.

In the left-right symmetric model we encounter also a new quark mixing matrix, V^R, which plays the same rôle in the right-handed gauge interactions of the different quarks as

the usual Kobayashi-Maskawa mixing matrix V^L for the left-handed ones. In case of no manifest or pseudo-manifest left-right symmetry, there are no experimental constraints on the elements of V^R and they are limited simply by unitarity. In fact, for specific forms of V^R given in Table II of Ref. [79], the $K_L - K_S$ mass difference imposes a lower bound on the W_R-boson mass $M_R \gtrsim 400$ GeV, not very much different from the experimental one [84].

We should give the possible ranges for the masses of the particles appearing in the different diagrams. We would definitely favor very heavy neutrinos, close to their perturbative limit of approximately 50 TeV. So in order to enhance the non-decoupling effects we will consider $m_N \sim 20 - 30$ TeV. For the charged Higgs particles it would be an obvious choice to set their mass close to the mass of the flavor changing neutral scalars. This means that $m_h \approx 10$ TeV is a natural value. For the right-handed gauge boson we will use the assumption $M_R \gg M_L$, a typical value used in our estimates will be $M_R = 1$ TeV.

In the previously defined range of the parameter space for the particle masses a certain mass hierarchy is present. We can conclude that in this region the hierarchy $\lambda_N \gg \lambda_h \gg 1/\beta \gg 1$ is valid. Using this assumption, we can write the analytical results obtained in Sec. 4.4 in an asymptotic form, which will make much easier the comparison between them.

4.5.1 Leading contributions to the box diagrams

All diagrams in Fig. 4.2 contain different particles, so we give the leading contributions to all of them:

$$\tilde{A}_A^a \approx 1.75 \times 10^{-5} V_{td}^L V_{ts}^L \lambda_t \left[3 + 2\ln\lambda_t + 4\ln\lambda_N\right] , \tag{4.65}$$

$$\tilde{A}_A^b \approx 3.5 \times 10^{-5} \beta^2 \lambda_t \left[3 - 3\ln\beta + \ln(\lambda_N/\lambda_t^4)\right] , \tag{4.66}$$

$$\tilde{A}_A^c \approx 3.5 \times 10^{-5} \beta^2 \lambda_t \left[\ln(\lambda_N/\lambda_h) - 1\right] . \tag{4.67}$$

The asymptotic behavior for the box diagrams of group B. will have a similar form to the expression given in Eq. (18) of Ref. [67], with the only difference being that with our present assumptions about the masses the we will have $\beta\lambda_t \ll 1$. The leading contribution, which can be traced back to diagram (c) in Fig. 4.7, can be expressed as

$$\tilde{A}_B \approx 3 \times 10^{-5} \eta V_{td}^L \beta^{3/2} \lambda_t^{3/2} \lambda_N^{1/2} \left(\ln\beta + \frac{\lambda_t \ln\lambda_t}{\lambda_t - 1}\right) . \tag{4.68}$$

For group C. we evaluate first the leading contributions to the two loop integrals, which gives

$$I_1^C(\lambda_i,\lambda_\alpha,\lambda_h) \approx \frac{1}{4\lambda_N}\ln(\lambda_N/\lambda_h)\ , \tag{4.69}$$

$$I_2^C(\lambda_i,\lambda_\alpha,\lambda_h) \approx \frac{\ln\lambda_h}{\lambda_N\lambda_h}\ . \tag{4.70}$$

Using this result we can identify the leading contribution originating from diagram (a) in Fig.4.4

$$\tilde{A}_C \approx 3\times 10^{-5}\eta V_{td}^L\beta^{1/2}\frac{\lambda_t^{3/2}\lambda_N^{1/2}}{\lambda_h}\ln\lambda_h\ . \tag{4.71}$$

In a similar manner we evaluate the leading contributions to the loop integrals for the group D.

$$I_1^D(\lambda_i,\lambda_\alpha,\lambda_h) \approx \frac{\beta}{4\lambda_N}\ln(\lambda_N/\lambda_h)\ , \tag{4.72}$$

$$I_2^C(\lambda_i,\lambda_\alpha,\lambda_h) \approx \frac{\beta}{\lambda_N\lambda_h}\left[\frac{\lambda_h}{\lambda_N}\ln\lambda_N - \ln\beta\lambda_h\right]\ , \tag{4.73}$$

which leads to

$$\tilde{A}_D \approx 3.5\times 10^{-5}\beta^2\lambda_t\ln(\lambda_N/\lambda_h)\ . \tag{4.74}$$

4.5.2 Non-decoupling effects in the box diagrams

The main reason for displaying the leading contributions of the different type of box diagrams is that it offers a clear insight in the behavior of the decay amplitude for very heavy neutrino masses. One can remark at a glance that the box diagrams of group B. and C. display a non-decoupling effect manifested in the proportionality of the corresponding reduced amplitudes to the mass of the heavy neutrino $m_N \sim \lambda_N^{1/2}$. This effects originates in the chirality-changing interactions of the left- and right-handed gauge bosons with the leptons, the same type of interaction existing also in the presence of the charged Higgs boson h. Despite of this similarity, the two amplitudes are not of the same order of magnitude, as we have

$$\left|\frac{\tilde{A}_B}{\tilde{A}_C}\right| \approx \frac{\ln\beta + \frac{\lambda_t\ln\lambda_t}{\lambda_t-1}}{\ln\lambda_h}\beta\lambda_h \sim 10^2\ . \tag{4.75}$$

This result means, that from all the box diagrams actually those of group B. can contribute most to the decay amplitude.

All along our analysis we have considered $(s_L^{\nu_e})^2 = (s_L^{\nu_\mu})^2 \leq 10^{-4}$ in our numerical estimates, in agreement with a global analysis of low-energy and LEP data [87]. We have identified $(s_L^{\nu_l})^2 \equiv \sum_{\alpha=1}^{n_G} |B^L_{lN_\alpha}|^2$, where l stands for an electron or a muon. Nevertheless, one may have to worry that diagrams similar to (d) and (h) in Fig. 4.7, which are present in the decay $\mu \to eee$, could lead to a violation of the experimental bound expressed in $B(\mu \to eee) < 10^{-12}$ [84]. Considering only the dominant non-decoupling terms, we have estimated that this happens when $\eta m_t V_{td}/(s_L^{\nu_e} m_N) < 1$ for $M_R \sim 1$ TeV. Unless the mass of heavy neutrinos $m_N > 10$ TeV for $M_R \lesssim 1$ TeV, the limits derived from the non-observation of $\mu \to e\gamma$ will be rather sufficient to perform our combined analysis.

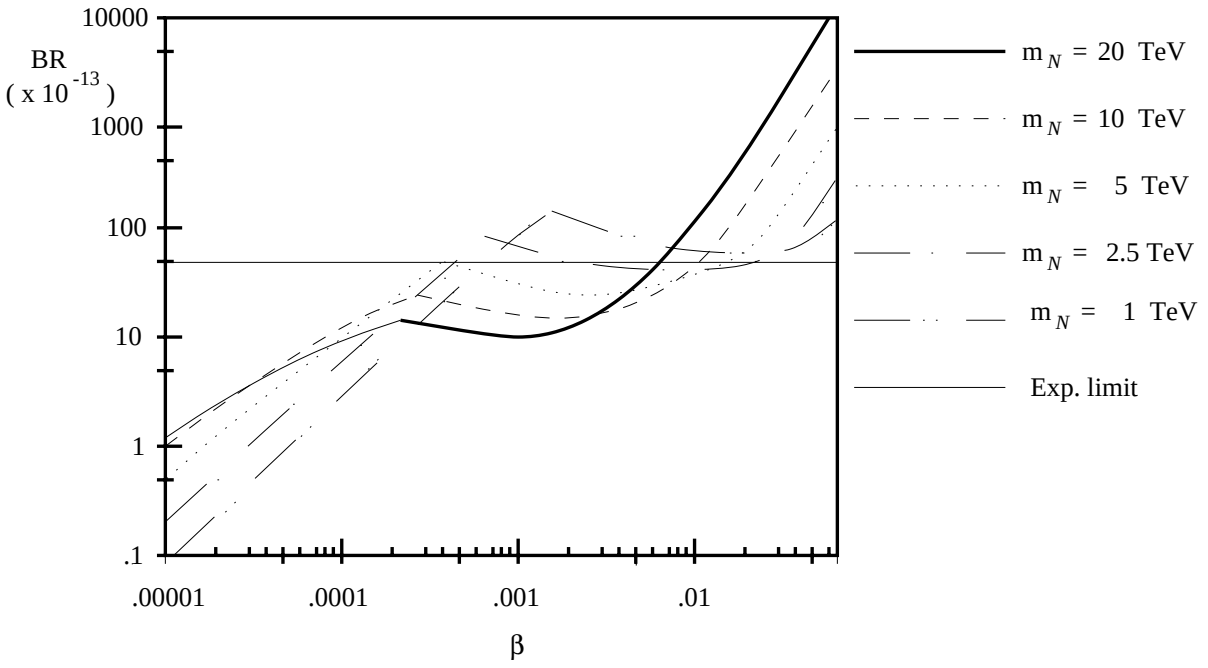

Figure 4.8: $B(K_L \to e\mu)$ as a function of $\beta = M_L^2/M_R^2$ in an $SU(2)_R \otimes SU(2)_L \otimes U(1)_{B-L}$ model, assuming that all heavy neutrinos are approximately degenerate with mass m_N.

As can be seen from Fig. 4.8, $B(K_L \to e\mu)$ depends strongly on M_R via the parameter β. Taking the constraints coming from $\mu \to e\gamma$ into account, we find that heavy neutrinos with few TeV masses can give rise to branching ratios of the order of 10^{-12} close to the

present experimental limit. Note that there is a local maximum in Fig. 4.8 for smaller values of β, where W_R bosons with several TeV masses can also account for $B(K_L \to e\mu) \sim 10^{-12}$. The origin of this local maximum can be traced back to Eq. (4.63), where the mathematical formulation of the constraints coming from $\mu \to e\gamma$ is displayed. Asymptotically, for very heavy neutrino masses, this leads to the result given in Eq. (4.64). The unitarity limit imposed on the mixing matrix B^R will be eventually reached for sufficiently heavy W_R (or, equivalently, for sufficiently small β), which means that further increase in M_R can not be compensated by an increase in the magnitude of the $B^R_{l\alpha}$ and the branching ratio will start to decrease monotonically. The local maxima in the plot of Fig. 4.8 mark the transition between these two regions, the first defined by constraints on B^R from low-energy processes, the second defined by the unitarity constraints on the same matrix.

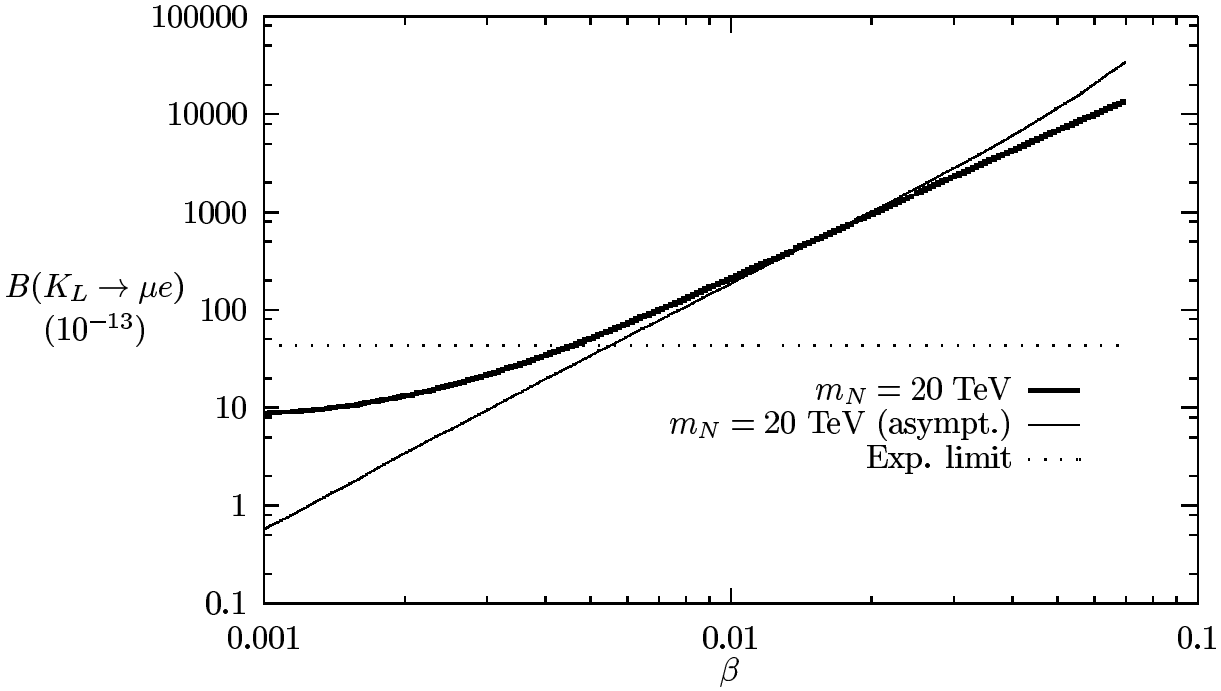

Figure 4.9: Validity check for the asymptotic formula in the case of two degenerate heavy neutrinos with mass $m_N = 20$ TeV

It is interesting to compare our asymptotic formula 4.68 with the complete result originating from Eq. (4.45). To illustrate the relationship between the two expressions, the branching ratio is calculated based on these formulas. The two curves shown in Fig 4.9

indicate that our approximation works surprisingly well in an appreciable region of the mass parameters. Note, however, that the heavier W_R gets (i.e. the smaller the parameter β), the discrepancies between the two results increase. One can see this feature as a direct consequence of the fact that the assumption $m_N/M_R \gg 1$ is less and less valid in that case. On the other hand, for $M_R \approx 1$ TeV both curves yield a value close to 10^{-12} for the branching ratio.

With these results at hand and increased confidence in our approximate formulas, we can estimate the level of suppression of the various different type box diagrams. This can be most conveniently done estimating the ratios

$$\left|\frac{\tilde{A}_A^a}{\tilde{A}_B}\right| \approx 0.2\frac{V_{ts}^L}{\eta}\frac{3+\ln\lambda_t+4\ln\lambda_N}{\beta^{3/2}\lambda_t^{1/2}\lambda_N^{1/2}} \approx 0.03 \ , \tag{4.76}$$

$$\left|\frac{\tilde{A}_A^b}{\tilde{A}_B}\right| \approx 0.4\frac{\beta^{1/2}}{\eta V_{td}^L}\frac{3-3\ln\beta+\ln(\lambda_N/\lambda_t^4)}{\lambda_t^{1/2}\lambda_N^{1/2}} \approx 1.4\times 10^{-3} \ , \tag{4.77}$$

$$\left|\frac{\tilde{A}_A^c}{\tilde{A}_B}\right| \approx 0.4\frac{\beta^{1/2}}{\eta V_{td}^L}\frac{\ln(\lambda_N/\lambda_h)-1}{\lambda_t^{1/2}\lambda_N^{1/2}} \approx 6\times 10^{-5} \ , \tag{4.78}$$

$$\left|\frac{\tilde{A}_C}{\tilde{A}_B}\right| \approx 0.3\frac{\ln\lambda_h}{\beta\lambda_h} \approx 0.03 \ , \tag{4.79}$$

$$\left|\frac{\tilde{A}_D}{\tilde{A}_B}\right| \approx 0.4\frac{\beta^{1/2}}{V_{td}^L}\frac{\ln(\lambda_N/\lambda_h)}{\lambda_t^{1/2}\lambda_N^{1/2}} \approx 5\times 10^{-3} \ . \tag{4.80}$$

In the above expressions we used the value obtained for $m_N = 30$ TeV and $M_R = 1$ TeV,

$$\left|\ln\beta+\frac{\lambda_t\ln\lambda_t}{\lambda_t-1}\right| \approx 3 \ . \tag{4.81}$$

The results of Eq. (4.76–4.80) demonstrate conclusively that diagrams where non-decoupling effects do not occur, could contribute only insignificantly to the branching ratio for the decay $K_L \to e\mu$.

Chapter 5

Gauge cancellations and renormalization

In this chapter we will focus our attention on the gauge structure of our results. Our discussion will bear many similarities with the case encountered in the analysis of the $K_L - K_S$ mass difference in the left-right symmetric model. Diagrams similar to diagrams (a) and (b) in Fig. 4.3 have been used to derive a stringent lower bound on M_R based on the smallness of Δm_K [88–91]. The authors of Ref. [92] pointed out for the first time in the literature that these one-loop diagrams are not gauge-invariant in the left-right symmetric model, contrary to the usual expectation, although a similar property was recognized earlier in the case of $\mu \to 3e$ [93]. By extensive use of Ward identities and quite general assumptions about the left- and right handed couplings they have found the general structure for the additional 1-loop graphs needed in order to restore gauge invariance. For these additional graphs it was shown that they must contain the flavor-changing neutral Higgs boson, namely the the self-energy and vertex-type graphs in diagrams (c)–(h) in Fig. 4.3. As these graphs present ultraviolet divergences, a renormalization procedure was needed. This study was successfully carried out in [86,94]. We note that the results obtained in [86] are completely transferable for the diagrams in Fig. 4.3, constituting the proof that they represent a gauge invariant subset.

We will gain some insight in this procedure when applying it to the diagrams shown in Fig. 4.4. The motivation for this resides in the fact that in order to find the gauge

complements of the box graphs, an important hint was the proportionality of the coupling $\phi_2^0 - G_L - G_R$ to the flavor-changing neutral Higgs mass $m^2_{\phi_2^0}$. For our group C. of diagrams this argument is not valid any more, the coupling $\phi_2^0 - G_L - h$ being proportional to the mass difference $m_h^2 - m^2_{\phi_2^0}$. The mass factor from the propagator in the vanishing momentum transfer limit is not canceled by this coupling. We will closely follow the method presented in Ref. [86] in order to derive the gauge invariance of the new type of diagrams of Fig. 4.4.

5.1 Gauge dependence of the box diagrams

The amplitude for diagram (a) in Fig. 5.1 can be written, omitting the integration over the loop momentum k, as

$$\mathcal{M}_a = T_\mu^{Wh}(p_1', p_2', k)\tilde{T}_\nu^{hW}(p_1, p_2, -k) i\Delta^{W\mu\nu}(k) iD_h(k') \ . \tag{5.1}$$

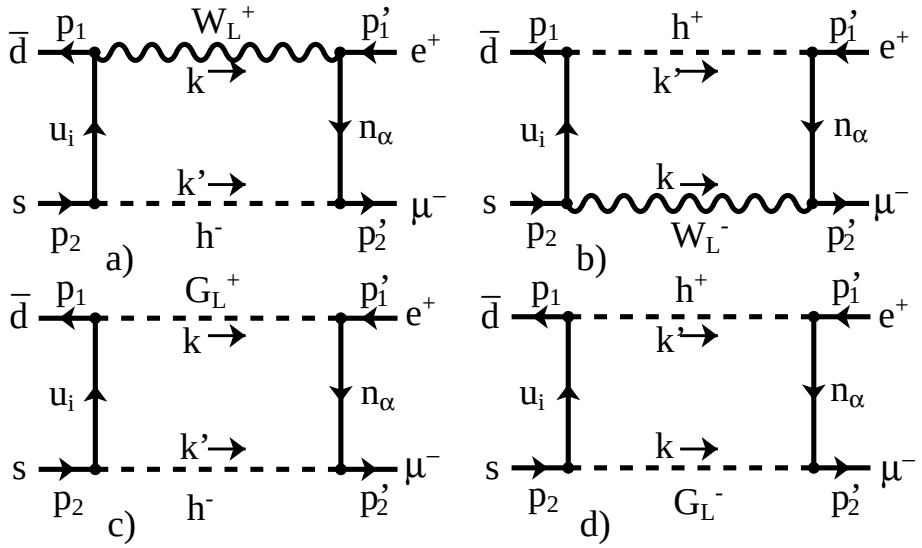

Figure 5.1: Box diagrams of group C. in a renormalizable R_ξ gauge

In this expressions T_μ^{Wh} and $\tilde{T}_\nu^{hW}$ represent the contribution of the different fermion lines, k is the internal loop momentum, chosen to be the momentum of W_L, k' is the momentum carried by the charged Higgs, p_1, p_2, p_1' and p_2' are respectively the momenta

of the external s, d, e^+ and μ^- particles and $iD_h(k)$ is the charged Higgs propagator with

$$D_h(k) = \frac{1}{k^2 - m_h^2}. \tag{5.2}$$

The contribution of the fermion lines can be evaluated using the Feynman rules listed in Appendix A. These give

$$\begin{aligned} T_\mu^{Wh}(p_1', p_2', k) &= \frac{-i}{c_\beta M_L}\left(\frac{ig_w}{\sqrt{2}}\right)^2 \sum_{\alpha,\gamma}\Bigg\{ \bar{u}_\mu(p_2')\left[c_\beta m_\mu B_{\mu\alpha}^R \mathrm{P}_R\right. \\ &\quad \left. + \left(s_\beta^2\delta_{\gamma\alpha} - C_{\gamma\alpha}^L\right) m_{n_\gamma} B_{\mu\gamma}^R \mathrm{P}_L\right] \\ &\quad \times \frac{1}{\not{p}_1' + \not{k} - m_{n_\alpha}} \gamma_\mu B_{e\alpha}^{L*} \mathrm{P}_L v_e(p_1')\Bigg\}\ , \end{aligned} \tag{5.3}$$

$$\begin{aligned} \tilde{T}_\mu^{hW}(p_1, p_2, k) &= \frac{i}{M_L}\left(\frac{ig_w}{\sqrt{2}}\right)^2 \sum_i \Bigg[\bar{v}_d(p_2)\gamma_\mu V_{id}^{L*} \frac{1}{\not{p}_1 + \not{k} - m_{u_i}} \\ &\quad \times c_\beta\left(m_{u_i}\mathrm{P}_R - m_s \mathrm{P}_L\right) V_{is}^R u_s(p_1)\Bigg]\ . \end{aligned} \tag{5.4}$$

We can decompose the gauge-boson propagator in Eq. (5.1) in the R_ξ gauge [95] as

$$\Delta_{\mu\nu}^W(k) = \Delta_{\mu\nu}(k) - \frac{k_\mu k_\nu}{M_L^2}\Delta_\xi(k), \tag{5.5}$$

where

$$\Delta_{\mu\nu}(k) = \frac{1}{k^2 - M_L^2}\left(-g_{\mu\nu} + \frac{k_\mu k_\nu}{M_L^2}\right) \tag{5.6}$$

is the gauge boson propagator for W_L in the unitary gauge and

$$\Delta_\xi(k) = \frac{1}{k^2 - \xi M_L^2} \tag{5.7}$$

is the part which has the dependence on the gauge parameter ξ and has the same form as the propagator of the unphysical Goldstone boson G_L corresponding to W_L.

Using this decomposition one can write

$$\mathcal{M}_a = \mathcal{M}_{a_1} + \mathcal{M}_{a_2}\ , \tag{5.8}$$

with

$$\mathcal{M}_{a_1} = T_\mu^{Wh}(p_1', p_2', k)\tilde{T}_\nu^{hW}(p_1, p_2, -k) i\Delta^{\mu\nu}(k) iD_h(k')\ , \tag{5.9}$$

$$\mathcal{M}_{a_2} = T_\mu^{Wh}(p_1', p_2', k)\tilde{T}_\nu^{hW}(p_1, p_2, -k)\left(\frac{-k_\mu k_\nu}{M_L^2}\right) i\Delta_\xi(k) D_h(k')\ . \tag{5.10}$$

Here we note that $\mathcal{M}_{a_1}$ is independent of the gauge parameter ξ and is the result of the box diagram in the unitary gauge where the unphysical Goldstone bosons are absent.

The contributions of the fermion lines satisfy the Ward identities

$$\frac{k^\mu}{M_L}T_\mu^{Wh}(p_1',p_2',k) = -T^{Gh}(p_1',p_2',k) - i\left(\frac{g_w}{\sqrt{2}}\right)^2\frac{c_\beta}{M_L^2}E_L(p_1',p_2')\ , \tag{5.11}$$

$$\frac{k^\mu}{M_L}\tilde{T}_\mu^{hW}(p_1,p_2,k) = \tilde{T}^{hG}(p_1,p_2,k) + i\left(\frac{g_w}{\sqrt{2}}\right)^2\frac{c_\beta}{M_L^2}\tilde{E}_R(p_1,p_2)\ , \tag{5.12}$$

where T^{Gh} and $\tilde{T}_{hG}$ are the corresponding contributions of the fermion lines when W_L is replaced by G_L, and we have defined

$$E_L(p_1',p_2') = \sum_\alpha \bar{u}_\mu(p_2')B_{\mu\alpha}^R B_{e\alpha}^{L*}m_{n_\alpha}\mathrm{P}_L v_e(p_1')\ , \tag{5.13}$$

$$\tilde{E}_R(p_1,p_2) = \sum_i \bar{v}_d(p_2)V_{id}^{L*}V_{is}^R m_{u_i}\mathrm{P}_R u_s(p_1)\ . \tag{5.14}$$

The amplitude for diagram (a) can be written then as

$$\mathcal{M}_a = \mathcal{M}_{a_1} - \mathcal{N}_{a_1} - \mathcal{N}_{a_2} - \mathcal{N}_{a_3} + \mathcal{N}_{a_4}\ , \tag{5.15}$$

or explicitly

$$\begin{aligned}\mathcal{M}_a = \mathcal{M}_{a_1} + i\Delta_\xi(k)iD_h(k')\Bigg[&-T^{Gh}(p_1',p_2',k)\tilde{T}_{hG}(p_1,p_2,-k)\\ &-i\left(\frac{g_w}{\sqrt{2}}\right)^2\frac{c_\beta}{M_L^2}\Big(T^{Gh}(p_1',p_2',k)\tilde{E}_R(p_1,p_2) + E_L(p_1',p_2')\tilde{T}_{hG}(p_1,p_2,-k)\Big)\\ &+\left(\frac{g_w}{\sqrt{2}}\right)^4\left(\frac{c_\beta}{M_L^2}\right)^2 E_L(p_1',p_2')\tilde{E}_R(p_1,p_2)\Bigg]\ .\end{aligned} \tag{5.16}$$

Following a similar procedure for diagram (b), we obtain

$$\mathcal{M}_b = \mathcal{M}_{b_1} - \mathcal{N}_{b_1} - \mathcal{N}_{b_2} - \mathcal{N}_{b_3} + \mathcal{N}_{b_4}\ , \tag{5.17}$$

with the result

$$\begin{aligned}\mathcal{M}_b = \mathcal{M}_{b_1} + i\Delta_\xi(k)iD_h(k')\Bigg[&-T^{hG}(p_1',p_2',k)\tilde{T}_{Gh}(p_1,p_2,-k)\\ &-i\left(\frac{g_w}{\sqrt{2}}\right)^2\frac{c_\beta}{M_L^2}\Big(T^{hG}(p_1',p_2',k)\tilde{E}_L(p_1,p_2) + E_R(p_1',p_2')\tilde{T}_{Gh}(p_1,p_2,-k)\Big)\\ &+\left(\frac{g_w}{\sqrt{2}}\right)^4\left(\frac{c_\beta}{M_L^2}\right)^2 E_R(p_1',p_2')\tilde{E}_L(p_1,p_2)\Bigg]\ ,\end{aligned} \tag{5.18}$$

where we have defined

$$E_R(p_1', p_2') = \sum_\alpha \bar{u}_\mu(p_2') B^L_{\mu\alpha} B^{R*}_{e\alpha} m_{n_\alpha} \mathrm{P}_R v_e(p_1') \ , \tag{5.19}$$

$$\tilde{E}_L(p_1, p_2) = \bar{v}_d(p_2) V^{R*}_{id} V^L_{is} m_{u_i} \mathrm{P}_R u_s(p_1) \ . \tag{5.20}$$

Adding the mutually correspondent terms in Eq. (5.16) and 5.18, the contribution of the box graphs takes the form

$$\mathcal{M}_{\rm box} = \mathcal{M}_1 - \mathcal{N}_1 - \mathcal{N}_2 - \mathcal{N}_3 + \mathcal{N}_4 \ . \tag{5.21}$$

Here $\mathcal{M}_1 = \mathcal{M}_{a_1} + \mathcal{M}_{b_1}$ and $\mathcal{N}_i = \mathcal{N}_{a_i} + \mathcal{N}_{b_i}$. $\mathcal{M}_1$ will have no gauge dependency, being the result of the two box diagrams in the unitary gauge. The gauge dependence in $\mathcal{N}_1$ will be canceled by the box diagrams involving the unphysical Goldstone bosons. However, the presence of the terms $\mathcal{N}_2$, $\mathcal{N}_3$ and $\mathcal{N}_4$, being proportional to the gauge dependent propagator $\Delta_\xi(k)$, implies that the two box diagrams do not form a gauge-invariant set. To find out which extra diagrams are needed to restore gauge invariance, one can look at the structure of these terms, which contain factors $E_L(p_1', p_2')$, $\tilde{E}_R(p_1, p_2)$ and the corresponding factors obtained interchanging $L \leftrightarrow R$. Taking into account the Feynman rules given in Appendix A. we can convince ourselves that the Yukawa couplings of ϕ_2^{0r} and ϕ_2^{0i}, when combined, are proportional to these factors. This provides us a hint which suggests that diagrams involving flavor-changing neutral Higgs scalars ϕ_2^{0r}, ϕ_2^{0i} should be taken into account. We will see that diagrams of the type $(c-f)$ in Fig. 4.4, where W_L is replaced by the non-physical Goldstone boson G_L, when added together, will have the same structure as the terms $\mathcal{N}_2$ and $\mathcal{N}_3$, proportional to the factor $E_{L,R}(p_1', p_2')$ or $\tilde{E}_{L,R}(p_1, p_2)$. For the term $\mathcal{N}_4$, which is proportional to $E_{L,R}(p_1', p_2')$ and $\tilde{E}_{L,R}(p_1, p_2)$, it is not hard to see that the self-energy corrections to the flavor-changing neutral Higgs scalars ϕ_2^{0r}, ϕ_2^{0i}, coming from diagrams $(g-h)$ in Fig. 4.4 with W_L replaced by G_L, can generate similar contributions. Here we note that both $\mathcal{M}_1$ and $\mathcal{N}_4$ in Eq. (5.21) are divergent. But it is easy to see that the combination $\mathcal{M}_1 + \mathcal{N}_4$ is finite as it should be because each box diagram is convergent in the renormalizable R_ξ gauge.

Even though the diagrams $(c-h)$ in Fig. 4.4 have the right structure to cancel the gauge-dependent terms $\mathcal{N}_2$, $\mathcal{N}_3$ and $\mathcal{N}_4$ in Eq. (5.21), the self-energy contribution is logarithmically divergent while the total contribution of box diagrams $\mathcal{M}_{\rm box}$ is finite. This

means that the vertex and self-energy graphs must be renormalized before being added to the box diagrams to cancel the gauge dependence. The renormalization prescription will be outlined in the following section.

5.2 Renormalization procedure

In general one has the freedom of choosing the subtraction points in the renormalization of the divergent Green's functions. Different subtraction points reflect themselves in giving different meanings to the parameters in the original Lagrangian and the physical results should be independent of the subtraction points. In theories with local gauge symmetries only the on-shell Green's functions are gauge invariant and thus have physical meaning. In the $SU(2)_L \otimes SU(2)_R \otimes U(1)_{B-L}$ model this is the case, therefore it is more convenient to choose the on-shell renormalization scheme, so that parameters after renormalization are gauge invariant and hence have direct physical interpretation. If we would decide for a subtraction not on-shell, the parameters might not be gauge invariant.

We can consider, for example, the renormalized scalar propagator given in the form

$$\Delta_R(p^2) = \frac{1}{p^2 - \mu^2 - \Sigma_R(p^2)} \ , \tag{5.22}$$

where μ^2 is the tree level mass of the scalar and $\Sigma_R(p^2)$ is the renormalized self-energy coming from higher-order contributions. If $\Sigma_R(p^2)$ is obtained from the unrenormalized self-energy by subtraction at $p^2 = \mu^2$, then $\Sigma_R(\mu^2) = 0$ and it is easy to see that $\Delta_R(p^2)$ in Eq. (5.22) has a pole at $p^2 = \mu^2$. In this case μ^2 is the physical mass of the scalar and it is gauge invariant because it is a physically measurable quantity. On the other hand, if the subtraction is done at $p^2 = 0$, then $\Sigma_R(0) = 0$ and the physical mass of the scalar, μ_p^2, will satisfy the equation

$$\mu_p^2 - \mu^2 - \Sigma_R(\mu_p^2) = 0 \ . \tag{5.23}$$

Since in general $\Sigma_R(\mu_p^2) \neq 0$ and is gauge dependent, the parameter μ^2 in this case is not the same as the physical mass μ_p^2 and has no reason to be gauge invariant. Thus to study the gauge invariance of a certain amplitude it is more convenient to use on-shell renormalization to avoid the implicit gauge dependence of the parameters. The procedure outlined in the next sections is equivalent with an on-shell skeleton-renormalization scheme.

5.3 On-shell renormalization of self-energy diagrams

The self-energy graphs of the scalar fields ϕ_2^{0r}, ϕ_2^{0i} are at most quadratically divergent, therefore we need to make two subtractions. If we denote the unrenormalized self-energy of ϕ_2^{0r} by $\Sigma^{(r)}(p^2)$, the renormalized one is given by the $R2$ operation defined as in Eq. (29) of Ref. [86]:

$$\left[\Sigma^{(r)}(p^2)\right]^{R2} \equiv \Sigma^{(r)}(p^2) - \Sigma^{(r)}(m_r^2) - (p^2 - m_r^2)\Sigma'^{(r)}(m_r^2) \ , \tag{5.24}$$

where $m_r = m_{\phi_2^{0r}}$ and $\Sigma'^{(r)}(m_r^2)$ denotes $d\Sigma^{(r)}(p^2)/dp^2$ evaluated at $p^2 = m_r^2$. A similar definition applies for $\Sigma^{(i)}(p^2)$, the self-energy of ϕ_2^{0i}. The Feynman rules derived for our model assure that there will be no one-loop contribution to the mixed propagator of ϕ_2^{0r} and ϕ_2^{0i}.

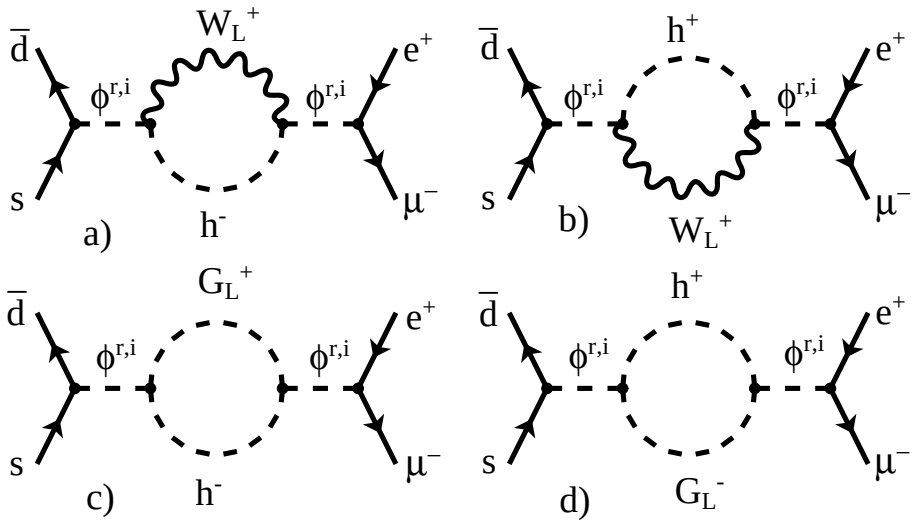

Figure 5.2: Self-energy diagrams of group C. in a renormalizable R_ξ gauge

We can write the contribution of the self-energy graphs in Fig. 5.2 as

$$\mathcal{M}_S = \sum_{f=r,i} A_f \frac{(i)^2}{(p^2 - m_f^2)^2} \left[\Sigma^{(f)}(p^2)\right]^{R2} \ , \tag{5.25}$$

where p is the momentum carried by the scalar particle and A_f contains all the fermion spinors and their couplings to the flavor-changing scalars and can be written as

$$A_r \ = \ \left(\frac{-ig_w}{2M_L}\right)^2 E_S(p_1', p_2') \tilde{E}_S(p_1, p_2) \ , \tag{5.26}$$

$$A_i = \left(\frac{g_w}{2M_L}\right)^2 E_P(p_1', p_2')\tilde{E}_P(p_1, p_2) \ , \tag{5.27}$$

where we have defined

$$E_S(p_1', p_2') = E_R(p_1', p_2') + E_L(p_1', p_2') \ , \tag{5.28}$$

$$E_P(p_1', p_2') = E_R(p_1', p_2') - E_L(p_1', p_2') \ , \tag{5.29}$$

$$\tilde{E}_S(p_1, p_2) = \tilde{E}_R(p_1, p_2) + \tilde{E}_L(p_1, p_2) \ , \tag{5.30}$$

$$\tilde{E}_P(p_1, p_2) = \tilde{E}_R(p_1, p_2) - E_L(p_1, p_2) \ . \tag{5.31}$$

The self-energy of the scalars can be separated as in

$$\Sigma^{(f)}(p^2) = \Sigma_G^{(f)}(p^2) + \Sigma_W^{(f)}(p^2) \ , \tag{5.32}$$

where $\Sigma_G^{(f)}(p^2)$ and $\Sigma_W^{(f)}(p^2)$ are the graphs with G_L or W_L in the loop. Using the identity

$$1 = \left(\frac{(p^2 - m_f^2) - (p^2 - m_h^2)}{m_h^2 - m_f^2}\right) \tag{5.33}$$

we can write

$$\Sigma_G^{(f)}(p^2) = \frac{(p^2 - m_f^2)^2 - 2(p^2 - m_h^2)(p^2 - m_f^2) + (p^2 - m_h^2)^2}{(m_h^2 - m_f^2)^2}\Sigma_G^{(f)}(p^2). \tag{5.34}$$

The renormalized self-energy will be then

$$\begin{aligned}\left[\Sigma_G^{(f)}(p^2)\right]^{R2} = & \left(\frac{p^2 - m_f^2}{m_h^2 - m_f^2}\right)^2 \Sigma_G^{(f)}(p^2) \\ & -2\frac{p^2 - m_f^2}{(m_h^2 - m_f^2)^2}\left[(p^2 - m_h^2)\Sigma_G^{(f)}(p^2)\right]^{R1} \\ & + \left[\left(\frac{p^2 - m_h^2}{m_h^2 - m_f^2}\right)\Sigma_G^{(f)}(p^2)\right]^{R2} \ ,\end{aligned} \tag{5.35}$$

where the $R1$ operation is defined as a simple subtraction

$$\left[f^{(f)}(p^2)\right]^{R1} \equiv f^{(f)}(p^2) - f^{(f)}(m_f^2) \ . \tag{5.36}$$

Then the total contribution from the self-energy graphs is given by

$$\begin{aligned}\mathcal{M}_S = & \sum_{f=r,i}(i)^2 A_f \left\{\frac{1}{(m_h^2 - m_f^2)^2}\Sigma_G^{(f)}(p^2)\right. \\ & -\frac{2}{(m_h^2 - m_f^2)(p^2 - m_f^2)}\left[(p^2 - m_h^2)\Sigma_G^{(f)}(p^2)\right]^{R1} \\ & \left. + \left[\left(\frac{p^2 - m_h^2}{m_h^2 - m_f^2}\right)\Sigma_G^{(f)}(p^2) + \Sigma_W^{(f)}(p^2)\right]^{R2}\right\} \ .\end{aligned} \tag{5.37}$$

The explicit expressions for the different self-energies can be obtained using the derived Feynman rules, and apart from the loop integration they read:

$$\begin{aligned}
\Sigma_G^{(r)}(p^2) &= \frac{2c_\beta^2}{M_L^2}\left(\frac{ig_w}{2}\right)^2 (m_h^2-m_r^2)^2 i\Delta_\xi(k) iD_h(k') \ , \\
\Sigma_G^{(i)}(p^2) &= -\frac{2c_\beta^2}{M_L^2}\left(\frac{g_w}{2}\right)^2 (m_h^2-m_i^2)^2 i\Delta_\xi(k) iD_h(k') \ , \\
\Sigma_W^{(r)}(p^2) &= 2c_\beta^2\left(\frac{ig_w}{2}\right)^2 i\left(\Delta_{\mu\nu}(k) - \frac{k_\mu k_\nu}{M_L^2}\Delta_\xi(k)\right) iD_h(k')(p+k')^\mu (p+k')^\nu \ , \\
\Sigma_W^{(i)}(p^2) &= \Sigma_W^{(r)}(p^2) \ .
\end{aligned} \tag{5.38}$$

These expressions make clear that the self-energies $\Sigma_G^{(f)}(p^2)$ are proportional to $(m_h^2-m_f^2)^2$ so we can evaluate the first term in Eq. (5.37) using the forms for A_f given in Eq. (5.26–5.27) and the Ward identities:

$$\begin{aligned}
\sum_{f=r,i}(i)^2 A_f\left[\frac{1}{(m_h^2-m_f^2)^2}\Sigma_G^{(f)}(p^2)\right] &= -2c_\beta^2\left(\frac{ig_w}{2}\right)^4 i\Delta_\xi(k) iD_h(k') \\
&\times\left[E_S(p_1',p_2')\tilde{E}_S(p_1,p_2) - E_P(p_1',p_2')\tilde{E}_P(p_1,p_2)\right] \\
&= -4c_\beta^2\left(\frac{ig_w}{2}\right)^4 i\Delta_\xi(k) iD_h(k') \\
&\times\left[E_R(p_1',p_2')\tilde{E}_L(p_1,p_2) + E_L(p_1',p_2')\tilde{E}_R(p_1,p_2)\right] \ .
\end{aligned} \tag{5.39}$$

Comparing this result with Eq. (5.16) and (5.18) it is clear that

$$\sum_{f=r,i}(i)^2 A_f\left[\frac{1}{(m_h^2-m_f^2)^2}\Sigma_G^{(f)}(p^2)\right] = -\mathcal{N}_{a_4} - \mathcal{N}_{b_4} = -\mathcal{N}_4 \ . \tag{5.40}$$

Thus, this term cancels the gauge-dependent term $\mathcal{N}_4$ of the box graphs.

For the last term in Eq. (5.37) we can write

$$\begin{aligned}
\left(\frac{p^2-m_h^2}{m_h^2-m_r^2}\right)\Sigma_G^{(r)}(p^2) + \Sigma_W^{(r)}(p^2) &= \\
&2c_\beta^2\left(\frac{ig_w}{2}\right)^2 i\Delta_{\mu\nu}(k) iD_h(k')(p+k')^\mu(p+k')^\nu \\
&-\frac{2c_\beta^2}{M_L^2}\left(\frac{g_w}{2}\right)^2\left[2(p^2-m_h^2) - (k'^2-m_h^2)\right]\Delta_\xi(k) \ .
\end{aligned} \tag{5.41}$$

The second term in Eq. (5.41), being linear in p^2, will vanish after the $R2$ operation defined in Eq. (5.24), which requires two subtractions. Then we obtain

$$\left[\left(\frac{p^2-m_h^2}{m_h^2-m_r^2}\right)\Sigma_G^{(r)}(p^2)+\Sigma_W^{(r)}(p^2)\right]^{R2} = \left[2c_\beta^2\left(\frac{g_w}{2}\right)^2\Delta_{\mu\nu}(k)D_h(k')(p+k')^\mu(p+k')^\nu\right]^{R2} , \quad (5.42)$$

which is clearly gauge-invariant. The similar result can be obtained also for ϕ_2^{0i}.

The second term in Eq. (5.37) can be written, using the expressions in Eq. (5.38) as

$$\mathcal{M}_{S_2} \equiv 2\sum_{f=r,i} A_f \frac{1}{(m_h^2-m_f^2)(p^2-m_f^2)}\left[(p^2-m_h^2)\Sigma_G^{(f)}(p^2)\right]^{R1} , \quad (5.43)$$

which gives

$$\begin{aligned}\mathcal{M}_{S_2} &= c_\beta^2\left(\frac{g_w}{\sqrt{2}M_L}\right)^4\left[(p^2-m_h^2)i\Delta_\xi(k)iD_h(k')\right]^{R1} \\ &\times\left[E_S(p_1',p_2')\tilde{E}_S(p_1,p_2)\frac{1}{p^2-m_r^2}-E_P(p_1',p_2')\tilde{E}_P(p_1,p_2)\frac{1}{p^2-m_i^2}\right] . \quad (5.44)\end{aligned}$$

As we will see, this contribution will combine with that of the vertex graphs to give a gauge-invariant result.

5.4 On-shell renormalization of the vertex diagrams

The contribution of the vertex diagrams in Fig.5.3 can be written as

$$\begin{aligned}\mathcal{M}_v &= \sum_{f=r,i}\left\{B_f(p_1',p_2')\frac{i}{p^2-m_f^2}\left[\tilde{\Gamma}^{(f)}(p_1,p_2,p^2)\right]^{R1}\right. \\ &\left.+\left[\Gamma^{(f)}(p_1',p_2',p^2)\right]^{R1}\frac{i}{p^2-m_f^2}\tilde{B}_f(p_1,p_2)\right\} , \quad (5.45)\end{aligned}$$

where we have defined

$$B_r(p_1',p_2') = \frac{-ig_w}{2M_L}E_S(p_1',p_2'); \quad B_i(p_1',p_2') = \frac{g_w}{2M_L}E_P(p_1',p_2') , \quad (5.46)$$

$$\tilde{B}_r(p_1,p_2) = \frac{-ig_w}{2M_L}\tilde{E}_S(p_1,p_2); \quad \tilde{B}_i(p_1,p_2) = \frac{g_w}{2M_L}\tilde{E}_P(p_1,p_2) , \quad (5.47)$$

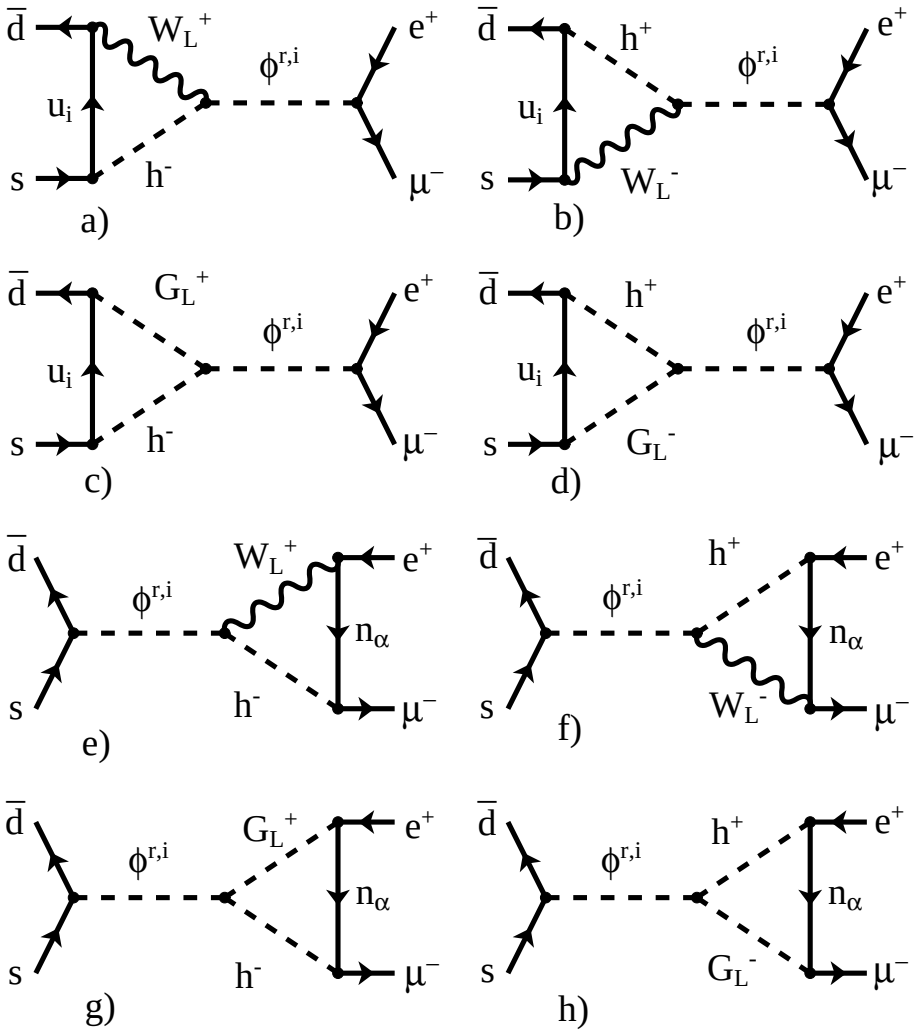

Figure 5.3: Vertex diagrams of group C. in a renormalizable R_ξ gauge

and the $R1$ operation of $\Gamma^{(f)}$ is defined as

$$\left[\Gamma^{(f)}(p_1,p_2,p^2)\right]^{R1} \equiv \Gamma^{(f)}(p_1,p_2,p^2) - \Gamma^{(f)}(p_1,p_2,m_f^2) \ . \tag{5.48}$$

Separating again the diagrams with non-physical Goldstone bosons and gauge bosons in the R_ξ gauge, one can write

$$\Gamma^{(f)}(p_1,p_2,p^2) = \Gamma^{(f)}_G(p_1,p_2,p^2) + \Gamma^{(f)}_W(p_1,p_2,p^2) \ . \tag{5.49}$$

Using again the identity from Eq. (5.33) results

$$\begin{aligned}\left[\Gamma^{(f)}_G(p_1,p_2,p^2)\right]^{R1} &= \frac{p^2-m_f^2}{m_h^2-m_f^2}\Gamma^{(f)}_G(p_1,p_2,p^2) \\ &\quad - \left[\frac{p^2-m_h^2}{m_h^2-m_f^2}\Gamma^{(f)}_G(p_1,p_2,p^2)\right]^{R1} \ .\end{aligned} \tag{5.50}$$

Using this result we will decompose $\mathcal{M}_v$ in two terms, $\mathcal{M}_v = \mathcal{M}_{v_1} + \mathcal{M}_{v_2}$, with

$$\begin{aligned}\mathcal{M}_{v_1} &= \sum_{f=r,i}\left[B_f(p_1',p_2')\frac{i}{p^2-m_f^2}\tilde{\Gamma}^{(f)}_G(p_1,p_2,p^2)\right. \\ &\quad \left. + \Gamma^{(f)}_G(p_1',p_2',p^2)\frac{i}{p^2-m_f^2}\tilde{B}_f(p_1,p_2)\right] \ ,\end{aligned} \tag{5.51}$$

$$\begin{aligned}\mathcal{M}_{v_2} &= \sum_{f=r,i}\left\{B_f(p_1',p_2')\frac{i}{p^2-m_f^2}\left[\tilde{\Gamma}^{(f)}_W(p_1,p_2,p^2) - \frac{p^2-m_h^2}{m_h^2-m_f^2}\tilde{\Gamma}^{(f)}_G(p_1,p_2,p^2)\right]^{R1}\right. \\ &\quad \left. + \left[\Gamma^{(f)}_W(p_1',p_2',p^2) - \frac{p^2-m_h^2}{m_h^2-m_f^2}\Gamma^{(f)}_G(p_1',p_2',p^2)\right]^{R1}\frac{i}{p^2-m_f^2}\tilde{B}_f(p_1,p_2)\right\} \ .\end{aligned} \tag{5.52}$$

The expressions of the vertex diagrams can be obtained using the Feynman rules of Appendix A.:

$$\begin{aligned}\Gamma^{(r)}_G(p_1',p_2',p^2) &= c_\beta\frac{ig_w}{2M_L}(m_h^2-m_r^2)i\Delta_\xi(k)iD_h(k') \\ &\quad \times\left[T^{hG}(p_1',p_2',k) + T^{Gh}(p_1',p_2',k)\right] \ ,\end{aligned} \tag{5.53}$$

$$\Gamma_G^{(i)}(p_1',p_2',p^2) = -c_\beta\frac{g_w}{2M_L}(m_h^2-m_i^2)i\Delta_\xi(k)iD_h(k') \times\left[T^{hG}(p_1',p_2',k)-T^{Gh}(p_1',p_2',k)\right] , \tag{5.54}$$

$$\tilde\Gamma_G^{(r)}(p_1,p_2,p^2) = c_\beta\frac{ig_w}{2M_L}(m_h^2-m_r^2)i\Delta_\xi(k)iD_h(k') \times\left[\tilde T^{hG}(p_1,p_2,-k)+\tilde T^{Gh}(p_1,p_2,-k)\right] , \tag{5.55}$$

$$\tilde\Gamma_G^{(i)}(p_1,p_2,p^2) = -c_\beta\frac{g_w}{2M_L}(m_h^2-m_i^2)i\Delta_\xi(k)iD_h(k') \times\left[\tilde T^{hG}(p_1,p_2,-k)-\tilde T^{Gh}(p_1,p_2,k)\right] , \tag{5.56}$$

$$\Gamma_W^{(r)}(p_1',p_2',p^2) = c_\beta\frac{ig_w}{2}(m_h^2-m_r^2)i\left(\Delta^{\mu\nu}(k)-\frac{k^\mu k^\nu}{M_L^2}\Delta_\xi(k)\right)iD_h(k') \times\left[-T_\nu^{hW}(p_1',p_2',k)(k'+p)_\mu+T_\nu^{Wh}(p_1',p_2',k)(k'+p)_\mu\right] , \tag{5.57}$$

$$\Gamma_W^{(i)}(p_1',p_2',p^2) = c_\beta\frac{g_w}{2}(m_h^2-m_i^2)i\left(\Delta^{\mu\nu}(k)-\frac{k^\mu k^\nu}{M_L^2}\Delta_\xi(k)\right)iD_h(k') \times\left[T_\nu^{hW}(p_1',p_2',k)(k'+p)_\mu+T_\nu^{Wh}(p_1',p_2',k)(k'+p)_\mu\right] , \tag{5.58}$$

$$\tilde\Gamma_W^{(r)}(p_1,p_2,p^2) = c_\beta\frac{ig_w}{2}(m_h^2-m_r^2)i\left(\Delta^{\mu\nu}(k)-\frac{k^\mu k^\nu}{M_L^2}\Delta_\xi(k)\right)iD_h(k') \times\left[\tilde T_\nu^{hW}(p_1,p_2,-k)(k'+p)_\mu-\tilde T_\nu^{Wh}(p_1,p_2,-k)(k'+p)_\mu\right] , \tag{5.59}$$

$$\tilde\Gamma_W^{(i)}(p_1,p_2,p^2) = -c_\beta\frac{g_w}{2}(m_h^2-m_i^2)i\left(\Delta^{\mu\nu}(k)-\frac{k^\mu k^\nu}{M_L^2}\Delta_\xi(k)\right)iD_h(k') \times\left[\tilde T_\nu^{hW}(p_1,p_2,-k)(k'+p)_\mu-\tilde T_\nu^{Wh}(p_1,p_2,k)(k'+p)_\mu\right] . \tag{5.60}$$

With these expressions we obtain, after some algebra and using the defining relations of B_f and $\tilde B_f$:

$$\begin{aligned}\mathcal{M}_{v_1} = {} & ic_\beta\left(\frac{g_w}{2M_L}\right)^2 i\Delta_\xi(k)iD_h(k') \\ & \times\Big[\tilde T^{hG}(p_1,p_2,-k)\left(E_S(p_1',p_2')-E_P(p_1',p_2')\right) \\ & +\tilde T^{Gh}(p_1,p_2,-k)\left(E_S(p_1',p_2')+E_P(p_1',p_2')\right) \\ & +T^{hG}(p_1',p_2',k)\left(\tilde E_S(p_1,p_2)-\tilde E_P(p_1,p_2)\right) \\ & +T^{Gh}(p_1',p_2',k)\left(\tilde E_S(p_1,p_2)+\tilde E_P(p_1,p_2)\right)\Big] .\end{aligned} \tag{5.61}$$

From Eq. (5.61) we can see that $\mathcal{M}_{v_1}$ takes the form

$$\mathcal{M}_{v_1}=\mathcal{N}_2+\mathcal{N}_3 \tag{5.62}$$

and it will cancel the corresponding terms from the box diagrams.

If we define

$$\bar{\Gamma}^{(f)}(p_1,p_2,p^2) \equiv \Gamma_W^{(f)}(p_1,p_2,p^2) - \frac{p^2-m_h^2}{m_h^2-m_f^2}\Gamma_G^{(f)}(p_1,p_2,p^2)\ , \tag{5.63}$$

we can evaluate, using Eq. (5.53–5.60) and the corresponding Ward identities

$$\begin{aligned}\bar{\Gamma}^{(r)}(p_1',p_2',p^2) &= \Gamma_{u.g}^{(r)}(p_1',p_2',p^2) - \\ &-c_\beta\frac{g_w}{2M_L}\left[T^{hG}(p_1',p_2',k)+T^{Gh}(p_1',p_2',k)\right]i\Delta_\xi(k) \\ &+c_\beta^2\frac{ig_w}{2M_L}\left(\frac{g_w}{\sqrt{2}M_L}\right)^2 E_S(p_1',p_2')i\Delta_\xi(k) \\ &-c_\beta^2\frac{g_w}{2M_L}\left(\frac{g_w}{\sqrt{2}M_L}\right)^2 (p^2-m_h^2)E_S(p_1',p_2')i\Delta_\xi(k)iD_h(k').\end{aligned} \tag{5.64}$$

Here $\Gamma_{u.g}^{(r)}(p_1',p_2',p^2)$ is the corresponding vertex contribution in the unitary gauge, and by definition it has no gauge dependence. The second and the third term vanish under the $R1$ operation, as they do not depend on p^2. Then we can obtain the renormalized vertex function as

$$\begin{aligned}\left[\bar{\Gamma}^{(r)}(p_1',p_2',p^2)\right]^{R1} &= \left[\Gamma_{u.g}^{(r)}(p_1',p_2',p^2)\right]^{R1} \\ -c_\beta^2\frac{g_w}{2M_L}\left(\frac{g_w}{\sqrt{2}M_L}\right)^2 &E_S(p_1',p_2')\left[(p^2-m_h^2)i\Delta_\xi(k)iD_h(k')\right]^{R1}\ .\end{aligned} \tag{5.65}$$

In a similar manner we can obtain

$$\begin{aligned}\left[\bar{\Gamma}^{(i)}(p_1',p_2',p^2)\right]^{R1} &= \left[\Gamma_{u.g}^{(i)}(p_1',p_2',p^2)\right]^{R1} \\ -c_\beta^2\frac{g_w}{2M_L}\left(\frac{ig_w}{\sqrt{2}M_L}\right)^2 &E_P(p_1',p_2')\left[(p^2-m_h^2)i\Delta_\xi(k)iD_h(k')\right]^{R1}\ ,\end{aligned} \tag{5.66}$$

$$\begin{aligned}\left[\bar{\tilde{\Gamma}}^{(r)}(p_1,p_2,p^2)\right]^{R1} &= \left[\tilde{\Gamma}_{u.g}^{(r)}(p_1,p_2,p^2)\right]^{R1} \\ -c_\beta^2\frac{g_w}{2M_L}\left(\frac{g_w}{\sqrt{2}M_L}\right)^2 &\tilde{E}_S(p_1,p_2)\left[(p^2-m_h^2)i\Delta_\xi(k)iD_h(k')\right]^{R1}\ ,\end{aligned} \tag{5.67}$$

$$\begin{aligned}\left[\bar{\tilde{\Gamma}}^{(i)}(p_1,p_2,p^2)\right]^{R1} &= \left[\tilde{\Gamma}_{u.g}^{(i)}(p_1,p_2,p^2)\right]^{R1} \\ -c_\beta^2\frac{g_w}{2M_L}\left(\frac{ig_w}{\sqrt{2}M_L}\right)^2 &\tilde{E}_P(p_1,p_2)\left[(p^2-m_h^2)i\Delta_\xi(k)iD_h(k')\right]^{R1}\ .\end{aligned} \tag{5.68}$$

Now we are enabled to write

$$\mathcal{M}_{v_2} = \mathcal{M}_{v_2}^{(1)} + \mathcal{M}_{v_2}^{(2)}\ , \tag{5.69}$$

where $\mathcal{M}_{v_2}^{(1)}$ is the contribution of the terms given in the unitary gauge, hence with no dependency on the gauge parameter ξ, $\mathcal{M}_{v_2}^{(2)}$ representing the contribution given by the remaining terms in Eq. (5.52) and which will have the expression

$$\begin{aligned}\mathcal{M}_{v_2}^{(2)} &= c_\beta^2 \left(\frac{g_w}{\sqrt{2}M_L}\right)^4 \left[(p^2 - m_h^2) i\Delta_\xi(k) iD_h(k')\right]^{R1} \\ &\times \left[-E_S(p_1', p_2')\tilde{E}_S(p_1, p_2)\frac{1}{p^2 - m_r^2} + E_P(p_1', p_2')\tilde{E}_P(p_1, p_2)\frac{1}{p^2 - m_i^2}\right] . \end{aligned} \tag{5.70}$$

Turning back to Eq. (5.44) we can see that this contribution will cancel the gauge dependent part of the self-energy diagrams contained in $\mathcal{M}_{S_2}$.

This result concludes our study of the gauge-invariance of the diagrams presented in Fig. 4.4. We have seen that the box diagrams are not independent of the gauge parameter ξ in the renormalizable R_ξ gauge. In order to obtain physical results we had to include the self-energy ant the vertex diagrams. The gauge independence is restored at the end through a subtle interplay between the general Ward identities and on-shell renormalization.

5.5 Gauge complement contributions

In Chapter 4. the contributions of the box diagrams to the decay amplitude for the process $K_L \to e\mu$ were studied in detail. In the present chapter we have seen that these diagrams are not gauge-independent, and in order to restore gauge-invariance additional Feynman diagrams containing flavor-changing neutral Higgs particles must be taken into account. In order to complete our study we will evaluate the contributions of the additional gauge-complement diagrams.

5.5.1 Self-energy complements

To estimate the order of magnitude for the contributions originating in the self-energy diagrams, we will evaluate in the Feynman–'t Hooft gauge one of the diagrams (g) or (h) in Fig. 4.3, namely when the gauge bosons are replaced with the corresponding unphysical Goldstone scalars G_L and G_R. The motivation for this choice is that this diagram will cancel the suppression by the heavy Higgs mass in the low momentum transfer limit, as the coupling $\phi_2^0 - G_L - G_R$ is proportional to the same heavy mass m_ϕ^2.

The scalar self-energy can be calculated using Eq. (B.21) of Ref. [96]. The result presented there for the corresponding loop function can be written in our case as

$$\Pi(p) = \frac{1}{16\pi^2}\left[C_{UV} - \int_0^1 dx \ln(D_2(x))\right] , \tag{5.71}$$

where C_{UV} is the ultraviolet divergent part in the dimensional regularization

$$C_{UV} \equiv \frac{1}{\epsilon} - \gamma + \ln 4\pi ,$$

γ is the Euler constant and the function $D_2(x)$ is defined as

$$D_2(x) \equiv M_R^2(1-x) + M_L^2 x - p^2 x(1-x) , \tag{5.72}$$

when p is the momentum flowing through the diagram. The self-energy $\Sigma(p)$ is obtained by multiplying with the relevant couplings.

We are interested in the regime of heavy right-handed gauge boson, when the condition $M_L \ll M_R$ is satisfied, so we can define the relevant loop function as

$$B_0(p^2, 0, b^2) \equiv C_{UV} - \int_0^1 dx \ln[b^2(1-x) - p^2 x(1-x)] . \tag{5.73}$$

Using this definition, we obtain also

$$B_0'(p^2, 0, b^2) = \int_0^1 dx \frac{x(1-x)}{b^2(1-x) - p^2 x(1-x)} . \tag{5.74}$$

The above defined integrals can be evaluated analytically, yielding:

$$B_0(0, 0, M_R^2) = C_{UV} + \ln(M_R^2) - 1 , \tag{5.75}$$

$$B_0(p^2, 0, M_R^2) = C_{UV} - 2 + \ln(M_R^2) + \left(1 - \frac{M_R^2}{p^2}\right) \ln\left|1 - \frac{p^2}{M_R^2}\right| , \tag{5.76}$$

$$B_0'(p^2, 0, M_R^2) = \frac{1}{p^2}\left[1 + \frac{M_R^2}{p^2} \ln\left|1 - \frac{p^2}{M_R^2}\right|\right] . \tag{5.77}$$

The renormalized self-energy will then be given by

$$\left[B_0(0, 0, M_R^2)\right]^{R2} = B_0(0, 0, M_R^2) - B_0(m_\phi^2, 0, M_R^2) + m_\phi^2 B_0'(m_\phi^2, 0, M_R^2) \tag{5.78}$$

$$= 2 - \left(1 - \frac{2M_R^2}{m_\phi^2}\right) \ln\left|1 - \frac{m_\phi^2}{M_R^2}\right| , \tag{5.79}$$

where m_ϕ^2 is identified with the mass of the flavor-changing Higgs particle.

Using this result we can estimate

$$\left|\frac{A_{\rm self}}{A_{\rm tree}}\right| = \frac{1}{(4\pi)^2}\left(\frac{g_w}{2}\right)^2 \left[B_0(0,0,M_R^2)\right]^{R2} \frac{m_\phi^2}{M_R^2}\ . \tag{5.80}$$

The expression above tells us that unless the the mass of the flavor-changing Higgs is unnaturally close to the mass of W_R, the self-energy graph will have a negligible contribution compared to that of the tree level diagram.

Our interest is to compare this self-energy contribution to other contributions at one-loop level. The most relevant comparison is the one with the dominant contribution of the box-diagrams. Based on the results obtained in the previous chapter we can write

$$\left|\frac{A_{\rm self}}{A_{\rm box}}\right| = \frac{\left[B_0(0,0,M_R^2)\right]^{R2}}{\beta\lambda_t\left(\ln\beta + \frac{\lambda_t \ln\lambda_t}{\lambda_t - 1}\right)}\ . \tag{5.81}$$

A numerical evaluation convinces us that when $3.35 M_R \leq m_\phi \leq 3.6 M_R$, the box graphs play the leading role among the loop corrections. Outside this limit, however, the self-energy graphs become dominant and they can not be neglected in a complete analysis. This result contradicts the common assumption in the literature that the gauge complement graphs can be safely neglected. This assumption was made in Ref. [79] using the results obtained in [86]. We must stress that in the context of $K_L - K_S$ mixing studied in Ref. [86] this conclusion remains valid. The main reason for the different situation in the $K_L \to e\mu$ decay occurs due to the different structure of the box integrals resulting from the presence of the heavy neutrinos. The main conclusion of this section is that the gauge complements of self-energy type can contribute substantially to a branching ratio $B(K_L \to e\mu)$ close to the present experimental limit without violating the perturbative bound on the mass of the flavor-changing neutral Higgs particles.

5.5.2 Vertex complements

Using a similar motivation as in the previous section, we will evaluate diagrams similar to diagrams $(c-f)$ in Fig. 4.3, with the left- and right-handed gauge bosons being replaced by the corresponding unphysical Goldstone bosons G_L and G_R. In our case there are very heavy fermions present on the fermionic lines, and therefore we will consider only this limiting case as one cannot obtain exact analytical expressions for the integrals involved.

The vertex diagram can be calculated using Eq. (B.36) of Ref. [96]. Neglecting safely the external momenta of the fermions, the result will be proportional to

$$\Gamma(p^2) \sim \frac{1}{16\pi^2}\int_0^1\int_0^1 \frac{y}{D_3(x,y)}dxdy \ , \tag{5.82}$$

where

$$D_3(x,y) \equiv (1-y)M_f^2 + y\left[\bar{M}^2 - p^2x(1-x)\right] \tag{5.83}$$

can be defined with $\bar{M}^2 = (1-x)M_R^2 + xM_L^2$ and M_f being the mass of the fermion in the loop.

Neglecting M_L compared to M_R, m_N and m_ϕ, we can define

$$C_0(0,p^2,0,m_N^2,0,M_R^2) \equiv \int_0^1\int_0^1 dxdy\frac{y}{(1-y)m_N^2 + y(1-x)(M_R^2 - p^2x)} \ . \tag{5.84}$$

We will have then

$$C_0(0,0,0,m_N^2,0,M_R^2) = \frac{\ln(m_N^2/M_R^2)}{m_N^2 - M_R^2} \ . \tag{5.85}$$

In the limit $m_N \gg M_R$ this leads to

$$C_0(0,0,0,m_N^2,0,M_R^2) \approx \frac{1}{m_N^2}\ln\left(\frac{m_N^2}{M_R^2}\right) \ . \tag{5.86}$$

The renormalized vertex function has different expressions for the various relationships between the heavy masses:

$$\left[C_0(0,0,0,m_N^2,0,M_R^2)\right]^{R1} \approx \frac{1}{m_N^2}\left[\ln\left(\frac{m_N^2}{M_R^2}\right) - \frac{1}{\sqrt{2}}\right] \quad \text{for } m_N^2 \approx m_\phi^2 \gg M_R^2, \tag{5.87}$$

$$\left[C_0(0,0,0,m_N^2,0,M_R^2)\right]^{R1} \approx \frac{1}{m_N^2}\left[\ln\left(\frac{m_\phi^2}{M_R^2}\right) - 1\right] \quad \text{for } m_N^2 \gg m_\phi^2 \gg M_R^2, \tag{5.88}$$

$$\left[C_0(0,0,0,m_N^2,0,M_R^2)\right]^{R1} \approx \frac{1}{m_N^2}\left[\ln\left(\frac{m_N^2}{M_R^2}\right) - \left(\frac{m_N^2}{m_\phi^2}\right)^2\right] \quad \text{for } m_\phi^2 \gg m_N^2 \gg M_R^2 \ . \tag{5.89}$$

In contrast to the self-energy contribution, the contribution of the vertex diagrams is always suppressed by the heavy fermion mass. Hence we can conclude that their contribution to the one-loop effects in the $K_L \to e\mu$ decay can be safely neglected.

Conclusions

In this thesis several aspects related to physics beyond the Standard Model were presented. Our attention was focused on rare processes, forbidden in the aforementioned model, particularly the lepton family number violating decay $K_L \to e\mu$. In order to accommodate the possibility of such a decay, we have adopted two minimal extensions of the Standard Model. In this sense, the most important part of our work was presented in the framework of the left-right symmetric model based on the gauge group $SU(2)_L \otimes SU(2)_R \otimes U(1)_{B-L}$. Particularities about the adopted model were presented in Chapter 1, with stress on the particular choice of a realistic scenario for the different vacuum expectation values of the symmetry-breaking scalar Higgs multiplets. The model chosen leads to particular expressions for the masses of the left- and right-handed gauge bosons as well as for the scalar particles, in terms of the gauge coupling constants and the different vacuum expectation values.

In addition to the gauge structure of the model one has to present considerations about the fermions, in particular the neutrinos. In a left-right symmetric model the natural choice is to have both left- and right-handed neutrinos present in the theory, and this further leads to the existence of neutrino mass terms in the Lagrangian. The neutrino masses will arise then from mass matrices with certain structure. Chapter 2 was dedicated to the study of a particular model for the massive neutrinos. Usual "see-saw" type scenarios constrain the heavy partners of the currently known light neutrinos to have a very large mass, however in the model adopted in this work these heavy neutrinos can be present with masses as low as few hundred GeV. One must keep in mind that this is possible only when more than one generation of heavy neutrinos are present. The model with two generations was of particular interest for our work, this model was used to obtain the corresponding matrix

elements for the neutrino mixing.

The main topic of this thesis, the study of the decay $K_L \to e\mu$, provided some interesting results. In the model still based on the $SU(2)_L \otimes U(1)_Y$ gauge group with heavy right-handed neutrinos present, it was shown that a branching ratio of the order $\sim 5.5 \times 10^{-15}$ is possible. This result is still orders of magnitudes below the present experimental limit of 4.7×10^{-12}, however it displays a serious enhancement compared to previous results in the literature [79,83].

Beside this value, new aspects related to the process were revealed. It has been shown that the main contribution to the decay amplitude in our model originates in the diagram with virtual top-quark present, the contribution of the charm-quark being negligible for the most regions of the parameter space of interest. Previously the charm-quark contribution was considered dominant, and the top-quark contribution treated as being at most of the same order. Our result originates partly from the large value of the measured top-quark mass, but an important role is played also by the new structure of the loop-function describing the corresponding box graph. The structure of the loop-function is providing the other important new aspect, namely the presence of the non-decoupling effects in the decay $K_L \to e\mu$. The fact that heavy neutrinos with masses of phenomenological interest are present in the theory, in correspondence with the particular structure of the neutrino mixing matrices lead to this effect. The consequence is that the branching ratio would increase with the increase of the heavy neutrino masses, the latter being constrained from above by perturbative unitarity considerations.

In the left-right symmetric model the decay $K_L \to e\mu$ requires a treatment of increased complexity. First of all, the process is allowed already at tree level due to the presence of flavour-changing neutral Higgs particles. It was important to notice that constrains from other low-energy processes (as the $K_0 - \bar{K}_0$ mixing) on the flavor-changing scalar masses do not suppress exceedingly the value of the branching ratio, actually one can impose new constrains on these masses based on the tree-level amplitude. At one-loop level a multitude of diagrams must be taken into account, and it turned out that there will be one-loop contributions to the decay amplitude which are not suppressed by the heavy FCNC scalars. Our study has concluded that diagrams with virtual gauge bosons of different chirality will give the dominant contribution to the decay amplitude, and this

contribution will exhibit the same non-decoupling behaviour. From a phenomenological point of view we concluded that a branching ratio close to the present experimental limit can be well accommodated in the framework of our model.

The fact that the box diagrams contributing to the $K_L \to e\mu$ decay amplitude in the left-right symmetric model are not gauge invariant was previously pointed out in the literature. In our work the first complete study dedicated to this particular question was performed. Although there exist many similarities with the well-known case of $K_0 - \bar{K}_0$ mixing, we have performed our analysis taking into account the presence of the charged Higgs particles. Our result provides a comprehensive treatment of the different gauge-complements to the box diagrams, and we arrived to the new conclusion that these gauge complements can become dominant compared to the box graphs. This conclusion differ from the point of view presented generally in the literature, where these gauge-complements were considered to be at least of the same order as the box graph contributions, mainly based on the results obtained in the study of $K_0 - \bar{K}_0$ mixing. Our result is based again on the different structure of the box diagrams compared to the ones present in the case of $K_0 - \bar{K}_0$ mixing. In our case the presence of neutrinos heavier than the right-handed gauge boson leads to the new behaviour described above.

The main motivation for our study was to provide a theoretical framework which can accommodate a branching ratio for the decay $K_L \to e\mu$ not far below the present experimental limit. We have presented a complete study of this decay in the left-right symmetric model and have obtained interesting new results. Should this decay be detected at DAPHNE or in other kaon factories, the left-right symmetric model would gain serious support, as it is the only model which predict a branching ratio for $K_L \to e\mu$ at this level.

Appendix A

Feynman rules of the model

Feynman rules for the $SU(2)_L \times SU(2)_R \times U(1)_{B-L}$ model with heavy Majorana neutrinos are given. If not explicitly stated otherwise (as for e.g. fermions), all particles are considered to enter the vertex.

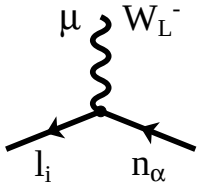

$$-i\frac{g_w}{\sqrt{2}}\gamma_\mu B^L_{l_i\alpha}\mathrm{P}_L$$

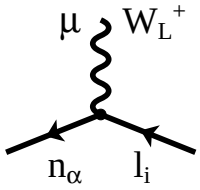

$$-i\frac{g_w}{\sqrt{2}}\gamma_\mu B^{L*}_{l_i\alpha}\mathrm{P}_L$$

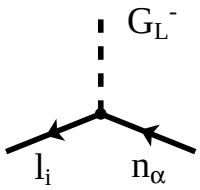

$$-i\frac{g_w}{\sqrt{2}M_L}B^L_{l_i\alpha}\left(m_{l_i}\mathrm{P}_L - m_{n_\alpha}\mathrm{P}_R\right)$$

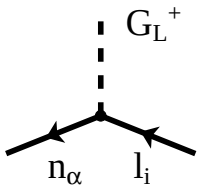

$$-i\frac{g_w}{\sqrt{2}M_L}B^{L*}_{l_i\alpha}\left(m_{l_i}\mathrm{P}_R - m_{n_\alpha}\mathrm{P}_L\right)$$

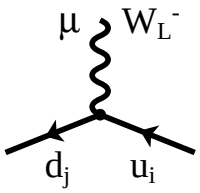

$$-i\frac{g_w}{\sqrt{2}}\gamma_\mu V_{ij}^{L*}\mathrm{P}_L$$

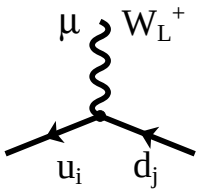

$$-i\frac{g_w}{\sqrt{2}}\gamma_\mu V_{ij}^{L}\mathrm{P}_L$$

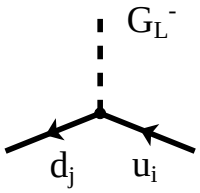

$$-i\frac{g_w}{\sqrt{2}M_L}V_{ij}^{L*}\left(m_{d_j}\mathrm{P}_L - m_{u_i}\mathrm{P}_R\right)$$

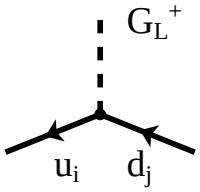

$$-i\frac{g_w}{\sqrt{2}M_L}V_{ij}^{L}\left(m_{d_j}\mathrm{P}_R - m_{u_i}\mathrm{P}_L\right)$$

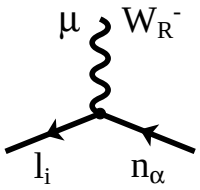

$$-i\frac{g_w}{\sqrt{2}}\gamma_\mu B_{l_i\alpha}^{R}\mathrm{P}_R$$

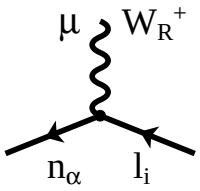

$$-i\frac{g_w}{\sqrt{2}}\gamma_\mu B_{l_i\alpha}^{R*}\mathrm{P}_R$$

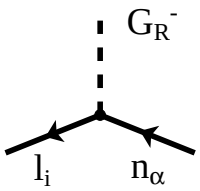

$$-i\frac{g_w}{\sqrt{2}M_L}s_\beta B_{l_i\alpha}^{R}\left(m_{l_i}\mathrm{P}_R - m_{n_\alpha}\mathrm{P}_L\right)$$

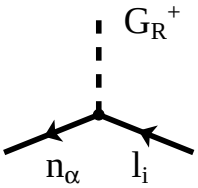

$$-i\frac{g_w}{\sqrt{2}M_L}s_\beta B^{R*}_{l_i\alpha}\left(m_{l_i}\mathrm{P}_L - m_{n_\alpha}\mathrm{P}_R\right)$$

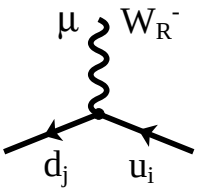

$$-i\frac{g_w}{\sqrt{2}}\gamma_\mu V^{R*}_{ij}\mathrm{P}_R$$

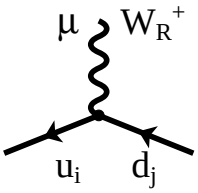

$$-i\frac{g_w}{\sqrt{2}}\gamma_\mu V^{R}_{ij}\mathrm{P}_R$$

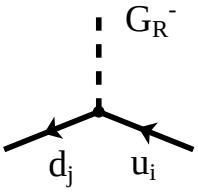

$$-i\frac{g_w}{\sqrt{2}M_L}s_\beta V^{R*}_{ij}\left(m_{d_j}\mathrm{P}_R - m_{u_i}\mathrm{P}_L\right)$$

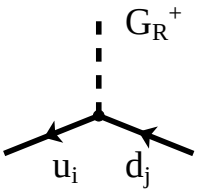

$$-i\frac{g_w}{\sqrt{2}M_L}s_\beta V^{R}_{ij}\left(m_{d_j}\mathrm{P}_L - m_{u_i}\mathrm{P}_R\right)$$

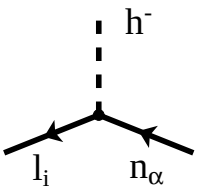

$$i\frac{g_w}{\sqrt{2}M_L}c_\beta\left[B^{R}_{l_i\alpha}m_{l_i}\mathrm{P}_R - \sum_{\gamma=1}^{2n_G}B^{R}_{l_i\gamma}\left(\delta_{\gamma\alpha}-\frac{C^{R*}_{\gamma\alpha}}{c^2_\beta}\right)m_{n_\gamma}\mathrm{P}_L\right]$$

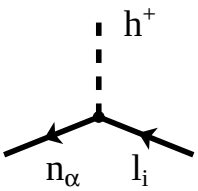

$$i\frac{g_w}{\sqrt{2}M_L}c_\beta\left[B^{R*}_{l_i\alpha}m_{l_i}\mathrm{P}_L - \sum_{\gamma=1}^{2n_G}B^{R*}_{l_i\gamma}\left(\delta_{\gamma\alpha}-\frac{C^{R}_{\gamma\alpha}}{c^2_\beta}\right)m_{n_\gamma}\mathrm{P}_R\right]$$

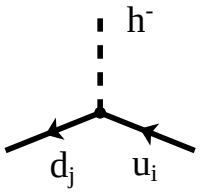

$$-i\frac{g_w}{\sqrt{2}M_L}c_\beta V_{ij}^{R*}\left(m_{d_j}\mathrm{P}_R - m_{u_i}\mathrm{P}_L\right)$$

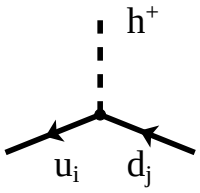

$$-i\frac{g_w}{\sqrt{2}M_L}c_\beta V_{ij}^{R}\left(m_{d_j}\mathrm{P}_L - m_{u_i}\mathrm{P}_R\right)$$

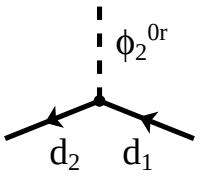

$$-i\frac{g_w}{2M_L}\sum_{i=u,c,t}\left(V_{id_2}^{L*}V_{id_1}^{R}m_i\mathrm{P}_R + V_{id_2}^{R*}V_{id_1}^{L}m_i\mathrm{P}_L\right)$$

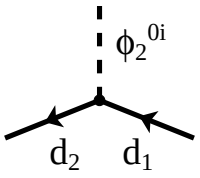

$$\frac{g_w}{2M_L}\sum_{i=u,c,t}\left(V_{id_2}^{L*}V_{id_1}^{R}m_i\mathrm{P}_R - V_{id_2}^{R*}V_{id_1}^{L}m_i\mathrm{P}_L\right)$$

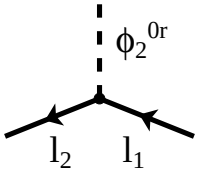

$$-i\frac{g_w}{2M_L}\sum_{\alpha=1}^{2n_G}\left(B_{l_2\alpha}^{L}B_{l_1\alpha}^{R*}m_{n_\alpha}\mathrm{P}_R + B_{l_2\alpha}^{R}B_{l_1\alpha}^{L*}m_{n_\alpha}\mathrm{P}_L\right)$$

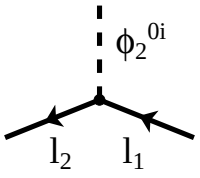

$$\frac{g_w}{2M_L}\sum_{\alpha=1}^{2n_G}\left(B_{l_2\alpha}^{L}B_{l_1\alpha}^{R*}m_{n_\alpha}\mathrm{P}_R - B_{l_2\alpha}^{R}B_{l_1\alpha}^{L*}m_{n_\alpha}\mathrm{P}_L\right)$$

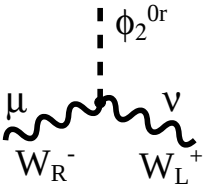

$$-ig_w M_L g_{\mu\nu}$$

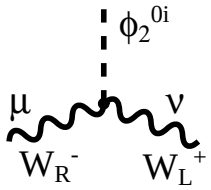

$g_w M_L g_{\mu\nu}$

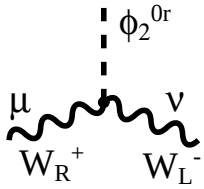

$-ig_w M_L g_{\mu\nu}$

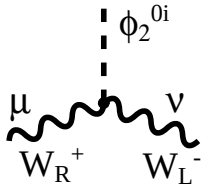

$-g_w M_L g_{\mu\nu}$

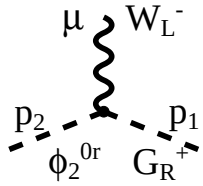

$-i\frac{g_w}{2}s_\beta(p_1-p_2)_\mu$

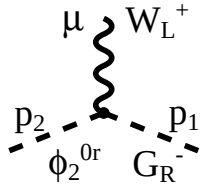

$i\frac{g_w}{2}s_\beta(p_1-p_2)_\mu$

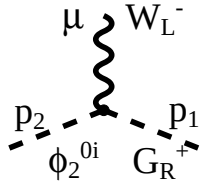

$-\frac{g_w}{2}s_\beta(p_1-p_2)_\mu$

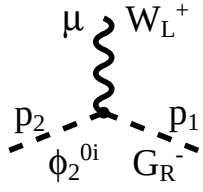

$-\frac{g_w}{2}s_\beta(p_1-p_2)_\mu$

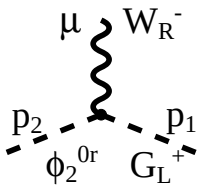

$$-i\frac{g_w}{2}(p_1 - p_2)_\mu$$

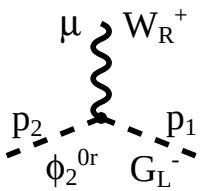

$$i\frac{g_w}{2}(p_1 - p_2)_\mu$$

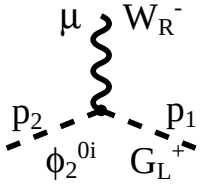

$$\frac{g_w}{2}(p_1 - p_2)_\mu$$

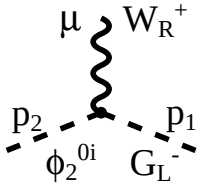

$$\frac{g_w}{2}(p_1 - p_2)_\mu$$

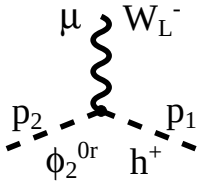

$$-\frac{g_w}{2}c_\beta(p_1 - p_2)_\mu$$

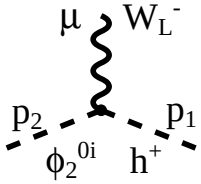

$$-i\frac{g_w}{2}c_\beta(p_1 - p_2)_\mu$$

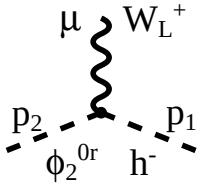

$$\frac{g_w}{2}c_\beta(p_1 - p_2)_\mu$$

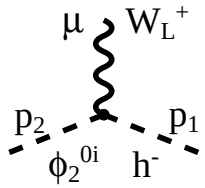

$$-i\frac{g_w}{2}c_\beta(p_1-p_2)_\mu$$

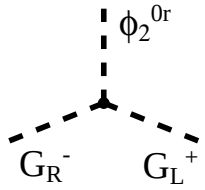

$$i\frac{g_w}{2}s_\beta\frac{m^2_{\phi_2^{0r}}}{M_L}$$

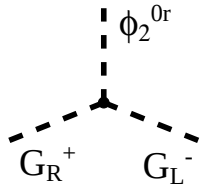

$$i\frac{g_w}{2}s_\beta\frac{m^2_{\phi_2^{0r}}}{M_L}$$

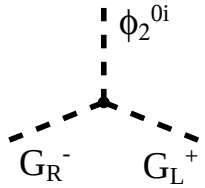

$$-\frac{g_w}{2}s_\beta\frac{m^2_{\phi_2^{0i}}}{M_L}$$

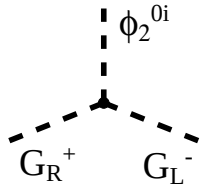

$$\frac{g_w}{2}s_\beta\frac{m^2_{\phi_2^{0i}}}{M_L}$$

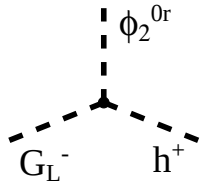

$$i\frac{g_w}{2M_L}c_\beta\left(m_h^2-m^2_{\phi_2^{0r}}\right)$$

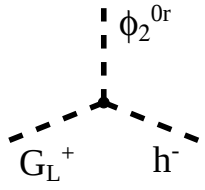

$$i\frac{g_w}{2M_L}c_\beta\left(m_h^2-m^2_{\phi_2^{0r}}\right)$$

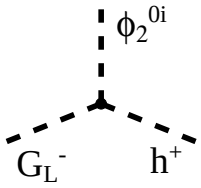

$$\frac{g_w}{2M_L} c_\beta \left(m_h^2 - m_{\phi_2^{0i}}^2 \right)$$

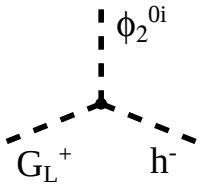

$$-\frac{g_w}{2M_L} c_\beta \left(m_h^2 - m_{\phi_2^{0i}}^2 \right)$$

Bibliography

[1] S. L. Glashow, *Nucl. Phys.* **22** (1961) 579,
S. Weinberg, *Phys. Rev. Lett.* **19** (1967) 1264,
A. Salam, in *Elementary Particle Theory*, ed. N. Svartholm (Almquist and Wiksel, 1968).

[2] J.C. Pati, A. Salam, *Phys. Rev.* **D10** (1974) 275,
R.N. Mohapatra, J.C. Pati, *Phys. Rev.* **D11** (1975) 566,
R.N. Mohapatra, J.C. Pati, *Phys. Rev.* **D11** (1975) 2558,
G. Senjanović, R.N. Mohapatra, *Phys. Rev.* **D12** (1975) 1502.

[3] Q. R. Ahmad *et al.* [SNO Collaboration], *Phys. Rev. Lett.* **89** (2002) 011301; *Phys. Rev. Lett.* **89** (2002) 011302; *Phys. Rev. Lett.* **87** (2001) 071301.

[4] S. N. Ahmed *et al.* [SNO Collaboration], arXiv:nucl-ex/0309004.

[5] Y. Fukuda *et al.* [Super-Kamiokande Collaboration], *Phys. Rev. Lett.* **81** (1998) 1562; *Phys. Rev. Lett.* **82** (1999) 2644.

[6] S. Fukuda *et al.* [Super-Kamiokande Collaboration], *Phys. Rev. Lett.* **86** (2001) 5651; *Phys. Lett.* **B539** (2002) 179.

[7] S.S. Gershtein, Ya.B. Zeldovich,*JETP Lett.* **4** (1966) 120,
R. Cowsik, J. McClelland,*Phys. Rev. Lett.* **29** (1972) 699.

[8] R.N. Mohapatra, R.E. Marshak, *Phys. Lett.* **B91** (1980) 222,
A. Davidson, *Phys. Rev.* **D20** (1979) 776.

[9] M. Kobayashi, T. Maskawa, *Prog. Theor. Phys.* **49** (1973) 652.

[10] R.N. Mohapatra, J.C. Pati, *Phys. Rev.* **D11** (1975) 566.

[11] R.E. Marshak, Riazuddin and C.P. Ryan, *Theory of Weak Interactions in Particle Physics*, Wiley, New York, 1969,
L. Wolfenstein, *Theory and Phenomenology in Particle Physics* (edited by A. Zichichi), Academic Press, New York, 1969,
E. Paul, in *Elementary Particle Physics*, Springer Tracts in Modern Physics, vol. 79.

[12] D. Chang, *Nucl. Phys.* **B214** (1983) 435,
G. Branco, J.M. Frere and J.M. Gerard, *Nucl. Phys.* **B221** (1983) 317.

[13] R.N. Mohapatra, G. Senjanović, *Phys. Rev. Lett.* **44** (1980) 912,
R.N. Mohapatra, G. Senjanović, *Phys. Rev.* **D21** (1981) 165.

[14] R.N. Mohapatra, R.E. Marshak, *Phys. Rev. Lett.* **44** (1980) 1316.

[15] J.F. Gunion *et al.*, *Phys. Rev.* **D40** (1989) 1546.

[16] D. Chang, R.N. Mohapatra and M.K. Parida, *Phys. Rev. Lett.* **50** (1984)1072,
D. Chang, R.N. Mohapatra and M.K. Parida, *Phys. Rev.* **D30** (1984) 1052.

[17] W. Pauli, private correspondence with O. Hahn and L.Meitner, 1931
W. Pauli, Proceedings of *The VII. Solvay Congress*, Brussels (1933) p. 324, Gauthier-Villars, Paris.

[18] T. Yanagida, Proceedings of the *Workshop on Unified Theory and Baryon Number of the Universe*, eds. O. Swada and A. Sugamoto (KEK, 1979) p. 95,
M. Gell-Mann, P. Ramond and R. Slansky, *Supergravity*, eds. P. van Nieuwenhuizen and D. Friedman (North-Holland, Amsterdam, 1979) p. 315,
A. S. Joshipura, A. Mukherjee and U. Sarkar, *Phys. Lett.* **B156**
(1985) 353,
P. Roy, O. Shanker, *Phys. Rev.* **D30** (1984) 1949.

[19] F. del Aguila, E. Laermann and P.M. Zerwas, *Nucl. Phys.* **B297**
(1988) 1.

[20] J. Maalampi, K. Mursula and R. Vuopionperä, *Nucl. Phys.* **B372** (1992) 23.

[21] C.A. Heusch, P. Minkowski, *Nucl. Phys.* **B416** (1994) 3.

[22] W. Buchmüller, C. Greub, *Nucl. Phys.* **B363** (1991) 345.

[23] D.A. Dicus, P. Roy, *Phys. Rev.* **D44** (1991) 1593.

[24] A. Datta, A. Pilaftsis, *Phys. Lett.* **B278** (1992) 162.

[25] A. Pilaftsis, *Z. Phys.* **C55** (1992) 275.

[26] D. Choudhury, R.M. Godbole and P. Roy, *Phys. Lett.* **B308** (1993) 394.

[27] A. Datta, M. Guchait and A. Pilaftsis, *Phys. Rev.* **D50** (1994) 3195.

[28] J.G. Körner, A. Pilaftsis and K. Schilcher, *Phys. Lett.* **B300** (1993) 381.

[29] A. Pilaftsis, *Phys. Lett.* **B285** (1992) 68.

[30] J.G. Körner, A. Pilaftsis and K. Schilcher, *Phys. Rev.* **D47** (1993) 1080.

[31] J. Bernabéu, J.G. Körner, A. Pilaftsis and K. Schilcher, *Phys. Rev. Lett.* **71** (1993) 2695.

[32] S. Bertolini, A. Sirlin, *Phys. Lett.* **B257** (1991) 179.

[33] E. Gates, J. Terning, *Phys. Rev. Lett.* **67** (1991) 1840.

[34] B.A. Kniehl, H.-G. Kohrs, *Phys. Rev.* **D48** (1993) 225.

[35] M.E. Peskin, T. Takeuchi, *Phys. Rev. Lett.* **65** (1990) 964; *Phys. Rev.* **D46** (1992) 381.

[36] G. Altarelli, R. Barbieri, *Phys. Lett.* **B253** (1991) 161.

[37] G. Altarelli, R. Barbieri and S. Jadach, *Nucl. Phys.* **B369** (1992) 3.

[38] I. Maksymyk, C. P. Burgess and D. London, *Phys. Rev.* **D50** (1994) 529

[39] A. Ilakovac, B. A. Kniehl and A. Pilaftsis, *Phys. Lett.* **B317** (1993) 609.

[40] B. A. Kniehl, A. Pilaftsis, *Nucl. Phys.* **B424** (1994) 18.

[41] P. Langacker, D. London, *Phys. Rev.* **D38** (1988) 886.

[42] G. Bhattacharyya *et al.*, *Mod. Phys. Lett.* **A6** (1991) 2921.

[43] E. Nardi, E. Roulet and D. Tommasini, *Nucl. Phys.* **B386** (1992) 239; *Phys. Rev.* **D46** (1992) 3040.

[44] C.P. Burgess et. al., *Phys. Rev.* **D49** (1994) 6115.

[45] W. Buchmüller, C. Greub and H.-G. Kohrs, *Nucl. Phys.* **B370** (1992) 3.

[46] E. Witten, *Nucl. Phys.* **B268** (1986) 79,
R.N. Mohapatra, J.W.F. Valle, *Phys. Rev.* **D34** (1986) 1642,
J. L. Hewett, T. L. Rizzo, *Phys. Rep.* **183** (1989) 193.

[47] S. Kelley, J.L. Lopez, D.V. Nanopoulos and H. Pois, *Nucl. Phys.* **B358** (1991) 27.

[48] R. Arnowitt, P. Nath, *Phys. Rev. Lett.* **66** (1991) 2708.

[49] D. Wyler, L. Wolfenstein, *Nucl. Phys.* **B218** (1983) 205.

[50] A. Ilakovac, A. Pilaftsis,*Nucl. Phys.* **B437** (1995) 491.

[51] W. Buchmüller, C. Greub, *Phys. Lett.* **B256** (1991) 465.

[52] P. Langacker, D. London, *Phys. Rev.* **D38** (1988) 886.

[53] S. P. Rosen, S. M. Gelb, *Phys. Rev.* **D34** (1986) 969.

[54] J. Bouchez et. al., *Z. Phys.* **C32** (1986) 499.

[55] M. Cribier et. al., *Phys. Lett.* **B182** (1986) 168.

[56] S. P. Mikheyev, A. Yu. Smirnov, *JETP* **64** (1986) 913.

[57] L. Wolfenstein, *Phys. Rev.* **D17** (1978) 2369.

[58] S. J. Parke, T. P. Walker, *Phys. Rev. Lett.* **57** (1986) 2322.

[59] J. N. Bahcall, *Nucl. Phys.* **B19** (1991) 94.

[60] W. Buchmüller, D. Wyler, *Phys. Lett.* **B249** (1990) 458.

[61] H. Harari, H. Haut, J. Weyers, *Phys. Lett.* **B78** (1978) 459.

[62] Y. Koide, *Phys. Rev.* **D39** (1989) 1391.

[63] T. Yanagida, *Prog. Theor. Phys.* **B135** (1978) 66,
Q. Shafi, F. W. Stecker, *Phys. Rev. Lett.* **53** (1984) 1292,
P. Langacker, R. D. Peccei, T. Yanagida, *Mod. Phys. Lett.* **A1** (1986) 541,
K. S. Babu, E. Ma, *Phys. Rev. Lett.* **61** (1988) 674.

[64] For reviews see, e.g. P. Langacker, *Phys. Rev.* **C72** (1981) 185,
R. N. Mohapatra, *Unification and Supersymmetry*, Springer-Verlag, New York, 1986.

[65] H. Georgi, C. Jarlskog, *Phys. Lett.* **B86** (1979) 297.

[66] E. Eichten et. al., *Phys. Rev.* **D34** (1986) 1547.

[67] Z. Gagyi-Palffy, A. Pilaftsis and K. Schilcher, *Phys. Lett.* **B343** (1995) 275.

[68] B. A. Campbell, *Phys. Rev.* **D28** (1983) 209.

[69] J. C. Pati, H. Stremnitzer, *Phys. Lett.* **B172** (1986) 441.

[70] I. I. Bigi, G. Köpp, P. M. Zerwas, *Phys. Lett.* **B166** (1986) 238.

[71] W.-S. Hou, A. Soni,*Phys. Rev. Lett.* **54** (1985) 2038.

[72] O. Shanker, *Nucl. Phys.* **B206** (1982) 253.

[73] L. J. Hall, L. J. Randall, *Nucl. Phys.* **B274** (1986) 157.

[74] B. A. Campbell et. al., *Int. J. Mod. Phys.* **A2** (1987) 831.

[75] B. W. Lee,R. E. Shrock, *Phys. Rev.* **D16** (1977) 1444.

[76] A. Barroso, G. C. Branco, M. C. Bento, *Phys. Lett.* **B134** (1986) 123.

[77] E.A. Paschos, *Phys. Rev. Lett.* **39** (1977) 858.

[78] T. Inami and C.S. Lim, *Prog. Theor. Phys.* **65** (1981) 2971.

[79] P. Langacker, S.U. Sankar, and K. Schilcher, *Phys. Rev.* **D38** (1988) 2841.

[80] S.L. Glashow, J. Iliopoulos, and L. Maiani, *Phys. Rev.* **D2** (1970) 1285.

[81] E. Ma and A. Pramudita, *Phys. Rev.* **D24** (1981) 1410.

[82] F. Abe *et al.* (CDF collaboration), *Phys. Rev. Lett.* **73** (1994) 225.

[83] A. Acker and S. Pakvasa, *Mod. Phys. Lett.* **A7** (1992) 1219.

[84] K. Hagiwara *et al.* (Particle Data Group), Review of Particle Physics, *Phys. Rev.* **D66** (2002) 010001.

[85] Z. Gagyi-Palffy, A. Pilaftsis and K. Schilcher, *Nucl. Phys.* **B513** (1998) 517

[86] J. Basecq, L.F. Li, and P.B. Pal, *Phys. Rev.* **D32** (1985) 175.

[87] C.P. Burgess *et al.*, *Phys. Rev.* **D49** (1994) 6115.

[88] G. Beall, M. Bander and A. Soni, *Phys. Rev. Lett.* **48** (1982) 848.

[89] R.N. Mohapatra, G. Senjanović and M.D. Tran, *Phys. Rev.* **D28** (1983) 546.

[90] F.J. Gilman, M.H. Reno, *Phys. Rev.* **D29** (1984) 937.

[91] M. Hwang, R.J. Oakes, *Phys. Rev.* **D29** (1984) 127.

[92] D. Chang, J. Basecq, L.F. Li, and P.B. Pal, *Phys. Rev.* **D30** (1984) 1601.

[93] C.S. Lim, T. Inami, *Prog. Theor. Phys.* **67** (1982) 1569.

[94] W.-S. Hou and A. Soni, *Phys. Rev.* **D32** (1985) 163

[95] K. Fujikawa, B.W. Lee and A.I. Sanda, *Phys. Rev.* **D6** (1972) 2923.

[96] K. Aoki *et al.*, *Prog. Theor. Phys.* **73** *Suppl.* (1982) 1.

Acknowledgments

This thesis can not be considered complete without mentioning those who contributed to its accomplishment.

★ First of all I would like to express my deep gratitude toward the Graduiertenkolleg "Elementarteilchenphysik bei mittleren und hohen Energien" for awarding me a scholarship that represented the main financial support along my years of study.

☼ I am grateful to Prof. K. Schilcher not only for supervising my thesis, but also for the continuous support he offered me in finalizing my doctoral studies.

ϟ I am glad to acknowledge the help received from Dr. A. Pilaftsis in developing this scientific project. His enthusiastic approach and relentless interest represented a permanent incentive in my work.

◷ Regarding the administrative aspects of the doctoral examination, I received an invaluable help from Roxana. Without her presence in Mainz it would have been really difficult to go successfully through all the paperwork.

☻ For years, my colleagues at ThEP represented the stimulating environment for my work. I thank them all, but I have to mention explicitly D. Pîrjol (who made easier my adaptation) and J. Plass (for broadening my horizon on computers).

♡ During the last months it was my wife, Ada, who offered me the greatest support in finalizing my thesis. Thank you for continuously trying to get the best out of me!

Curriculum Vitae

Personal Data

Name:	Zoltán Gagyi-Pálffy
Date of birth:	December 9-th, 1967
Place of birth:	Arad, Romania
Nationality:	Romanian
Marital status:	Married since June 2003 with Adriana-Claudia

Employment:

Since 1997	Teaching assistant at the Faculty of Physics, University of Bucharest
11.1993 – 03.1997	Scholarship of the Graduiertenkolleg "Elementarteilchenphysik bei mittleren und hohen Energien"
10.1992 – 10.1993	Associate teaching assistant at the University of Bucharest
10.1986 – 06.1987	Military service

Studies

February 19-th, 2004	Doctoral examination
11.1993 – 03.1997	Doctoral studies in Physics at the Johannes-Gutenberg University, Mainz
09.1987 – 06.1992	Student in Physics at the University of Bucharest

School

June 1986	High-school final examination ("Bacalaureat")
09.1982 – 06.1986	Ioan Slavici High-school in Arad

Lebenslauf

Persönliche Daten

Name:	Zoltán Gagyi-Pálffy
Geburtsdatum:	9. Dezember 1967
Geburtsort:	Arad, Rumänien
Staatsangehörigkeit:	rumänisch
Familienstand:	verheiratet seit Juni 2003 mit Adriana-Claudia

Beschäftigung:

Seit 1997	Wissenschaftlicher Angestellter am Fakultät für Physik der Universität Bukarest
11.1993 – 03.1997	Stipendiat des Graduiertenkollegs "Elementarteilchenphysik bei mittleren und hohen Energien"
10.1992 – 10.1993	Wissenschaftliche Hilfskraft an der Universität Bukarest
10.1986 – 06.1987	Wehrdienst

Studium

19. Februar 2004	Mündliche Doktorprüfung
11.1993 – 03.1997	Promotion (Physik) an der Johannes-Gutenberg Universität Mainz
09.1987 – 06.1992	Studium (Physik Diplom) an der Universität Bukarest

Schulbildung

Juni 1986	Abitur
09.1982 – 06.1986	Ioan Slavici Lyzeum in Arad